Comparison between IMU-based and Pressure Insoles-based Thresholds for Biofeedback in Postural Transitions

handed in
MASTER'S THESIS

B.Sc. Vincent Hessfeld

born on the 26.05.1995

living in:
Paul-Hindemith-Allee 4
80939 Munich

Tel.: 01578/6915110

Human-centered Assistive Robotics
Technical University of Munich

Univ.-Prof. Dr.-Ing. Dongheui Lee

Supervisor:	M.Sc. Katrin Schulleri
Start:	16.06.2020
Intermediate Report:	13.10.2020
Delivery:	16.01.2021

June 16, 2020

M A S T E R ' S   T H E S I S

for

Vincent Hessfeld

Student ID 03663884, Degree HFE

Comparison between IMU-based and Pressure Insoles-based Thresholds for Biofeedback in Postural Transitions

Problem description:

Wearable devices provide a good opportunity for people with postural instability to improve postural control in everyday life [3]. Different feedback devices have been investigated in the research area of postural control[1, 2, 3, 4] and in the context of wearable sensors inertial measurement units (IMUs) located on various parts of the body or plantar force sensors [3, 4, 5] have been widely used to measure static and dynamic balance. However, when using a feedback based on one single sensor at the trunk in situations of postural transition, like bending forward, one might get an unreliable feedback, as being still in a stable position. Consequently the following research questions will be investigated:

1) Is a pressure insole (PPS) based feedback more reliable than an IMU suit based system?

2) Is a combined feedback (PPS + IMU suit based) more reliable than the PPS based system?

3) Optional: Is the reliability of the systems dependent on the definition of threshold?

Tasks:

- Literature research and develop the study design
- Write/adapt scripts for communication and synchronisation of the different hardwares (IMU suit, force plate, pressure insoles)
- Write/adapt scripts for capturing and saving data with IMU suit, force plate pressure insoles
- Define the thresholds for feedback by pilot testing
- Carry out user study with 20 participants
- Data post processing and statistical analysis

Bibliography:

[1] P. Hur, Y.-T. Pan, and C. DeBuys. Free energy principle in human postural control system: Skin stretch feedback reduces the entropy. 09 2019.

[2] B. C. Lee, B. J. Martin, and K. H. Sienko. Directional postural responses induced by vibrotactile stimulations applied to the torso. *Exp Brain Res*, 222:471–82, 2012.

[3] C. Z. Ma, A. H. Wan, D. W. Wong, Y. P. Zheng, and W. C. Lee. A vibrotactile and plantar force measurement-based biofeedback system: Paving the way towards wearable balance-improving devices. *Sensors (Basel)*, 15:31709–22, 2015.

[4] D. W. Ma, C. Z.and Wong, W. K. Lam, A. H. Wan, and W. C. Lee. Balance improvement effects of biofeedback systems with state-of-the-art wearable sensors: A systematic review. *Sensors (Basel)*, 16:434, 2016.

[5] W. C. Ma, C. Z.and Lee. A wearable vibrotactile biofeedback system improves balance control of healthy young adults following perturbations from quiet stance. *Human Movement Science*, 55:54–60, 2017.

Supervisor: M. Sc. Katrin Schulleri
Start: 16.06.2020
Intermediate Report: 13.10.2020
Delivery: 16.01.2021

(D. Lee)
Univ.-Professor

Abstract

Previous studies have shown that biofeedback can enhance balance control. The additional information provided on one's body posture supports the postural perception. Researchers mostly focused on static balance or gait analysis; less research was done on balance during postural transitions. Scientists have used IMU-systems and PPS-systems to track the CoM and CoP trajectory, respectively. The definition of criteria and corresponding thresholds is crucial for reliable and effective biofeedback. This study compares an IMU-system and a PPS-system (insoles) regarding their reliability in providing biofeedback during postural transitions. Applying the CoM trajectory measured by an IMU-system to control biofeedback is a novel approach. Furthermore, we compare a threshold based on the postural sway during quiet standing (BL-threshold) with one based on the Limits of Stability (LoS-threshold).

We measured the parameters of 16 subjects and calculated their BL-threshold and LoS-threshold of each system. In the evaluation, the subjects carried out a postural transition by bending forward and shifting their body until they tipped over. This procedure was repeated for each direction along the anterior-posterior and medio-lateral axes separately. We calculated the time discrepancy Δt between the point the subject exceeded the respective threshold and the tipping point.

Considering the LoS-threshold, the PPS-system shows a lower Δt than the IMU-system, except in the posterior direction. The LoS-threshold's Δt-values are lower than these of the BL-threshold by 650 - 2325ms, when compared within each system. The PPS-system's LoS-threshold demonstrates the lowest Δt and best performance. We observe high variations in the BL-threshold, confirming previous findings that postural sway is a highly individual-specific parameter. Our results indicate that the LoS-threshold is more reliable than the BL-threshold and that a PPS-system is better suited. So future research should focus on mobile PPS-based systems. On average, time discrepancies are high compared to reaction times on vibrotactile stimuli. Further investigation into threshold parameters is needed.

Declaration of Authorship

I hereby declare that the thesis submitted is my own unaided work. All direct or indirect sources used are acknowledged as references.

I am aware that the thesis in digital form can be examined for the use of unauthorized aid and in order to determine whether the thesis as a whole or parts incorporated in it may be deemed as plagiarism. For the comparison of my work with existing sources I agree that it shall be entered in a database where it shall also remain after examination, to enable comparison with future theses submitted. Further rights of reproduction and usage, however, are not granted here.

This paper was not previously presented to another examination board and has not been published.

Vincent Hessfeld

first and last name

Munich, 16.01.21

date and signature

Contents

Chapter 1

Introduction

We as humans are a species that stands and moves on two legs for much of our time. When we change position, we tend naturally to control our balance in the process and keep our bodies stable. A person not able to do so loses his balance and might fall, risking physical injury. In particular adults older than 65 years suffer from severe injuries as a consequence of falls [HLBB19]. At least 300,000 older people are hospitalized in the US because of fall injuries every year, and falling causes 95% of hip fractures according to the Centers for Disease Control and Prevention [cdc17]. Similar numbers are reported for Germany, where 50% of all injuries in this age group are related to falls [RKSL17]. The prevalence of falls and fall-related mortality in this age group, moreover, has steadily increased over the past 20 years [HLBB19]. Figure 1.1 shows that the mortality rate in 2016 has doubled compared to the year 2000 for both women and men aged 75 and older. In 2015, the treatment of fall-related injuries generated medical costs of more than $50 billion [cdc17]. Most of this amount is shouldered by public health services, but the cost to individuals can be considerable - and goes beyond financials. Aside from the injuries themselves, a patient who falls repeatedly often experiences anxiety and reduces her physical activity [Sal10]. She may face chronic pain and loss of independence, seriously damping her quality of life.

In the older population, people most commonly fall because of gait and balance disorders - aspects of keen interest from the medical community [Sal10]. These disorders are themselves associated with certain risk factors, such as chronic illnesses, physical decline or lack of exercise, which increase with advancing age [who07, Sal10, CT17]. Salzman describes the detailed correlations as well as suggesting possible clinical diagnoses and interventions [Sal10]. Where he evaluates non-instrumented tests carried out by physicians, other researchers looking into balance disorders follow a more technical approach and have implemented state-of-the-art technology to objectively monitor and quantify balance performance [MWL$^+$16, KJBC18].

The sensor technologies employed in such research can also provide instant biofeedback to help the individual improve his balance over the long-term. The biofeedback is delivered, however, through technology that is hardly convenient to patients.
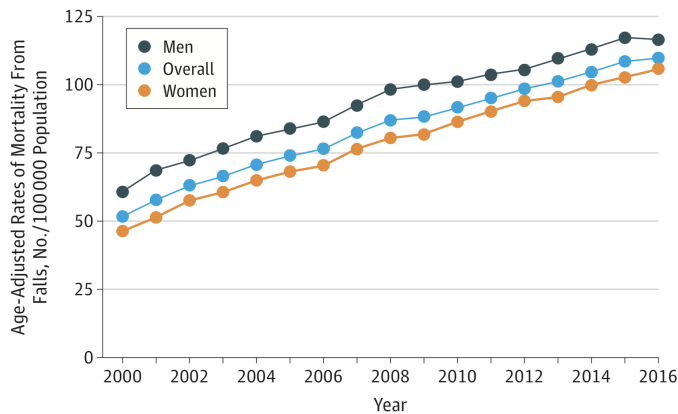
Figure 1.1: Mortality rates from falls among persons aged 75 and older in the US, 2000-2016 [HLBB19]

These are mostly stationary systems in hospitals or laboratories, which means that patients have to come to the facilities and that the technology cannot be applied in real-world scenarios. In response, researchers and industry are developing a growing number of wearable devices that aim at improving a person's stability during daily activities [MWL+16]. Compact devices attached to the body or integrated into clothing could greatly enhance balance and reduce the risk of falls among the elderly.

1.1   Concept of Balance

We earlier spoke about balance and its importance in postural transition. But what exactly are balance and posture and how do they relate? To answer this question, we first must address terminology.

The center of mass (CoM) is understood in biomechanics as "the point around which the sum of the torques produced by the weights of the body segments is equal to zero" [Ste20, p. 57-58]. It is also often referred to as the center of gravity. For the human body, the CoM usually sits in the area of the lower back - more exactly, at the end of the lumbar spine [Ste20, p. 57-58]. The center of pressure (CoP) indicates the point of application of the ground reaction force (GRF) vector on the ground plane [BRK94]. In static quiet standing, the CoP is assumed to be the CoM's vertical projection on this plane (cf. Figure 1.2).

The base of support (BoS) describes a person's contact area with a supporting surface [MP20, p. 547-548], such as the ground, a chair or a handrail. In this study, the BoS refers to the area beneath the feet (cf. Figure 1.3). The BoS is an important biomechanical constraint on balance [KSGH13].

From a mechanical perspective, balance is defined as "the state of an object when the resultant load actions acting upon it are zero" [PDRP00]. An object is balanced
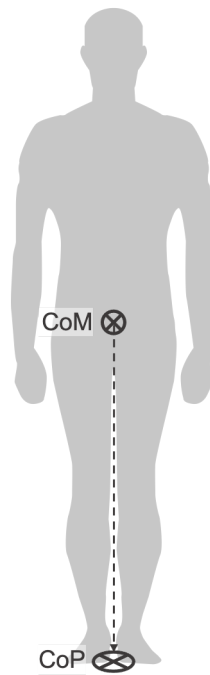
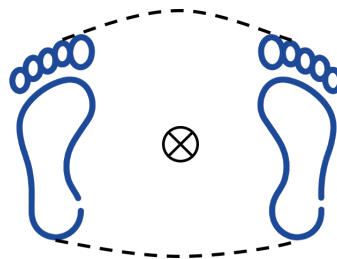Figure 1.2: Center of Mass (CoM) and Center of Pressure (CoP) in bipedal stance

Figure 1.3: Base of Support (BoS) in bipedal stance; $\otimes$ = CoP

when either the CoM's vertical projection or the CoP lies within the BoS. If the CoM or CoP shifts outside the BoS, the object is no longer balanced and will tip due to the gravitational force acting upon it. Humans, however, are able to cope with a certain degree of imbalance in order to prevent falls [PDRP00]. We can sense instabilities and activate our muscles to counteract gravitational forces. This ability is called "balance control" or "postural control".

Postural control is a complex motor skill [PDRP00]. It involves the somatosensory system, the cognitive system, and the motor system to detect and react to perturbations. Any impairment in one of these systems can result in a postural control deficit. Impairments can stem from diseases, such as a stroke, Parkinson's disease or sarcopenia and often occur in older adults, the group most affected by falls [who07, CT17].

Physiologists and medics have experimented with numerous measures to prevent patients from falling. They have proposed physical exercises, with a focus on flexibility, endurance, strength, and balance [CT17, KJBC18], recommendations supported by findings that patients who exercised regularly reduced their risk of falling by 21%. [CT17].

Sensor technology has helped medical teams to closely monitor a patient's training progress and increase her awareness for situations in which she might fall [KJBC18]. Sensors coupled with biofeedback can stimulate patients who deal with an impaired or degenerated somatosensory system [AAB+17]. Tactile stimulation in particular has shown to effectively evoke postural responses in individuals by providing their nervous systems with additional sensory input.

When speaking about balance in humans, we frequently distinguish between static and dynamic balance. Static balance refers to postural control when a person is standing still in an upright position [Rag96]. But it includes postural sway, continuous corrective involuntary movements around the CoM. This is a relevant detail when examining falls, as studies in the 1980s to 1990s have shown that postural sway increases with age [PJA90, WWD+93, Rag96].

Dynamic balance, on the other hand, describes postural control during voluntary movements or external perturbations [Rag96]. It is a fairly general term covering a wide range of situations, from gait to sit-to-stand transitions. Dynamic balance is difficult to quantify across a range of movements, and instead mostly specified for certain types of movements. A number of clinical test have aimed to assess dynamic balance but only a few studies have tried to use technology to objectively quantify dynamic balance - outside of gait analysis [MWL+16, ALHPI+18, LPJ+18].

Even though researchers distinguish between static and dynamic balance, both are present in daily activities simultaneously. Researchers tend, therefore, to look at balance in a series of movements, and develop a system able to assess balance in different situations.

1.2 Balance Assessment

Scientists and physicians differentiate between non-instrumented and instrumented tests to assess balance [MWL+16].

Physicians mostly use non-instrumented tests in a clinical context, visually assessing postural sway or abnormal evasive movements. A common test to assess static balance is the Romberg Test, in which the patient stands still in an upright position and the physician compares postural sway during trials with the patient's eyes open and closed [MWL+16]. In the Timed Up and Go (TUG) test, the physician measures the time a patient needs to complete a defined sequence of tasks. This test aims to detect dynamic balance deficits. Both tests are a first step to objectively quantify balance, but non-instrumented tests tend to lack objectivity and depend heavily on the clinician's expertise [PDRP00, KJBC18].

In instrumented test, researchers and physicians use sensor technologies to objectively assess balance parameters. They most frequently measure the CoM or CoP trajectory; a great displacement and high variability in these indicate balance disturbances [KSGH13, MWL+16, DSL19]. Researchers are able to quantify static balance by means of force plate measurements, when assessing dynamic balance, however, they mostly focus on gait parameters, such as step length and time [AOL+15, CCD+15, MWL+16]. In one pilot study, Lou et al. developed a method to measure dynamic balance during postural transition with a force plate in a game like environment [LPJ+18]. Their new method correlates with results obtained from the TUG test. The study showed that patients with a leg injury have a greater CoP displacement on the injured side compared to the normal side indicating balance instabilities in the injured leg. Still, most studies utilize force plates for measurements and are thus limited to indoor settings [MWL+16].

At this point we want to present another concept how to assess balance. As mentioned earlier, humans are able to cope with a certain degree of imbalance when the CoM or CoP shifts outside the BoS [PDRP00]. A metric to quantify this ability are the so called Limits of Stability (LoS). Ragnarsdottir (1996) defines the LoS as "the outmost range in any direction a person can lean from the vertical, without changing the original base of support" [Rag96]. There are two common approaches how to assess the LoS in humans: In the circular-leaning test, the person is asked to lean forward and carry out a circular movement around the BoS, leaning to each side as far as possible without loosing his balance [TSL+17]. Alternatively, in the four-way-leaning test, the person leans in anterior, left, right and posterior direction each separately. In one study from 2017, Thomsen et al. found out that the four-way-leaning test shows larger LoS than the circular-leaning test [TSL+17]. Sensor technologies, in particular force plates, can aid researchers in the LoS assessment as well.
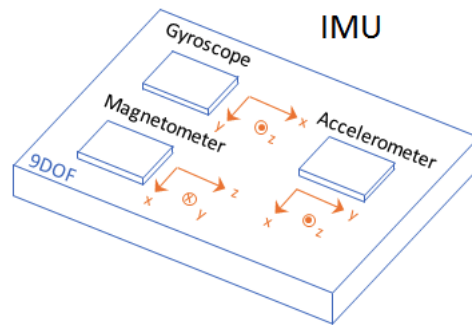
Figure 1.4: Schematic structure of an IMU [mat]

1.3   State-of-the-Art in Wearable Technology

1.3.1   Sensor Technology

The market for wearable sensor technology is growing, even more as hardware and components become cheaper [MMD17, DSL19]. Wearables range from smart shoes to smartphones, most of which already have multiple types of sensors inside. The challenge is to make wearables monitoring balance commercially available and guarantee reliable and valid functionality [MWL+16, DSL19].

The *FRAIL* project (*www.frail.eu*) is one example where researchers are developing a compact device for daily use. Led by experts in rehabilitation research at the Technical University of Munich (TUM), they work on a mobile app which processes sensor data obtained by a smartwatch. The app targets the health care market and aims at monitoring daily physical activity and detecting frailty among the users. An evaluation of the system is due to be presented this year.

This example, however, focused solely on the detection of falls by means of a single sensor at the wrist. If researchers want to get more insights into body motions and balance, they need more sophisticated systems. According to a systematic review conducted by Ma et al., researchers most commonly use inertial measurement units and plantar pressure sensors to investigate body motions and evaluate balance stability [MWL+16]. The sensors differ in the way they are attached to the human body and the parameters they measure.

An Inertial Measurement Unit (IMU) consists in its basic configuration of a tri-axial accelerometer and a tri-axial gyroscope [SK08, pp.483-484]. This allows it to sense changes on six axes in a single integrated circle, based on microelectromechanical systems (MEMS). As such, it can detect an object's position (X,Y,Z) and orientation (pitch,roll,yaw). State-of-the-art IMUs also incorporate magnetometers [MWL+16]. The basic structure of an IMU is similar among different manufacturers (cf. Figure 1.4); the primary differences lie in the software and algorithms used to analyze and interpret the data [DSL19].

The IMU's accelerometer detects the acceleration of a rigid object in a three-
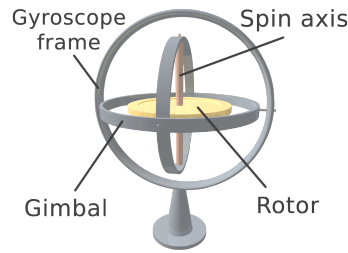
Figure 1.5: Basic structure of a gyroscope [Vie06]

dimensional space. It measures the acceleration in each of the three axes, X,Y and Z. A single signal is then calculated by combining the output in each direction. The IMU can obtain the direction of the object's linear movement by detecting changes in the magnitude of the gravitational acceleration [MWL+16]. However, an accelerometer cannot distinguish the differences between the acceleration resulting from motion and the acceleration due to gravitational forces. The gravitational forces can be subtracted from the measured acceleration, because the Earth's gravitation is known, but any residual vector results in a quadratic error in position [SK08, p. 484].

Gyroscopes measure the rotation of an object in a three dimensional space, i.e. the pitch, roll and yaw angle. They embrace a spinning disc in which the axis of rotation is free to take any orientation (cf. Figure 1.5). Thus, they are independent of the object's position and orientation, they are attached to. The principle behind a gyroscope is based on the Coriolis effect, which states that a mass moving with a defined velocity experiences a defined force and conserves its angular momentum [SK08, pp. 479-81]. This allows the gyroscope to detect movements more accurately than an accelerometer in a short period of time [MWL+16]. On the other hand, errors in the gyroscope's measures accumulate over time due to the integration of the angular rate resulting in a growing drift [SK08, p. 482]. These errors need to be corrected by an alternative reference measurement, often using the accelerometer's output [MWL+16].

Over a long period of time all IMUs eventually drift and external reference systems are beneficial. Magnetometers are non-inertial sensors and provide information about the absolute orientation relative to the Earth's magnetic field [MWL+16]. They help to capture the body's motion more accurately and correct for the errors of the gyroscope and accelerometer.

IMUs are attached to different body segments; the lumbar area, as an approximation of the CoM's position, is the most common location to mount a single IMU [DSL19]. Additional locations for gait and balance analysis are the sternum, thigh and shank [ALHPI+18]. The output of a single IMU unit can be used to determine the orientation and position of the respective segment. By combining several IMUs and implementing a biomechanical model, the CoM's position can be estimated

[KBS$^+$16]. There are different approaches for CoM estimation and motion capture, which we will explain in more detail in Chapter 2. A high frequency and variability in the CoM's trajectory indicate balance instabilities [AOL$^+$15, BFC$^+$20, NMAP$^+$12]. The other group of sensors are plantar pressure sensors (PPS) placed beneath the feet. They measure the pressure distribution on the plantar surface. Depending on the number of sensor units and their position, they can measure the GRF in one to three dimensions [MWL$^+$16]. The trajectory of the CoP is a common metric to evaluate postural stability. Great displacement and high variability in the CoP's position indicate balance disturbances [KSGH13, MWL$^+$16]. Force plates are regarded as the gold standard for the measurement of the GRF and CoP in several studies [ALHPI$^+$18, DSL19, PSCB20]. Because they are not suitable for investigating daily activities, pressure insoles appeared as a more compact alternative. These are insoles with embedded force sensors, which can easily be worn in shoes. They have shown to reliably measure the CoP's trajectory [CCD$^+$15, KSGH13, MWW$^+$15].

Physiologists and sport scientists have used both sensor systems to track the CoM's or CoP's trajectory in static and dynamic balance as well as gait analysis [DSL19, KSGH13, LPJ$^+$18]. They could diagnose balance impairments in patients by quantifying the postural sway.

Researchers have also used these systems to detect postural transitions. In one approach, Hickey et al. implemented wavelets to discriminate different postures and postural transitions [HGM$^+$16]. A wavelet transform decomposes a signal into several components and thus recognizes certain patterns in the sensor data. The study's results show that a wavelet transform with a 1st to 5th order scale detects sit-to-stand transitions with an accuracy between 87% and 97%. Data was recorded by a single IMU attached to the lower back (L5). Alternatively to a wavelet, a neural network-based classifier algorithm can learn data patterns recorded by a smartphone's IMU [CBG$^+$19]. The algorithm developed by Chandrasekaran et al. achieved an error rate of 1.47% and accuracy of 97% in the classification of activity and postural transition [CBG$^+$19].

Moufawad el Achkar et al. offer another approach comparing an IMU sensor and pressure insoles [ALHPI$^+$18]. They defined thresholds which, when exceeded, indicate a postural transition. For the single IMU attached to the trunk, a negative peak in the trunk's tilt angle implies a transition from sitting to standing (cf. Figure 1.6b). This corresponds to a forward inclination of the trunk. For the force plate and insoles, a transition is indicated by a sudden increase in vertical force (cf. Figure 1.6a & c) because the weight on the insoles increases in a standing position. In addition to predicting the event of a transition, the transition duration was estimated as well. The force plate functioned as the reference system. The IMU overestimated the transition duration for sit-to-stand by up to 31.9% whereas the insoles showed errors of less than 20% [ALHPI$^+$18]. The authors have argued that the IMU-based estimation is less accurate compared to the insoles-based one because the IMU might be prone to the detection of false positives due to frequent trunk tilt movements. Their statement is based on findings that the IMU sensor
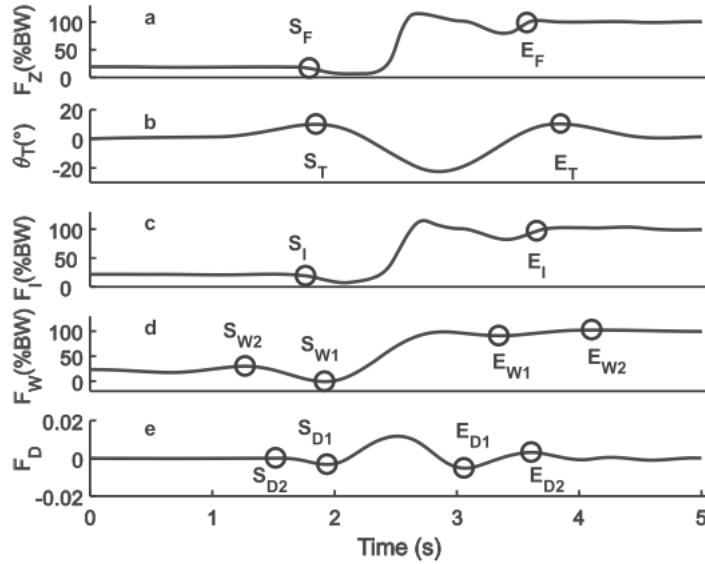
Figure 1.6: Thresholds in the output signal indicating a postural transition; a=force plate, b=IMU (trunk angle), c=pressure insoles, d-e=pressure insoles (wavelet transform) [ALHPI+18]

classified unsuccessful transitions as actual transitions while the pressure insoles did not.

Scientists are still in dissent which sensor location is most appropriate to detect postural transitions or balance instability [DSL19]. They have reported a variety of locations, but the lower back and sternum are the most common positions. Just recently, Atrsaei et al. investigated exactly this issue and compared the accuracy in the detection of postural transitions between different sensor locations [ADH+20]. In detail, they contrasted the performance of sensors attached to the sternum, lower back (L5), anterior superior iliac spine (SIAS) and clipped to the belt. An algorithm detected postural transitions by identifying peak vertical accelerations. It reached a classification accuracy of 98% in healthy participants and 89% in patients with severe neurological diseases and a sensitivity of 95% and 89%, respectively [ADH+20]. Estimation was best for the sensor attached to the lower back (L5). The sensor mounted on the sternum measured higher accelerations because of the greater angular momentum. This negatively influences the accuracy to detect postural transitions. The lower back's sensor most accurately estimated the tilt angle of the trunk with a relative absolute error of 5.6%.

1.3.2 Biofeedback Systems

Furthermore, researchers have coupled IMU-based and PPS-based systems with biofeedback systems. They have discovered that biofeedback can provide supple-
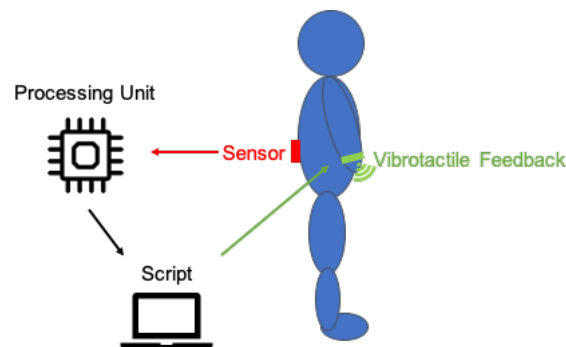
Figure 1.7: Visualization of signal transmission and processing from sensor to biofeedback

mentary information about the patient's balance condition and improve postural control [DSL19, MWL+16]. In a review, Ma et al. compared different studies regarding their effect of feedback systems [MWL+16]. They came to the conclusion that IMU-based feedback can lead to significant reductions of postural sway in static balance [AS10, NMAP+12, WWSK01] while PPS-based feedback is more effective in dynamic balance [AOL+15, CCD+15, MWW+15]. However, the latter shows reductions in the CoP's sway in static standing as well [MWW+15].

Most studies have either investigated static or dynamic balance, the latter primarily being gait patterns [AOL+15, CCD+15, MWL+16]. One study in 2012 assessed both conditions, but tests regarding static and dynamic balance were carried out in different tasks [NMAP+12]. In this particular study, patients with Parkinson's disease carried out a total of twelve tasks; six tasks assessed static balance and the other six dynamic balance. The subjects were divided into two groups, of which one group received a biofeedback during balance training. Results showed that roll sway and pitch sway angular velocity were significantly reduced in the group receiving feedback. The authors have suggested that biofeedback is more beneficial than conventional training in improving balance stability in patients with Parkinson's disease in both static and dynamic balance tasks.

The definition of criteria, which indicate balance instability and the moment to give feedback, is crucial for the implementation of biofeedback. Figure 1.7 illustrates the basic structure of the signal transmission from the sensor unit to the biofeedback system. The sensor unit detects the balance parameter and triggers a signal forwarded to a processing unit [BFC+20]. The processing unit provides the signal for the feedback system which is in the end transmitted to the patient.

In case of a single IMU attached to the trunk, researchers have often defined a certain inclination of the torso as the biofeedback's threshold [KFG+18, NMAP+12]. When postural sway increases and the torso exceeds the defined threshold, biofeedback is applied. Alternatively, the signal intensity is coupled with the CoM's kinematics and feedback intensity increases with a growing postural sway [BFC+20]. The problem

remaining is how to determine this particular threshold. By now, it is either defined beforehand [KFG+18] or based on baseline measures [NMAP+12]. Nanhoe-Mahabier et al. defined thresholds for each subject and task separately during pre-training assessment [NMAP+12]. Activation thresholds were set to 40% of a 90% range in peak-to-peak pitch and roll angular velocity measured by a sensor mounted on the trunk's back. Lee et al. determined the participant's LoS and set the thresholds to 90% of the measured LoS in each direction [LFT18]. These thresholds triggered a vibrotactile biofeedback in a weight-shifting balance exercise.

Similarly, thresholds are defined for the parameters measured by PPS. Ma et al. suggest a threshold of 110% of the average pressure amplitude recorded during baseline readings where the subjects stand still with closed-eyes for 90s in three repeated trials [MWW+15]. In another study, Vuillerme et al. set the threshold to one standard deviation (SD) of the CoP's displacement during a baseline recording for 10s [VCDP06]. This was done for the anterior-posterior and medio-lateral direction separately. In the end, they defined a so called "dead zone". Once the CoP had shifted outside this zone, a feedback signal was given.

1.4 Problem Statement

Physiologists and sport scientists have used IMU-based and PPS-based biofeedback systems to assess and improve a patient's balance in both static and dynamic conditions. However, while researchers have extensively studied these situations separately, they have yet to investigate how to apply biofeedback in situations of postural transition between states. Tasks regarding static and dynamic balance were always carried out separately and the transition between postures was not considered in the assessment [NMAP+12]. Moufawad el Achkar et al. suggest that a single threshold for the angle of a person's torso is an insufficient measure and prone to the detection of unintended movements in an IMU-based feedback system where a single unit is attached to the lower back [ALHPI+18]. During the transition from one posture to another, the patient could receive feedback even though the posture itself is stable (cf. Figure 1.8). The torso shifts because of the postural transition, and the inclination is detected by the IMU and leads to an unintended trigger signal. At the same time, the reference system indicates that the CoP is still inside the LoS and threshold area. This discrepancy between both systems' outputs is referred to as *misclassification*. A PPS-based system might be better suited for balance assessment in transition phases because it can more accurately distinguish between transitions and static states [ALHPI+18]. Another possible advantage of the PPS-based system is its focus on the CoP, which is less dependent on body parameters and more accurate in its calculation as described before. This work explores whether for these reasons or others a PPS-system might be more reliable.

As discussed, researchers still disagree about the IMU's optimal sensor location. There is no clear evidence which location is the best to extract balance parameters
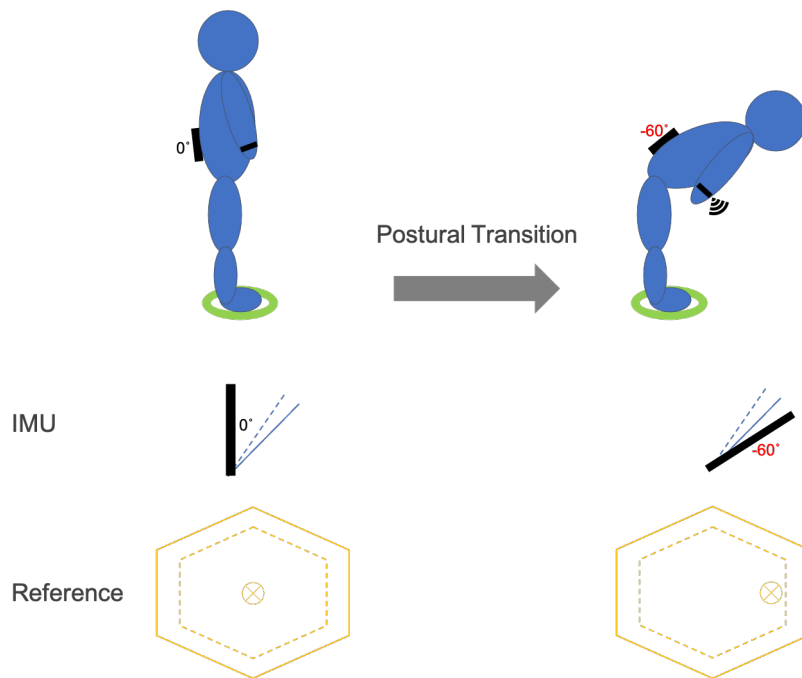
Figure 1.8: Visualization of the problem; solid line = LoS, dashed line = system threshold, $\bigotimes$ = CoP

[DSL19]. Even though a person's back or sternum are the most common locations for a single IMU, misclassification errors can occur [ALHPI+18]. A recent study suggests that placement on the lower back (L5) best helps a single IMU to detect postural transitions and estimate the trunk's inclination [ADH+20]. In another study, an IMU placed on the front of the subject's thighs worked as a reference for the detection of sit-to-stand postural transitions [ALHPI+18]. But researchers have yet to couple these investigations with questions about what works best for an IMU-based feedback system. The approach to use several IMUs on multiple body segments is intensive in processing power and energy consumption. Furthermore, it might influence the patient's motion and his acceptance of a biofeedback system [DSL19].

1.5 Aim of This Work

This work investigates whether (I) an IMU-system threshold, (II) a PPS-system threshold or (III) a combined threshold based on both systems is most reliable in triggering a biofeedback; reliability is defined as the temporal and spatial accuracy of the trigger signal [AS10]. Furthermore, we compare the performance within each system of a threshold based on the baseline postural sway (BL-threshold) during quiet standing to a threshold based on the LoS measurements (LoS-threshold). The second question is, which sensor locations and in the end how many sensors

are necessary in providing valid information for the IMU-system's thresholds. For this purpose we will attach multiple IMUs to defined body locations and evaluate whether they contribute to an accurate threshold.

The system should trigger feedback only when the participant's CoM or CoP exceeds the defined threshold and puts him in a position of balance instability. We compare the moment the feedback is triggered and the moment the feedback was supposed to be triggered. This is the point when the subject looses his balance, hereafter referred to as 'tipping point'. The tipping point is determined by a force plate as the gold standard for GRF-measurements. The BL-threshold is based on the CoP/ CoM trajectory's variance during quiet standing. This metric is commonly used to evaluate postural sway as described before. The LoS-threshold, on the other hand, requires LoS measurements. We will describe the exact procedure in the next chapter.

Previous findings suggest that a biofeedback system with a threshold based on PPS is more reliable than one based on multiple IMUs. Time lags for feedback are shorter in the PPS-system. Furthermore, we expect the combined threshold will be more reliable than for either single threshold and the time discrepancy will be shorter.

H_1: The PPS-system threshold is more reliable than the multiple IMU-system threshold ($\Delta t_{2,4} < \Delta t_{1,4}$)

H_2: The combined system threshold is more reliable than the threshold of each system alone ($\Delta t_{3,4} < \Delta t_{1,4}$ && $\Delta t_{3,4} < \Delta t_{2,4}$)

H_3: The LoS-threshold is more reliable than the BL-threshold within all systems. ($\Delta t_{LoSth} < \Delta t_{BLth}$)

Hypothesis H_1 states that the time discrepancy Δt between the point the PPS-system threshold is exceeded and the tipping point is significantly shorter than Δt between the point the multiple IMU-system threshold being exceeded and the tipping point. Hypothesis H_2 states that Δt between the point the combined threshold is exceeded and the tipping point is significantly shorter than Δt of each single system. Figure 1.9 illustrates the hypotheses in more detail. Hypothesis H_3 states that the time discrepancy between the point the LoS-threshold of all systems is exceeded and the tipping point is significantly shorter than between the BL-threshold and the tipping point.
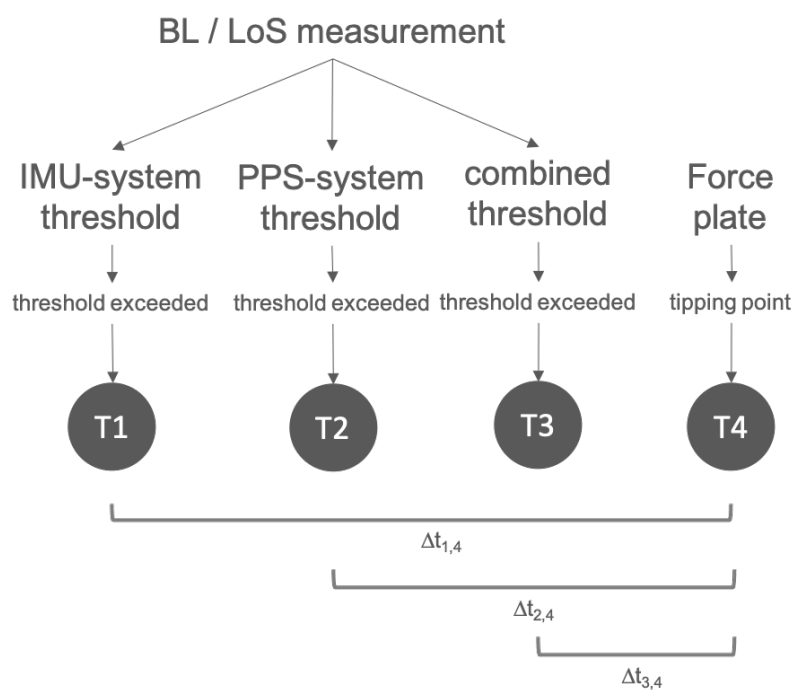
Figure 1.9: Visualization of the time discrepancy Δt between the different approaches; T = numeration of conditions

Chapter 2

Methodology

2.1 Inclusion Criteria

Participants were eligible to participate in this study if they were able to stand upright for up to three minutes without any physical support. To ensure a homogeneous sample, we limited the age range to 18 - 35 years. Because of the equipment's dimensions, body height was restricted to 1.50 - 1.95m and the shoe size to EU 37 - 45. Participants were not able to participate if they had any medical history of vestibular or other neurological diseases, which could influence their balance control. Furthermore, they could not participate if they feel pain while standing for up to three minutes. We checked theses conditions in a questionnaire and by asking the participant before the measurements.

2.2 CoM, CoP and LoS

2.2.1 Estimation of CoM

Calculation of the CoM based on the IMU-system's data

How to precisely estimate the body CoM's position has been the focus of research for years. Still, there is no standard method and most approaches are based on assumptions of the human body's biomechanics. Scientists have established different approaches to estimate the CoM of the whole body and track its trajectory during dynamic motions.

Sensor fusion is one approach to connect the output of multiple IMUs attached to the different body segments. At first, the orientation of each IMU or segment, respectively, is calculated using quaternion rotation [CGD+18]. In the second step, the orientation of the whole body is estimated by means of an Extended Kalman Filter based on a defined mathematical kinematic model. This method is limited to the estimation of the relative body position and orientation of the body segments to each other. It cannot estimate the CoM's absolute position in space.

De Leva [Lev96] segment classification	Xsens MVN equivalent	*mass* (%)		CoM_Z (%)	
		male	female	male	female
head	*head + trunk*	*6.94*	*6.66*	*50.02*	*48.41*
upper trunk	*T8 + T12 + shoulders*	*15.96*	*15.45*	*50.66*	*50.50*
middle trunk	*L5 + L3*	*16.33*	*14.65*	*45.02*	*45.12*
pelvis	*pelvis*	*11.17*	*12.47*	*61.15*	*49.20*
upper arm	*upper arm*	*2.71*	*2.55*	*57.72*	*57.54*
forearm	*forearm*	*1.62*	*1.38*	*45.74*	*45.59*
hand	*hand*	*0.61*	*0.56*	*36.24*	*34.27*
upper leg	*upper leg*	*14.16*	*14.78*	*40.95*	*36.12*
lower leg	*lower leg*	*4.33*	*4.81*	*43.95*	*43.52*
foot	*foot*	*1.37*	*1.29*	*44.15*	*40.14*

Table 2.1: Segment parameters; $mass$ = segment mass relative to body weight; CoM_Z = segment CoM position relative to segment length; data adopted from [HAMJ+20]

Researchers, however, more commonly use biomechanical models of the human body to reliably estimate the body CoM's absolute position in space. These models assume that the whole body is composed of a chain of rigid body segments connected by joints with a defined number of DoF [WHCR14, p. 63-64]. The difficult step is to obtain each segment's properties, namely the mass and center of mass. In 1990, Zatsiorsky and Seluyanov measured the relative segment mass and center of mass for a sample of 115 subjects (male & female); these were later adjusted by De Leva to match the commonly used bone landmarks and joint centers [Lev96]. The parameters are scaled to the specific subject's segment dimensions and body weight. The body CoM can then be calculated by weighting each segment's CoM [WHCR14, p. 69-70]. In this work, we followed the approach proposed by Hedegaard et al. regarding the segment classification and calculated the CoM's position as described in Robertson et al. [HAMJ+20, WHCR14].
The IMU-system used was the *Xsens MVN Link* together with the corresponding *MVN Studio (v3.4.0)* software (*Xsens Technologies B.V., Netherlands,* `www.xsens.com`); an established system employed in several studies before [KBS+16, HAMJ+20, PSCB20]. It was validated against estimations by Optical Motion Capturing (OMC). Errors (rRMSE) were less than 13% in vertical, anterior and sagittal direction and less than 30% in lateral, frontal and traverse direction [KBS+16]. The system consists of 17 IMUs attached to the body, as shown in Figure 2.1, and divides the body into 23 segments. We reduced these to 16 segments to calculate the body CoM's position, following Hedegaard et al. in order to match the classification by De Leva (1996) as shown in Table 2.1 [HAMJ+20, Lev96] .
The software outputs the position of each segment's proximal endpoint (origin) over time (cf. Figure 2.2). Because the human body is a continuous chain of
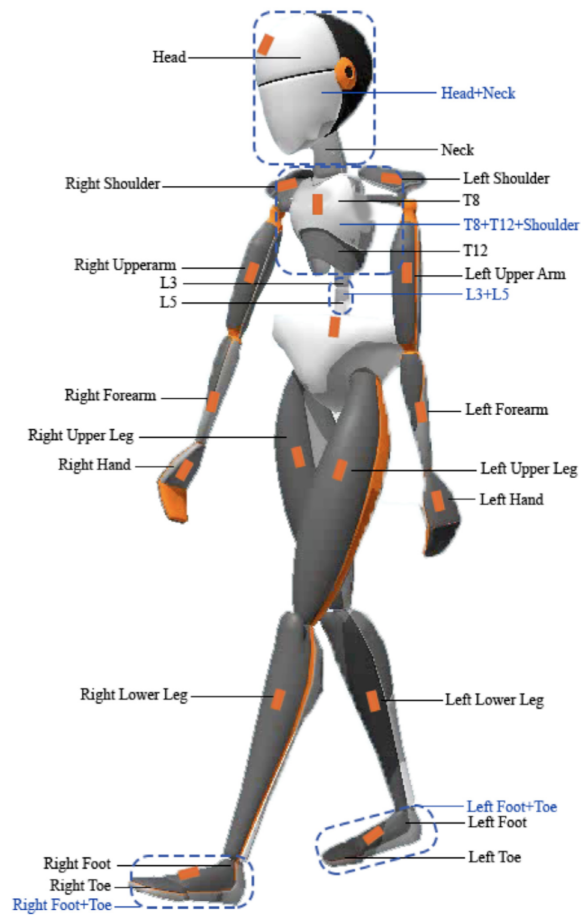
Figure 2.1: Placement of Xsens sensors (orange boxes) and segment classification; combined segments (blue squares) according to De Leva [HAMJ+20]
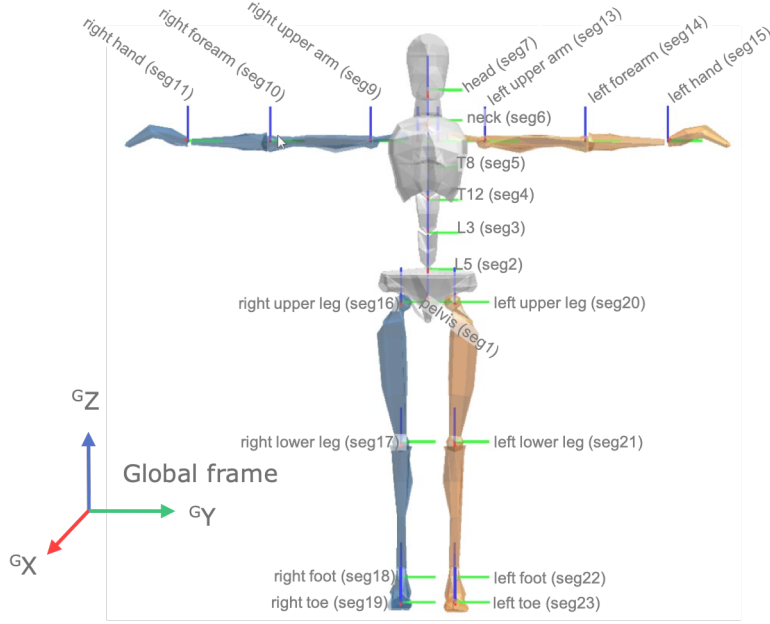
Figure 2.2: Segment origins (proximal endpoints) as defined in *Xsens MVN Studio* (graphic from *Xsens* user manual and modified by author)

connected segments, the distal endpoint of one segment is the proximal endpoint of the following segment. We had to manually measure the distal endpoints only for the head and hands as the chain's ends. We used the position of the metatarsals, which are outputted by *MVN Studio*, as the distal endpoint of the feet, neglecting the toes' length.

The segment CoM's position is calculated by Equation 2.1 adopted from Robertson et al. [WHCR14, p. 69-70].

$$p_{CoM;s} = p_{prox} + CoM_{Z;s} \left(p_{dist} - p_{prox} \right) \tag{2.1}$$

$p_{CoM;s}$ is the segment CoM's position, p_{prox} and p_{dist} are the segment's proximal and distal endpoints, and $CoM_{Z;s}$ is the proportion factor of the CoM's position (cf. Table 2.1). The body CoM's position is calculated by the weighted sum of each segment CoM with the corresponding segment's mass according to Equation 2.2.

$$p_{bCoM} = \sum_{s=1}^{s} m_s \, p_{CoM;s} \tag{2.2}$$

Here, p_{bCoM} is the body CoM's position and m_s is the mass proportion of each segment as shown in Table 2.1. Calculations were carried out in *Matlab (v2020a)*. Unfortunately, the software did not allow us to access each sensor's output independently and thus we were not able to investigate each sensor's contribution to the CoM trajectory's calculation. We did though reduce the original 23 segments to

three segments (upper body, left leg & right leg) by combining the respective segments' positions during the segment CoM calculations. The resulting CoM based on the reduced segmentation is hereafter referred to as 'CoMred' and compared to the previous approach.

For details regarding the exact calculations refer to Figure A.7 and the scripts on the enclosed data drive.

Set up and calibration of IMU-system

The 17 single IMUs are attached to the body via Velcro straps and via a headband and gloves at the head and hand according to the specifications in the *Xsens* user manual. This allows for the flexible adjustment to each participant's body dimensions. The IMUs are then connected with each other via cables in a defined sequence and to the computer's *MVN Studio* software via USB. There is also a possibility for a wireless transmission but we decided for the wired alternative to reduce any disturbance caused by surrounding wireless devices such as the WLAN insoles.

In order for the IMU-system to accurately match each sensor unit to the corresponding body segment and to determine the sensors' positions to each other, we needed to calibrate the system beforehand. This was done in a stepwise process in the *MVN studio* software and was carried out before each measurement trial. At first, the participant stood quietly in the N-pose for six seconds, followed by the T-pose for another six seconds. The software indicates the calibration's quality and the calibration process was repeated until the calibration showed the best result ('Good'). At last, the IMU-system's coordinate system was rotated so that the x-axis points into the direction of the participant's feet.

2.2.2 Estimation of CoP

Set up and CoP calculation of force plate

The force plate (FP) used in this study is an *AMTI HPS-SC* strain-gauge plate (*AMTI, USA*, `www.amti.biz`) with the corresponding *AMTI Gen 5* signal conditioner. It outputs the forces and moments along the system's coordinate system as shown in Figure 2.3. According to the manufacturer, the force plate can measure forces between 0N and 9,000N with an accuracy of 0.1% of the applied load.

The force plate was operated with a written C-script. In the beginning of each trial and before the subject stepped onto the plate, it was initialized and zeroed.

We calculated the force plate's CoP based on the output forces and moments using the equations 2.3 derived from Robertson et al. [WHCR14, p.95-96]. Because Robertson et al. used a different coordinate system, the force plate's output was adjusted to the different coordinate system (cf. Figure 2.4).

$$CoP_x = -(M_y + F_x \cdot FPz)/F_z$$
$$CoP_y = (M_x - F_y \cdot FPz)/F_z$$
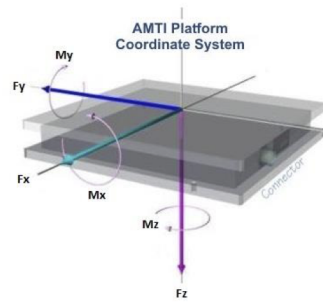
$$(2.3)$$

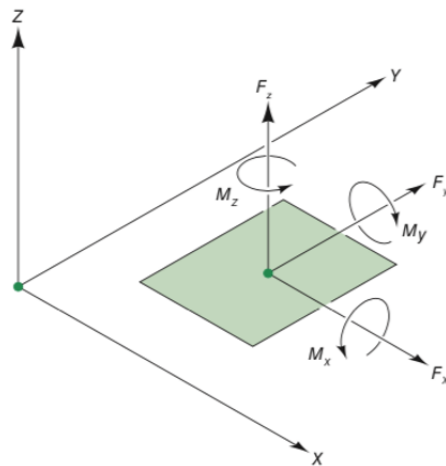Figure 2.3: Coordinate system of force plate according to *AMTI* user manual

Figure 2.4: Coordinate system according to Robertson et al. [WHCR14, p.95-96]
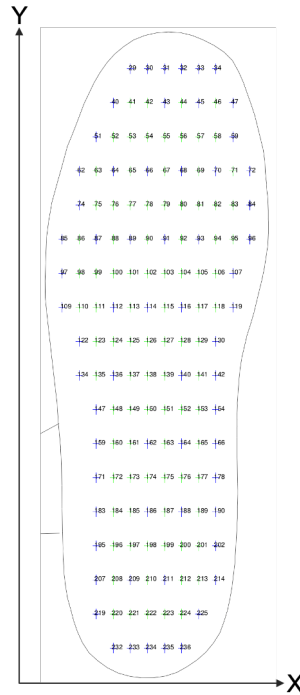
Figure 2.5: Sensor placement in an insole of size 45 (graphic adopted from *medilogic* user manual)

CoP_x and CoP_y refer to the CoP's x- and y-coordinates, F_x, F_y, F_z, M_x and M_y are the output forces and moments, respectively. FPz is an offset value indicating the vertical distance between the force plate's coordinate system and the plates surface. This value is provided by the manufacturer in the calibration certificate.

Data acquisition was done in *Visual Studio Code (v2019)*, calculations were carried out in *Matlab (v2020a)*.

Set up and CoP calculation of insoles

We used two *medilogic* WLAN pressure insoles (*T&T medilogic Medizintechnik GmbH, Germany*), which employ up to 240 SSR sensors depending on the insole's size and shape. Each sensor unit can measure a pressure between 0.6 to 64 N/m² with an accuracy of 5% FSO. The manufacturer provides a detailed description and graphic of each sensor's position in the insole (cf. Figure 2.5). For more details refer to the information on the enclosed data drive.

The insoles were operated with the manufacturer's software. Each sensor's force was recorded over time and exported to a *csv* file afterwards. Based on this output and the provided specifications we calculated the insole's CoP based on the equations 2.4 derived from Crea et al. [CDR+14].

$$vGRF = \sum_{s=1}^{s} F_s$$

$$CoP_x = \sum_{s=1}^{s} F_s \cdot x_s / vGRF \qquad (2.4)$$

$$CoP_y = \sum_{s=1}^{s} F_s \cdot y_s / vGRF$$

F_s is the force measured by a single sensor and $vGRF$ the sum of forces by all sensors, so the vertical GRF. CoP_x and CoP_y refer to the CoP's x- and y-coordinates, x_s and y_s are each sensors location in the insole. Calculations were done in *Matlab (v2020a)*.
The PPS-system is hereafter referred to as IS-system and the PPS-system thresholds as the IS-system thresholds because the insoles are a specific system in the family of PPS-systems.

2.2.3   Synchronization of systems

All systems recorded the data with a frequency of 100Hz, corresponding to one log every 10ms. To synchronize the time points between all systems, the *Xsens MVN studio* software triggered the force plate's C-script and *medilogic* software.
The systems and software differ in their coordinate systems. In order to compare the measurements, we adjusted the coordinate systems to a standard one. Figure 2.6 shows each system's and the standard coordinate system. Furthermore, we standardized the CoM/CoP's unit to millimeters across all systems.

2.2.4   Assessment of LoS

In the introduction we described the Limits of Stability (LoS) and ways to assess them. We used the four-way-leaning test, asking the subject to lean in anterior, left, right and posterior direction separately with a short stop between each direction. This follows the procedure reported by Thomson et al. [TSL+17]. The measurement was repeated over three trials to assess reliable limits.
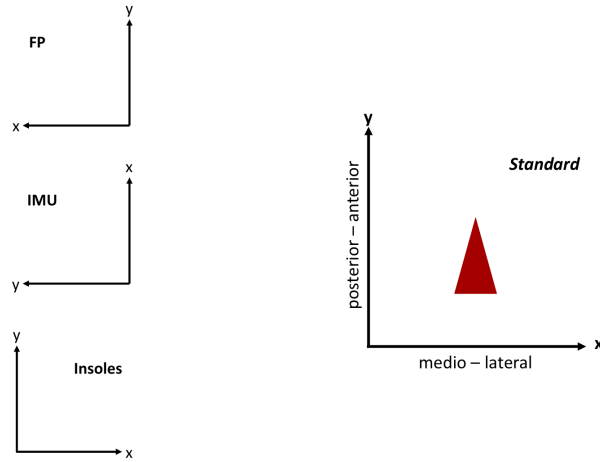
Figure 2.6: Coordinate systems of different systems and standardized coordinate system; red triangle indicates position of subject

2.3   Thresholds

Thresholds were calculated for each system separately, because each system showed different results in the measurements and to compare the systems' performances. The combined threshold is a combination of both the IMU-system and IS-system threshold. For the combined threshold to be exceeded, both thresholds need to be exceeded before a feedback would be triggered.

The BL-threshold is based on the baseline measurements' results, namely the variance in the CoP and CoM trajectories. Before calculating the threshold, we eliminated any linear trends in the trajectory over time, which indicate a slight motion during the measurement. We propose that only the high frequent involuntary sway movements are of importance for this threshold (cf Figure 2.7) because these are present in all standing postures.

After elimination, we calculated the trajectory's mean and standard deviation across the entire 45s of the baseline measurement, separately in medio-lateral (x) and anterior-posterior (y). The BL-threshold in anterior, left, right and posterior was then calculated using the following equations 2.5, where $BLth$ is the BL-threshold in each direction, $mean_x$ / $mean_y$ the mean value and SD_x / SD_y the standard deviation in medio-lateral and anterior-posterior, respectively.

$$BLthAnterior = (mean_y + 2 \cdot SD_y)/\sqrt{0.0077}$$
$$BLthLeft = (mean_x - 2 \cdot SD_x)/\sqrt{0.0077}$$
$$BLthRight = (mean_x + 2 \cdot SD_x)/\sqrt{0.0077}$$
$$BLthPosterior = (mean_y - 2 \cdot SD_y)/\sqrt{0.0077}$$

(2.5)

The value of $\sqrt{0.0077}$ was derived from Johannson et al., who found out that the
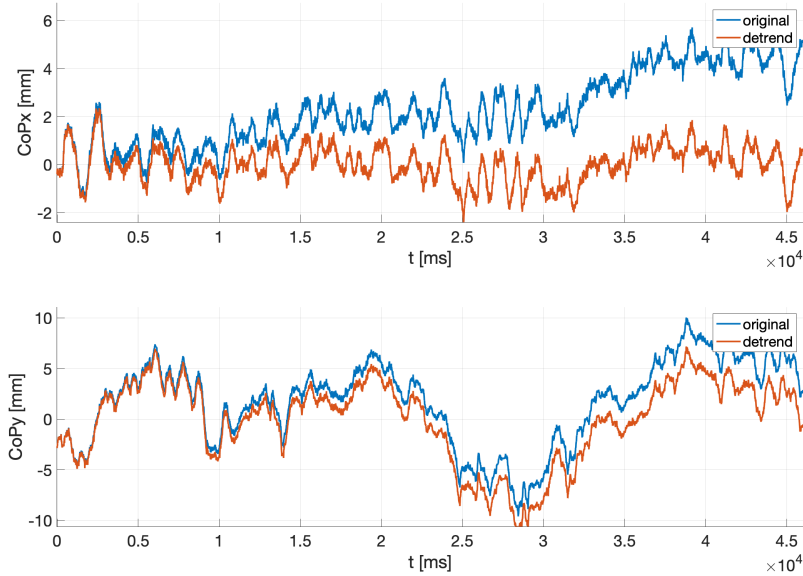
Figure 2.7: Elimination of linear trends in the CoP trajectory during baseline measurement (example FP CoP trajectory of subject 4)

ratio between the postural sway area and LoS area is 0.0077 [JJW+19]. We used two standard deviations to exclude possible extreme values. Based on the threshold values in each direction, we defined an elliptical area connecting these values as the threshold area. We refer to the area simply as 'threshold' even though it is in fact a two-dimensional area rather than a single value.

The LoS are the CoP's and CoM's maximal displacement in each direction. We calculated the average displacement of the three trials in each direction (anterior, left, right, posterior) separately. The LoS-threshold was defined as 90% of these average LoS values in each direction. The percentage value of 90% is the same used by Lee et al. to control a vibrotactile feedback as mentioned in the introduction [LFT18]. Out of practical considerations the threshold should lie before the actual LoS, so that the feedback is triggered before the limits are reached. The values were connected to an elliptical threshold area, too.

Further details regarding the calculations can be found in the scripts on the enclosed data drive.

2.4   Study Design

In the beginning of each experiment the participant filled out a questionnaire containing questions on demographics and regarding medical history and physical activity in daily life, especially sport activities with a focus on balance. This ensured

that the participant meets the requirements and in addition provides information whether the participant might be trained in balance control. We furthermore orally asked for the participant's well-being on the day of the experiment, i.e. if the subject felt any dizziness or pain, factors which might influence the subject's behavior during the measurements. We determined the subject's dominant (standing) leg asking with which foot she or he would kick a ball.

After this introduction phase, we measured the required body dimensions for the *Xsens* IMU-system and insoles to be fitted before attaching the sensor systems. The detailed procedure is described in the *Xsens MVN Studio* manual. We also measured the insoles offset resulting from the continuous pressure applied by the shoes. For this, we asked the subject to lift his feet for 10s and recorded the pressure distribution during this time interval. The measured pressure offset values for each sensor were then later subtracted from the sensors' values.

The experiment consisted of four scenarios with three trials each. The first scenario was a baseline measurement to measure the participant's baseline postural sway in a straight upright position. The second scenario quantified the LoS according to the four-way-leaning test. The third scenario measured the body position during a stable postural transition (sPT). In this scenario the participant kept balance at all times. Here, the thresholds as well as the LoS should not be exceeded. On the other side, we forced the subject in the fourth scenario to get in a state of balance instability. The participant was asked to shift his body until he can no longer keep balance and tips over; in other words an unstable postural transition (uPT). Each scenario was consecutively repeated in three trials. A trial started from the starting position, a position where the participant stands straight and upright (cf. Figure 2.8 - *Scenario 1*). All subjects did the scenarios in the same order starting from the first one.

Baseline postural sway was measured for 45s per trial. Before each trial, the subject stood in the starting position for 10s in which he could shift his position until reaching the most relaxed one. During the baseline measurement the subject remained in this position and was asked to stand as quiet as possible, especially to avoid shifting his weight on one leg. We repeated the baseline measurements three times but in the end only considered two trials of each subject because of occasional failure of the IMU-system.

In one trial of the LoS measurements the participant leaned his body in the four directions as far as that he could hold the end position for three seconds. The order was anterior - left - right - posterior. During the inclination the participant kept his body straight and arms parallel along the side. During the measurements, the subject returned to the starting position and stopped for 10s after each direction as well as rested for 10s before the first direction.

The sPT-scenario was a simple bending forward as far as possible (max 90 degree) from the starting position. This position was held for 3s after which the participant raised up back to the starting position. In the starting position the participant stopped for 10s before bending over again. The participant bent forward for three
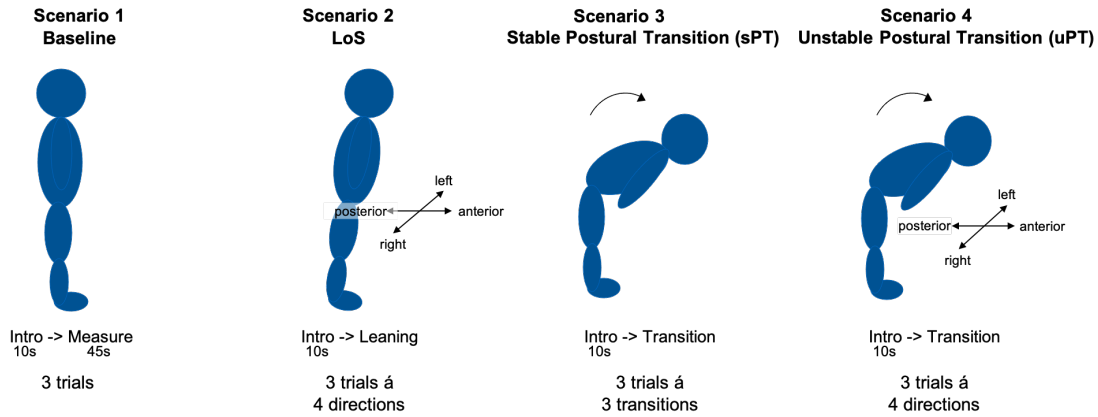
Figure 2.8: Visualization of the experiment's procedure

times and repeated this procedure over the three trials.

In the uPT-scenario the subject bent over once more and in the final position he shifted his body in one of the four directions until he lost balance and tipped over. In one trial this was done for each direction. After tipping over and potentially leaving the force plate the subject returned to the starting position. There, he stopped for 10s before attempting the next transition as well as rested for 10s before the first transition. The order was again anterior - left - right - posterior. The entire procedure is visualized in Figure 2.8.

During all measurements the participant stood on the force plate in a bipedal stance. The position was defined once in the beginning. The subject's feet were a hip-width apart and parallel so that the shoes' tips and heels were on the same height. This position was marked for the participant to return to the exactly same position before each trial. All movements were demonstrated to the participant and he or she tried each movement while the investigator corrected the starting position and transitions visually.

Because the IMU-system is prone to a drift in the sensors' positions we calibrated the IMU-system and force plate before each trial. According to the *Xsens MVN Studio* software we carried out the N-pose and T-pose calibration while the participant was standing on the force plate in the defined feet position.

There is a slight risk of injury for the participant, especially during the uPT-scenario, so the investigator stood next to the participant at any time to provide physical support in case he or she looses balance. A measurement was repeated if the participant carried out the required movements in a wrong way, needed physical support or left the defined feet position. Furthermore, we aborted measurements if any of the sensors became loose.

In order to simplify the following data processing we used a basic 3 Volt trigger to divide each repetition (sPT-scenario) or direction (LoS and uPT-scenario). Furthermore, we set a trigger between the intro (10s resting before) and the actual measure, and at the beginning and end of a measurement. Each trial was itself a separate
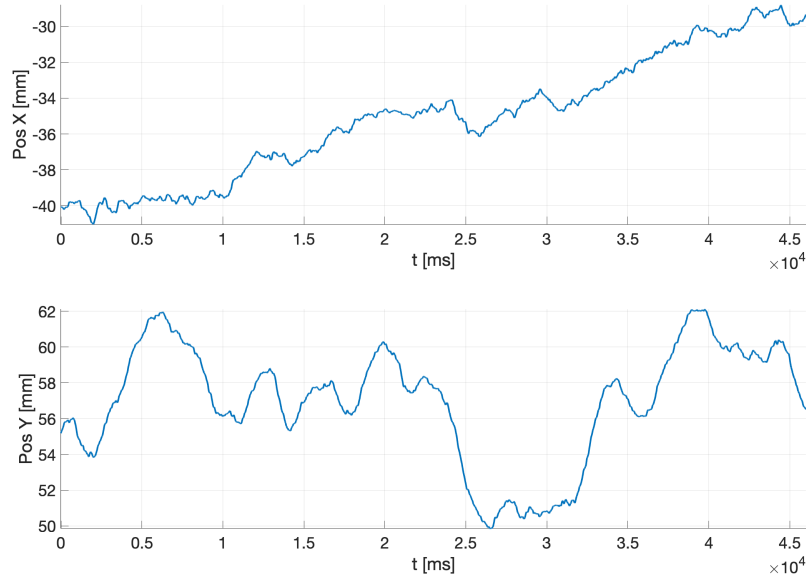
Figure 2.9: Position of segment 1 (pelvis) over time measured by the IMU-system during the BL-scenario (example data of subject 4)

measurement.

2.5 Data Analysis

Data Analysis was carried out in *Matlab (v2020a)*. At first, we cut each system's measurement at the respective triggers. This way, we obtained single datasets for each single transition/ direction of each trial. In the next step, we calculated the CoP/ CoM trajectory according to the formulas described before. Because the subjects obviously never stood in the origin of each system during the starting position, we eliminated this offset using the *Matlab's detrend*-function. This function subtracts offsets and linear trends from time-domain input data, but we kept any linear trends in the data and just subtracted the offset. In the data from the LoS-scenario, sPT-scenario and uPT-scenario, we took the intro interval (10s resting before) to determine the offset. Looking at the BL-scenario's IMU-data, we observed a noticeable drift in positive x-direction (cf. Figure 2.9). We eliminated this sensor drift by applying the FP-data's trend to the IMU-data and adjusted the IMU CoM trajectory in all datasets (cf. Figure 2.10).

Based on the baseline and LoS measurements we determined the BL- and LoS-thresholds for each system according to the approach described before (see Section 2.3). In the end we obtained six different thresholds: FP BL-threshold, FP LoS-threshold, IS BL-threshold, IS LoS-threshold, IMU BL-threshold and IMU LoS-
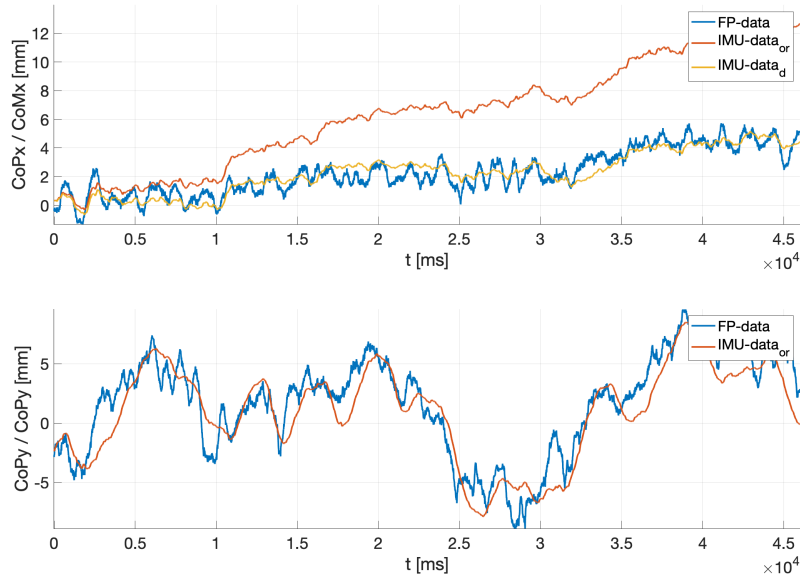
Figure 2.10: IMU CoM trajectory over time before ($IMU-data_{or}$) and after ($IMU-data_d$) the drift correction of CoM_x (example data of subject 4)

threshold.

We applied these thresholds to the data of the sPT- and uPT-scenarios' measurements and evaluated whether and at which time point the thresholds were exceeded. Because we could assume that the thresholds were not exceeded in the sPT-scenario, we looked here at the maximal distance between the CoP/CoM trajectory and the respective threshold's boundary. We calculated the maximal distance for each trial, transition and system separately. We could not calculate this distance for the combined thresholds though, because there is no separate system's threshold but only the combination of the IMU-system and IS-system thresholds. The distance of the FP-data's CoP trajectory and the FP-system thresholds were considered as the reference and we calculated the distance discrepancy Δd between FP-system and IMU-system and between FP-system and IS-system. This sums up to four pairs (2 systems x 2 thresholds) times nine (3 transitions x 3 trials) number of values for each subject.

The evaluation of the uPT-scenario was carried out similarly but as mentioned in the hypotheses, we here looked at the time discrepancy Δt between the point the respective threshold is exceeded and the tipping point (cf. Figure 2.11). The tipping point was defined as 20ms before the point in time when the vertical force F_z measured by the force plate falls below 85% of the average F_z during the intro interval (cf. Figure 2.12). This corresponds to a decrease in the measured force of 15% and indicated that the subject tips over and leaves the force plate. Initially we intended to use a limit value of 105%, an increase in F_z indicating an vertical impulse.
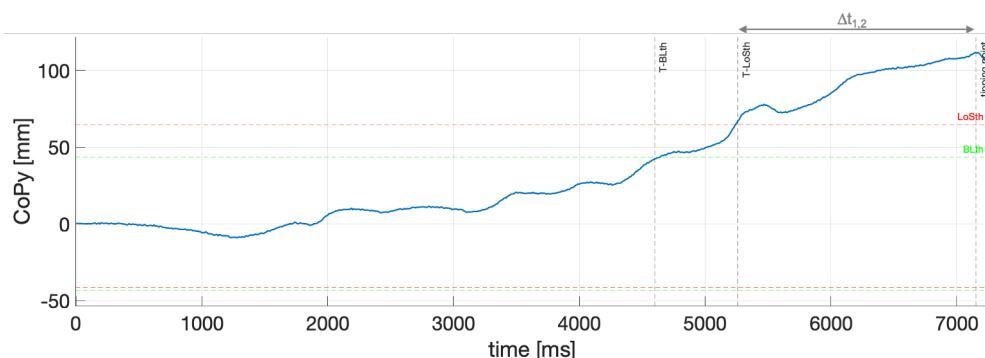
Figure 2.11: Time discrepancy Δt between the point the respective threshold is exceeded and the tipping point; BLth = BL-threshold, LoSth = LoS-threshold, T-BLth = time point when BL-threshold is exceeded, T-LoSth = time point when LoS-threshold is exceeded (example data of subject 5)

But we observed that some subjects did not apply such an impulse but simply tipped over. For standardization we decided on the first approach and subtracted the 20ms to approximately define the correct point. Δt was again calculated for each trial, direction and system separately; this time including the combined threshold, as the point in time when both the IMU-system and IS-system threshold were exceeded. Here we obtained eight pairs (4 systems x 2 thresholds) times three trials number of values for each subject, though the FP-system was only considered for reference and not included in the statistical evaluations. The combined threshold (COMB) is considered as the fourth 'system' in the analysis.
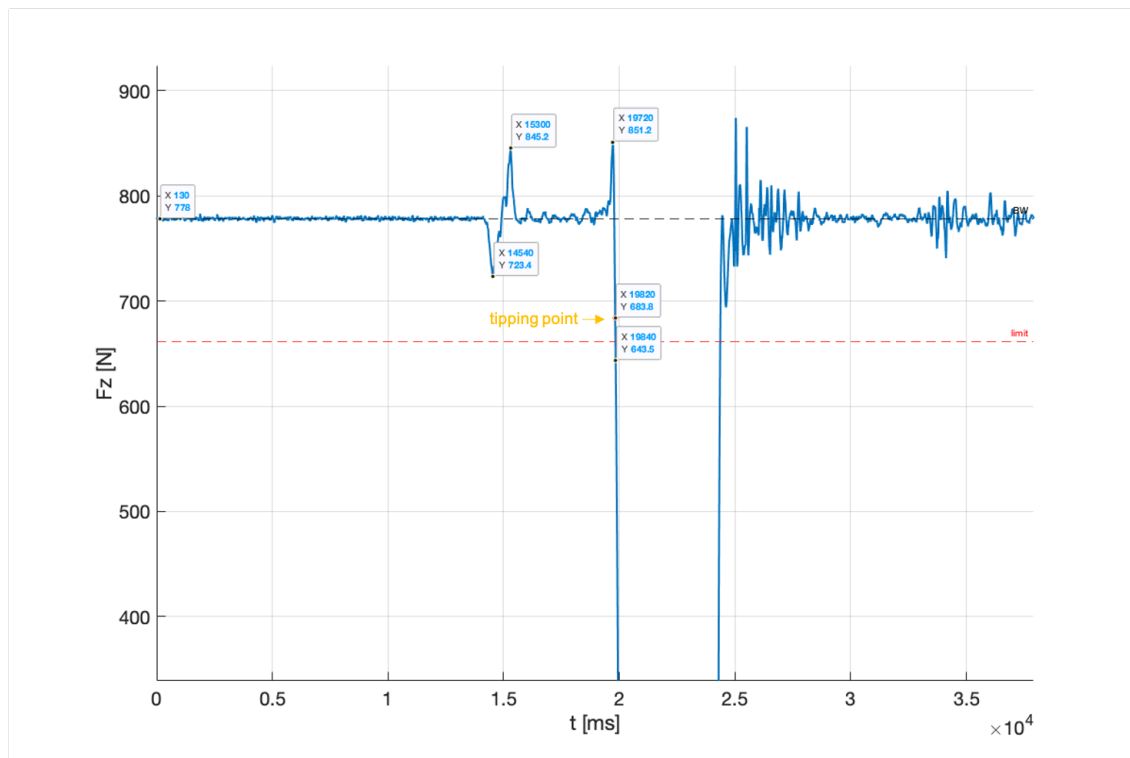
Figure 2.12: Tipping point marked in the FP's F_z curve during the uPT-scenario's measurement; 'limit' = 85% BW, 1. point (from left) = approx. BW (for reference), 2. point = first local minimum (93% BW), 3. point = first local maximum (109% BW), 4. point = local maximum before tipping point (109% BW), 5. point = tipping point (88% BW), 5. point = first time point below limit (83% BW) (example data of subject 8)

2.6   Statistical Analysis

The statistical analysis was done in the *Matlab - Statistics and Machine Learning Toolbox*. The Δd- and Δt- values are average values over the three trials of each subject, in case of the sPT-scenario average values of the three transitions and trials. Thus, we obtained a sample size n equal to the number of subjects tested. Level of significance was set to $\alpha = 0.05$.

The statistical model is slightly different in the sPT-scenario's evaluation compared to the uPT-scenario's one. In the sPT-scenario we have a 2x2 within-subject design: Distance discrepancy Δd is the dependent variable, Factor A comprises the two levels A1 - BL-threshold and A2 - LoS-threshold, and Factor B with the two levels B1 - FPvsIS and B2 - FPvsIMU, resulting into four balanced groups with n samples each. Significance between the mean values of each group was tested by a two-way repeated measure ANOVA. This way, we could evaluate main effects of each factor as well as interactions between the two factors. Using the Tukey-Kramer post-hoc test, we also looked into each factor level combination separately.

The uPT-scenario follows a 2x3 within-subject design: Time discrepancy Δt is the dependent variable, Factor A with two levels A1 - BL-threshold and A2 - LoS-threshold, and Factor B contains three levels B1 - IMU, B2 - IS and B3 - COMB, resulting into six groups with n samples each. We again applied a two-way repeated measure ANOVA and Tukey-Kramer post-hoc test.

We checked for the assumption of normal distribution using the Shapiro-Wilk test and Mauchly's test to check for sphericity. In case normal distribution was violated, the data was transformed with the natural logarithm. If sphericity was not given, we reported the adjusted p-value according to Greenhouse-Geisser.

In order to investigate the difference between the CoM - based on 16 segments - and the CoMred - based on only three segments - we compared the standard deviation during the baseline measurements in medio-lateral and anterior-posterior direction separately. Differences in mean values were statistically tested using a t-Test. The same was done to evaluate differences in the LoS between the two approaches; separately for anterior, left, right and posterior.

In addition to the tests evaluating diversity between metrics, we explored correlations between the BL-threshold and LoS-threshold. We calculated the Pearson correlation coefficients between both thresholds separately for each direction and checked their significance.

Chapter 3

Results

3.1 Participants

We considered the data of 16 subjects (9 female, 7 male, age 25.75 ± 2.62) - out of 21 - in the analysis. The other five subjects had missing datasets or made mistakes in the exercises. The 16 subjects reported an average exercise volume of 5.03 ± 3.52 hours per week. The most frequently stated sports discipline was running followed by climbing and hiking. Seven participants mentioned that they occasionally face situations of balance instabilities during their exercises. 14 subjects stated the left leg as their dominant (standing) leg. The participants were on average 172.94 ± 9.71cm tall and weighted 69.26 ± 11.71kg. For the statistical tests we thus obtained a sample size of $n = 16$.

3.2 BL-scenario

At first, we present two exemplary subjects' data to show the general patterns in the CoP/ CoM trajectories during the BL-scenario's measurements. Figure 3.1 shows subject 5's CoP/ CoM trajectories measured by the three systems, Figure 3.2 these of subject 8.
We see an elliptical shape in the trajectories, especially in the FP CoP trajectory, demonstrating the constant postural sway around the initial position. The general elliptical shape in subject 8's trajectories is similar but we observe, particularly in the IS CoP trajectory, a great shift in the left-posterior direction of around 8 to 16mm. The FP and IS CoP trajectories indicate though that this was a short displacement, after which the participant shifted back, because the trajectory's density is higher around the initial position.
Figure 3.3 shows the CoP/ CoM trajectories over time. Here, we can even more clearly see the differences between the systems. The IMU CoM trajectory shows a smoother development and smaller frequency compared to the pressure-based systems, FP and IS. The IS CoP trajectory's amplitude is smaller compared to the IMU
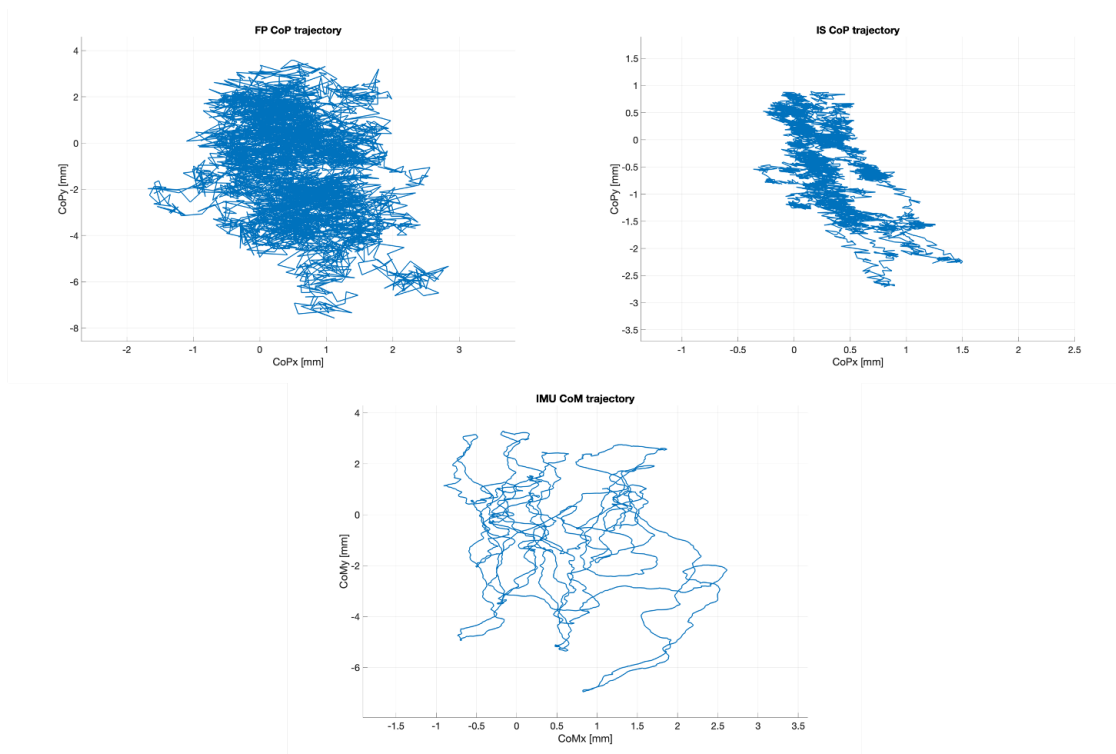
Figure 3.1: CoP/ CoM trajectories during the 45s of one baseline measurement (Subject 5 - Trial 1)
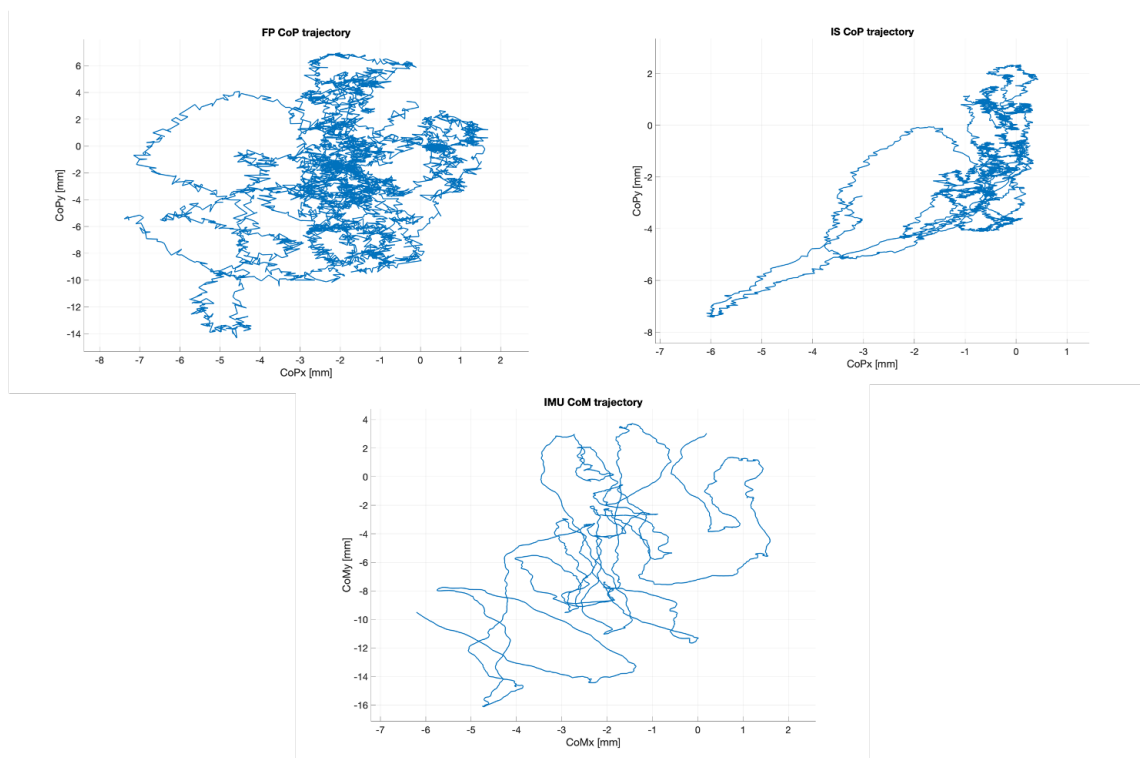
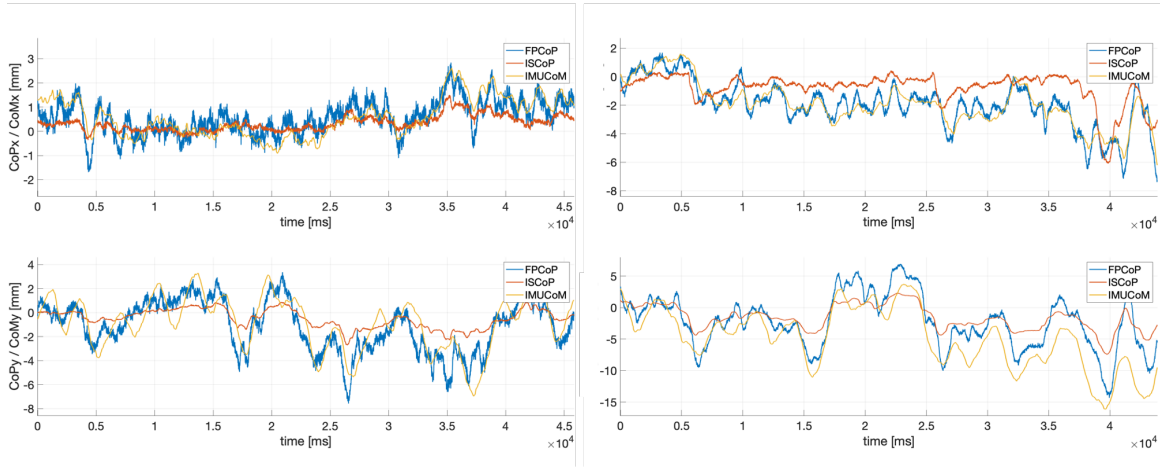Figure 3.2: CoP/ CoM trajectories during the 45s of one baseline measurement (Subject 8 - Trial 1)

Figure 3.3: CoP/ CoM trajectories over time during the 45s of one baseline measurement of subject 5 (left) and subject 8 (right) (Trial 1)

and FP. On the other side, we spot a similar shape in all three plots, indicating that all systems detected the postural sway accurately.

Looking at the right side of Figure 3.3, we realize the increasing amplitude in medio-lateral (x) and anterior-posterior (y) direction. Values of subject 8 diverge more around the mean than these of subject 5. Furthermore, there is a drift into the left-posterior direction in subject 8's trajectories. Both facts indicate that subject 8 staggered more during the BL-scenario than subject 5.

Table 3.1 presents the standard deviation (SD), as a metric of variance, in the data points of both BL-scenario trials separately for each system and direction. Because the IMU-system did not record all three trials of all subjects, we only considered two trials of each subject in the Data Analysis to keep the sample size at $n = 16$. The SDs decreased after applying the *Matlab's detrend*-function in preparation for the BL-threshold's calculation. The values confirm our observation that subject 8 shows a greater postural sway than subject 5 because SDs of subject 8 are higher.

The boxplots in Figure 3.4 and 3.5 show the variance in medio-lateral and anterior-posterior direction measured by each system across all subjects. In both directions the variance in the IS CoP trajectories is significant lower compared to the FP CoP and IMU CoM trajectories, respectively.

The exact differences between the mean values and the results of the statistical test are shown in Table 3.2. Differences in medio-lateral are below 1mm, in anterior-posterior between IS and FP and between IS and IMU around 1.6mm. The difference between FP and IMU amounts to less than 0.02mm.

		Subject 5			Subject 8		
		Trial1	Trial2	Mean	Trial1	Trial2	Mean
BL ml FP SD	or	0.6926	0.5863	0.6394	1.6040	3.0203	2.3121
	d	0.6109	0.5462	0.5785	1.1665	2.6675	1.9170
BL ap FP SD	or	2.1530	2.1053	2.1292	4.2233	6.6632	5.4432
	d	2.0559	1.7472	1.9016	4.0129	6.4620	5.2375
BL ml IS SD	or	0.3168	0.4285	0.3726	1.0982	3.1763	2.1373
	d	0.2538	0.2821	0.2680	1.0004	2.3453	1.6728
BL ap IS SD	or	0.7689	0.6291	0.6990	2.0025	4.2047	3.1036
	d	0.7163	0.5832	0.6498	1.7832	3.9940	2.8886
BL ml IMU SD	or	0.7866	0.5638	0.6752	1.5127	3.2355	2.3741
	d	0.7158	0.5220	0.6189	1.0375	2.9089	1.9732
BL ap IMU SD	or	2.2101	2.1330	2.1715	4.7331	6.7052	5.7192
	d	2.1559	1.7179	1.9369	3.7844	6.2537	5.0191

Table 3.1: SD of CoP/ CoM trajectories during the 45s of baseline measurement of subject 5 and 8; ap = anterior-posterior, ml = medio-lateral, or = original data, d = *detrend*-data; unit: [mm]
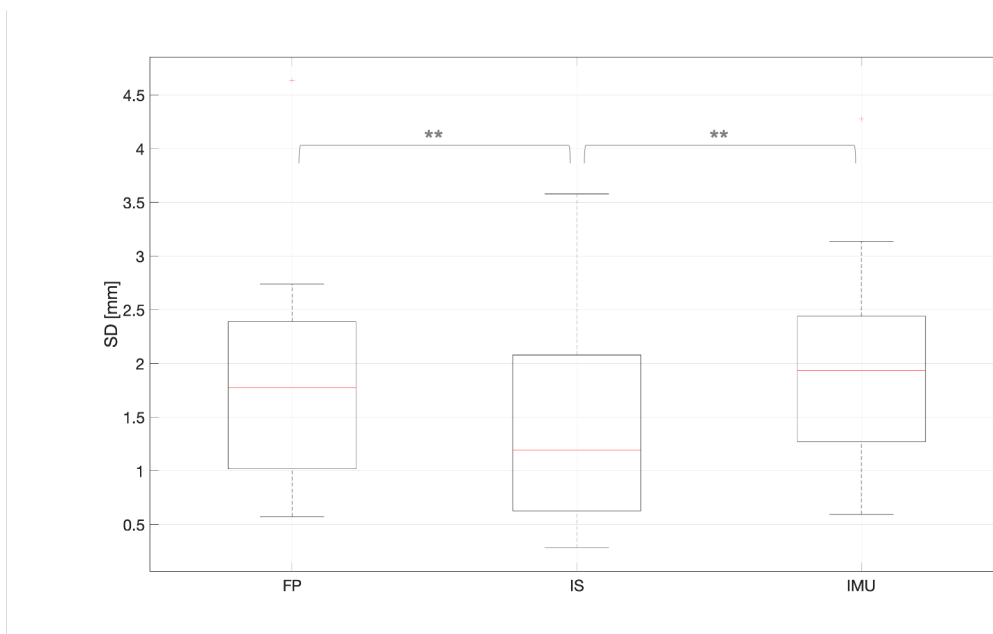
Figure 3.4: Comparison between the CoP/ CoM trajectory's SD in medio-lateral direction of each system across all subjects during baseline measurements; red line = median, whiskers = min/max, * = p<0.05, ** = p<0.01
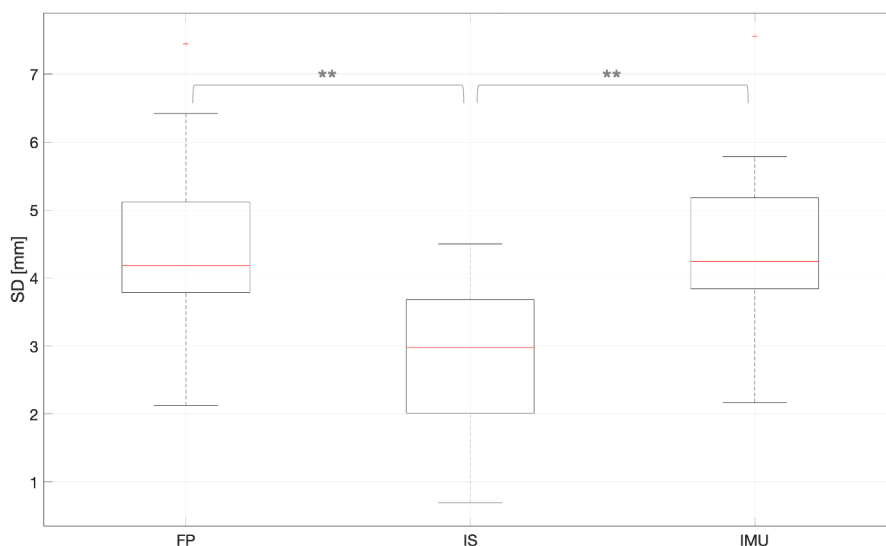
Figure 3.5: Comparison between the CoP/ CoM trajectory's SD in anterior-posterior direction of each system across all subjects during baseline measurements; red line = median, whiskers = min/max, * = p<0.05, ** = p<0.01

	Difference	StdError	p-value
FP ml vs IS ml	0.4922	0.0760	0.0001**
FP ml vs IMU ml	-0.1225	0.0588	0.3448
IS ml vs IMU ml	-0.6146	0.0762	0.0000**
FP ap vs IS ap	1.6337	0.1560	0.0000**
FP ap vs IMU ap	0.0176	0.0992	1.0000
IS ap vs IMU ap	-1.6160	0.1662	0.0000**

Table 3.2: Results of Tukey-Kramer post-hoc test regarding differences in means between SD values of the systems; ap = anterior-posterior, ml = medio-lateral; unit 'Difference': [mm]; * = p<0.05, ** = p<0.01

3.3 LoS-scenario

The LoS measurements served the purpose to determine the maximal voluntary displacement the participant could reach without tipping over. Figure 3.6 pictures subject 5's and subject 8's CoP/ CoM trajectories of one trial. The characteristic star-like shape indicates the displacement in each direction during the four-way-leaning test. We see that the leaning movement is not a straight line but the subject still shows postural sway.

Plotting the trajectories over time (Figure 3.7), we clearly observe the sudden deviations during each leaning movement. For example, when the participant leaned forward, the plot in the lower half shows a shift in positive direction. A point to mention are the local peaks after each major excursion, in particular in anterior-posterior (y), indicating a short overshoot when the subject returned to the initial position. The resting periods between each direction were cut out in this and the following figures.

Patterns and shape in the CoP/ CoM trajectories of subject 8 are similar though amplitudes are greater in left and posterior direction. Furthermore, we observe that the participant moved slightly to anterior (+y) when leaning to the left (-x). In general, the leaning movements in each direction were less independent of each other; during the shift in the medio-lateral direction we also see changes in anterior-posterior.

Table 3.3 lists the displacement over the three trials and the mean value for each system and direction separately. We notice that subject 8 shows on average broader LoS than subject 5. There is variance between the trials; in most cases values are higher in trial 2 and 3 compared to trial 1, indicating that the LoS increased and a learning effect was present.
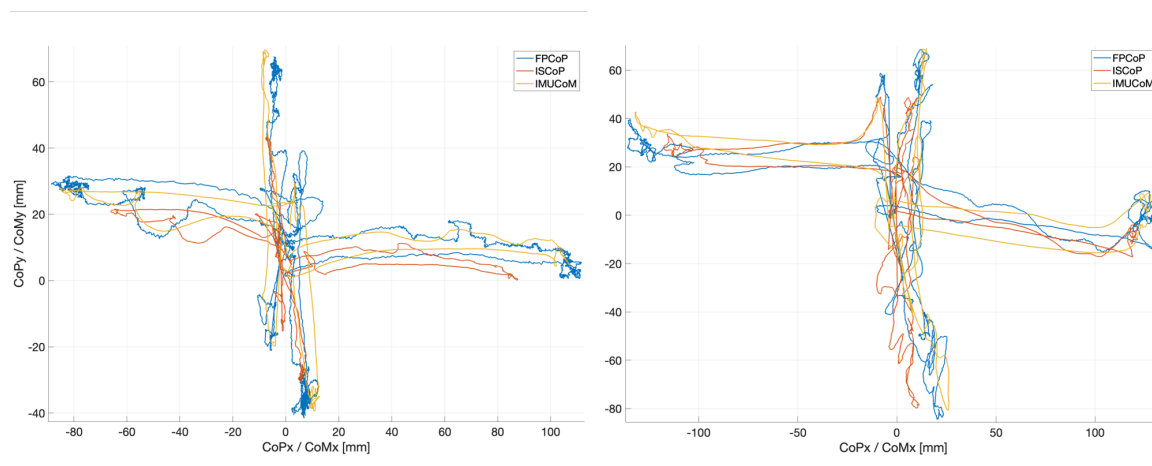
Figure 3.6: CoP/ CoM trajectories during one LoS measurement of subject 5 (left) and subject 8 (right) (Trial 1)
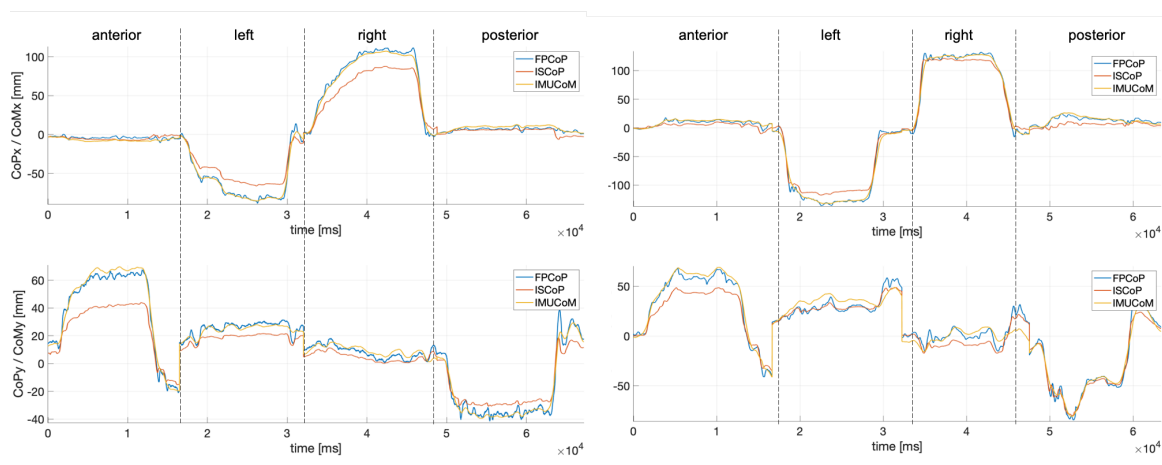

Figure 3.7: CoP/ CoM trajectories over time during one LoS measurement of subject 5 (left) and subject 8 (right) (Trial 1)

	Subject 5				Subject 8			
	Trial1	Trial2	Trial3	Mean	Trial1	Trial2	Trial3	Mean
LoS anterior FP	67.6021	72.0534	76.2195	71.9583	68.6671	90.9524	99.5923	86.4039
LoS anterior IS	43.8694	45.7230	45.6650	45.0858	48.7370	65.5112	78.4380	64.2287
LoS anterior IMU	69.7268	75.6620	74.3981	73.2623	69.0879	78.2508	94.7879	94.7879
LoS left FP	-88.5527	-98.1326	-98.7957	-95.1604	-135.8252	-142.7972	-126.8033	-135.1419
LoS left IS	-66.0398	-70.2429	-75.2742	-70.5190	-117.5403	-134.3654	-120.4201	-124.1086
LoS left IMU	-85.3880	-102.1198	-103.5816	-97.0298	-132.0309	-139.5162	-116.0843	-129.2105
LoS right FP	111.6304	119.1042	117.5832	116.1059	132.4207	118.3624	120.7977	123.8603
LoS right IS	87.5751	87.1395	81.3754	85.3633	121.4193	111.6702	116.3192	116.4696
LoS right IMU	107.1448	117.7940	113.3836	112.7741	128.0224	119.3523	123.5206	123.6319
LoS posterior FP	-41.5864	-45.9597	-50.5546	-46.0336	-84.5708	-86.2914	-86.6775	-85.8465
LoS posterior IS	-30.7703	-23.9669	-34.1285	-29.6219	-79.7917	-77.1646	-74.2625	-77.0730
LoS posterior IMU	-39.4706	-41.1915	-49.6865	-43.4495	-80.8507	-84.1112	-82.9902	-82.6507

Table 3.3: Displacement in CoP/ CoM trajectories during LoS measurements of subject 5 and 8; unit: [mm]
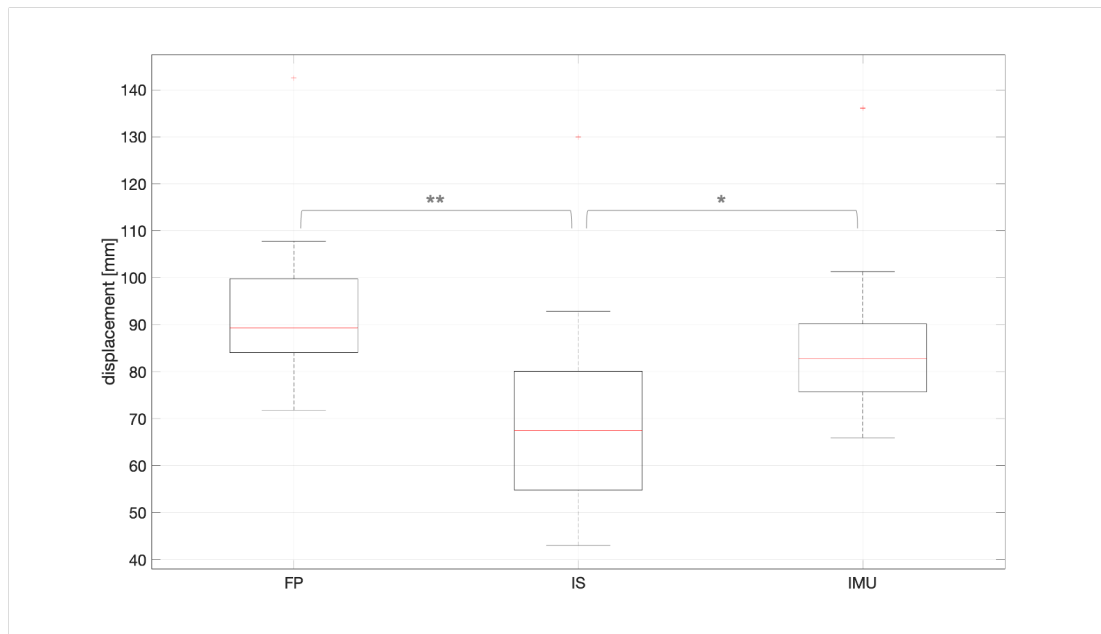
Figure 3.8: Comparison between the LoS in anterior measured by each system across all subjects; red line = median, whiskers = min/max, * = p<0.05, ** = p<0.01
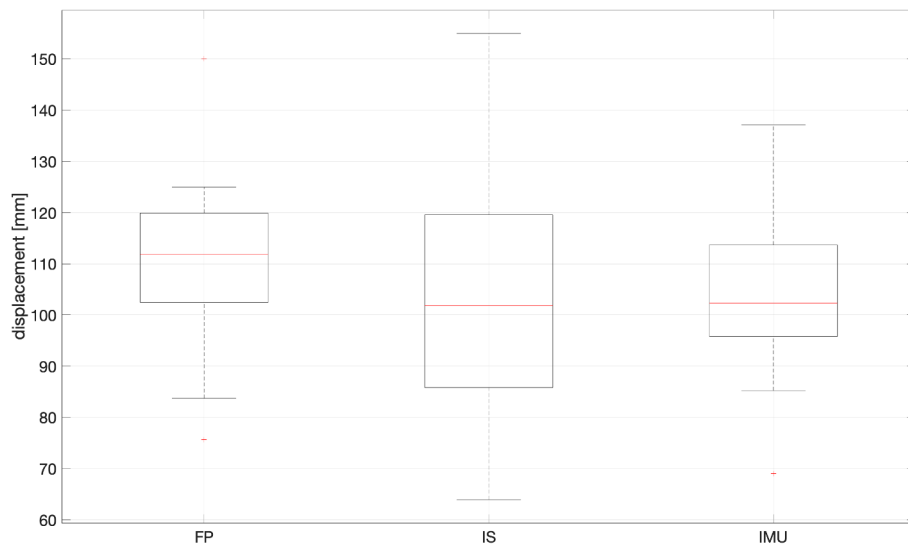
Across all subjects, the LoS in anterior measured by the FP-system are significantly higher than those measured by the IS-system with a difference in means of 21.84mm (cf. Figure 3.8). The same is true for the difference of 15.32mm between IMU-system and IS-system.

In the left direction, the LoS measured by the FP-system are significantly higher than those by the IMU-system by a margin of 7.29mm between mean values (cf. Figure 3.9). The difference between the IS-system's and IMU-system's means are less than 1mm.

This difference is less than 1mm in the right direction as well. Variations in means measured by the FP-system compared to the other systems are around 5mm though not significant (cf. Figure 3.10).

The statistical results of the LoS in posterior are similar to those in anterior but here the LoS measured by the FP-system and IS-system are higher by only 13.09mm (cf. Figure 3.11).

Table 3.4 presents the differences and statistical results of all system combinations. We need to mention that two groups in the ANOVA violated the assumption of normal distribution, namely the 'FP anterior' and 'IMU anterior'. Considering the Shapiro-Wilk test's output and after a visual inspection, the assumption was only marginally violated and we decided to not correct the distribution.
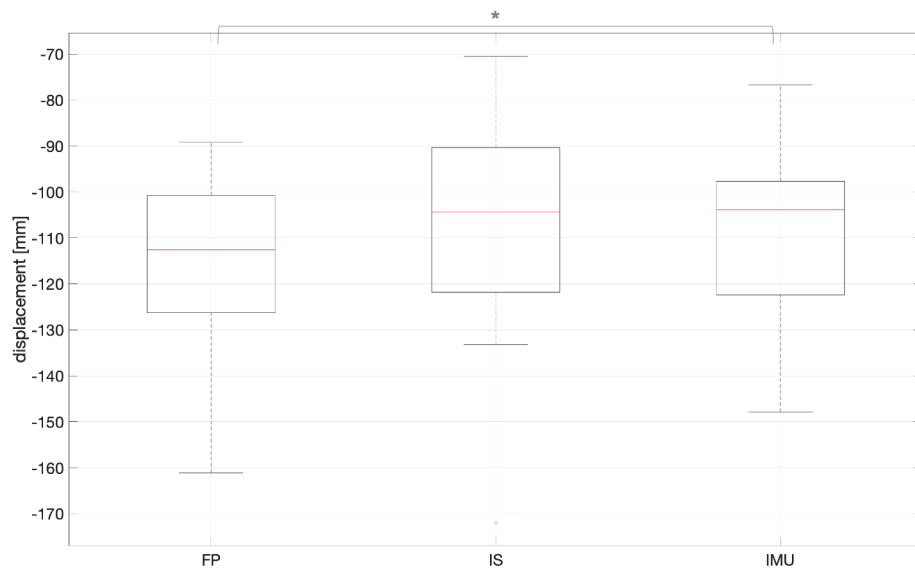
Figure 3.9: Comparison between the LoS to the left measured by each system across all subjects; red line = median, whiskers = min/max, * = p<0.05, ** = p<0.01

Figure 3.10: Comparison between the LoS to the right measured by each system across all subjects; red line = median, whiskers = min/max, ** = p<0.05, ** = p<0.01

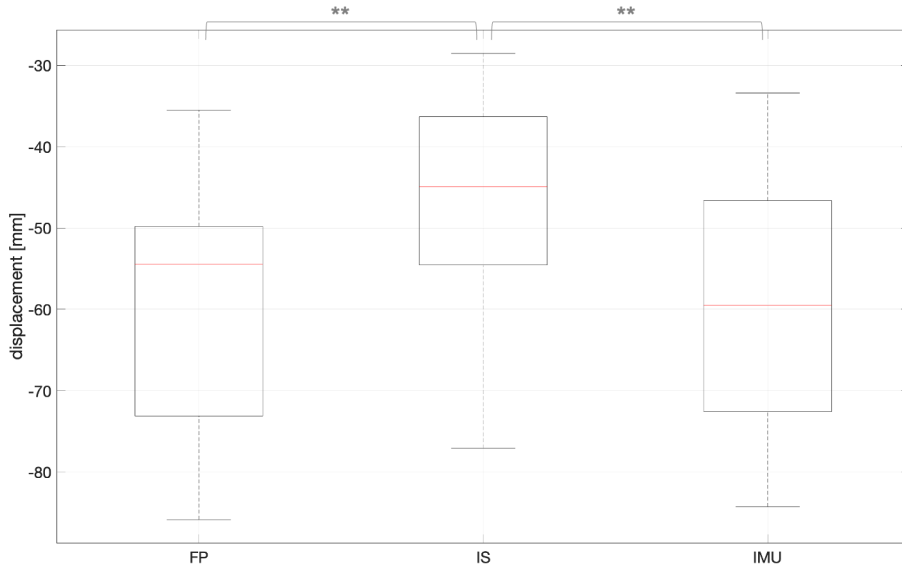Figure 3.11: Comparison between the LoS in posterior measured by each system across all subjects; red line = median, whiskers = min/max, * = p<0.05, ** = p<0.01

		Difference	StdError	p-value
anterior	FP vs IS	21.844	2.3132	0.0000**
	FP vs IMU	6.5277	1.8049	0.0716
	IS vs IMU	15.3160	3.4686	0.0171*
left	FP vs IS	-8.2480	3.8736	0.6130
	FP vs IMU	-7.2888	1.8651	0.0428*
	IS vs IMU	-0.9592	4.5216	1.0000
right	FP vs IS	5.4586	4.2064	0.9669
	FP vs IMU	5.2856	1.7421	0.1891
	IS vs IMU	0.1730	4.6863	1.0000
posterior	FP vs IS	-13.0900	1.3126	0.0000**
	FP vs IMU	-0.2935	1.5389	1.0000
	IS vs IMU	-12.7690	1.8857	0.0003**

Table 3.4: Results of Tukey-Kramer post-hoc test regarding differences in means between LoS values of each system ; ap = anterior-posterior, ml = medio-lateral; unit 'Difference': [mm]; * = p<0.05, ** = p<0.01

3.4 BL- & LoS-threshold

As mentioned in the previous chapter, we calculated two thresholds for each system:
The first one based on the postural sway in the baseline measurements and the
second one based on the measured LoS. Figure 3.12 shows the CoP/ CoM trajectories
of trials 1-3 during the LoS measurements together with the calculated BL- and LoS-
threshold of subject 5. As expected, the LoS-threshold encloses nearly the entire
CoP/ CoM trajectories' range, leaving out the extreme 10% in each direction. The
BL-threshold is quite narrow, especially in the IS-system. This is not surprising
when we remember the low SD in subject 5's baseline measurements (cf. Table 3.1).
Comparing subject 5's thresholds to these of subject 8 (cf. Figure 3.13), we clearly
see that subject 8 has a much broader BL-threshold because he showed a larger
postural sway in the baseline measurements. Looking into Table 3.5, we notice that
subject 8 has consistently higher threshold values, in particular when it comes to
the BL-threshold.
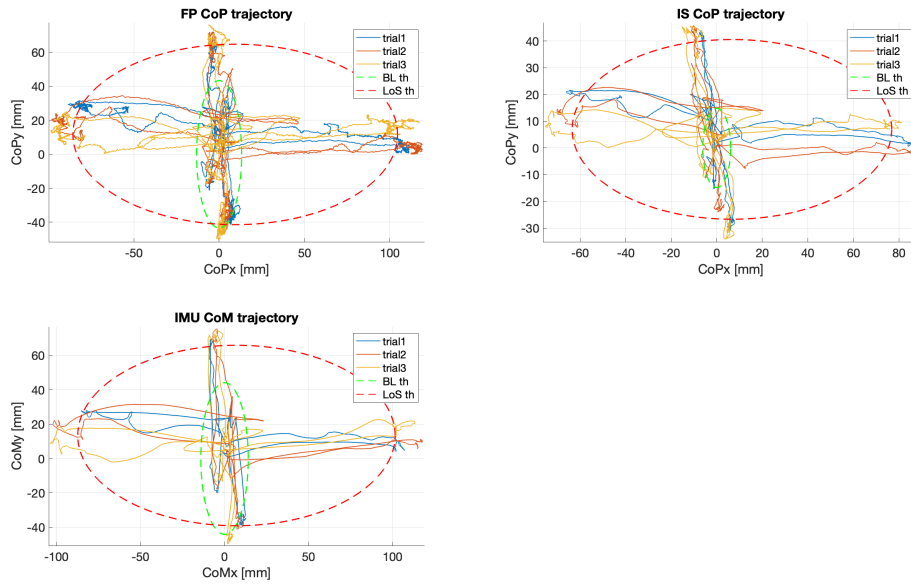
Figure 3.12: CoP/ CoM trajectories of trials 1-3 during LoS measurements and the calculated BL- and LoS-threshold for each system separately (Subject 5)
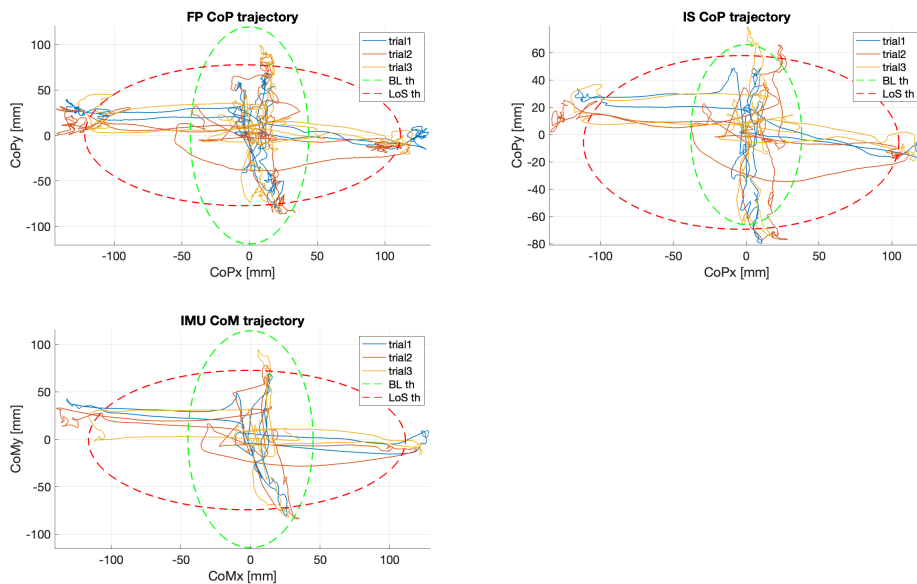
Figure 3.13: CoP/ CoM trajectories of trials 1-3 during LoS measurements and the calculated BL- and LoS-threshold for each system separately (Subject 8)

		Subject 5		Subject 8	
		BL-threshold	LoS-threshold	BL-threshold	LoS-threshold
anterior	FP	43.3406	64.7625	119.3727	77.7635
	IS	14.8093	40.5772	65.8372	57.8058
	IMU	44.1470	65.9361	114.3951	72.6380
left	FP	-13.1858	-85.6443	-43.6923	-121.6277
	IS	-6.1072	-63.4671	-38.1270	-111.6977
	IMU	-14.1054	-87.3268	-44.9736	-116.2894
right	FP	13.1858	104.4953	43.6923	111.4742
	IS	6.1072	76.8270	38.1278	104.8226
	IMU	14.1054	101.4967	44.9736	111.2686
posterior	FP	-43.3406	-41.4302	-119.3727	-77.2619
	IS	-14.8093	-26.6597	-65.8372	-69.3657
	IMU	-44.1470	-39.1046	-114.3951	-74.3856

Table 3.5: Threshold values of subject 5 and 8; unit: [mm]

3.5 Correlation BL- & LoS-threshold

The figures in the previous section, which showed the thresholds of subject 5 and 8, already pointed out that the BL-threshold and LoS-threshold do differ. We looked deeper into the relation between both thresholds and correlated them across all subjects separately for each direction. This is the same as a correlation between the baseline measurements' average SD and the LoS, because the thresholds are calculated by adding constant factors which do not have an influence on the relative relation of the data points and therefore correlation. In the first calculation we observed two outliers in the data points, thus we repeated the correlation after eliminating the outliers in all factions (directions), reducing the sample size to $n = 14$. Outliers were values that diverged more than three scaled median absolute deviations away from the median.

Figure 3.14 depicts the correlation between the anterior component of the BL-threshold and LoS-threshold. We observed a correlation of $R = 0.4169$ ($p = 0.1380, n = 14$) excluding the outliers. For the posterior components we obtained a correlation of $R = 0.5204$ ($p = 0.0564, n = 14$) after eliminating the outliers (cf. Figure 3.15). Figures of the left and right components are in the Appendix (Figure A.1 & A.2). Table 3.6 lists the correlations.
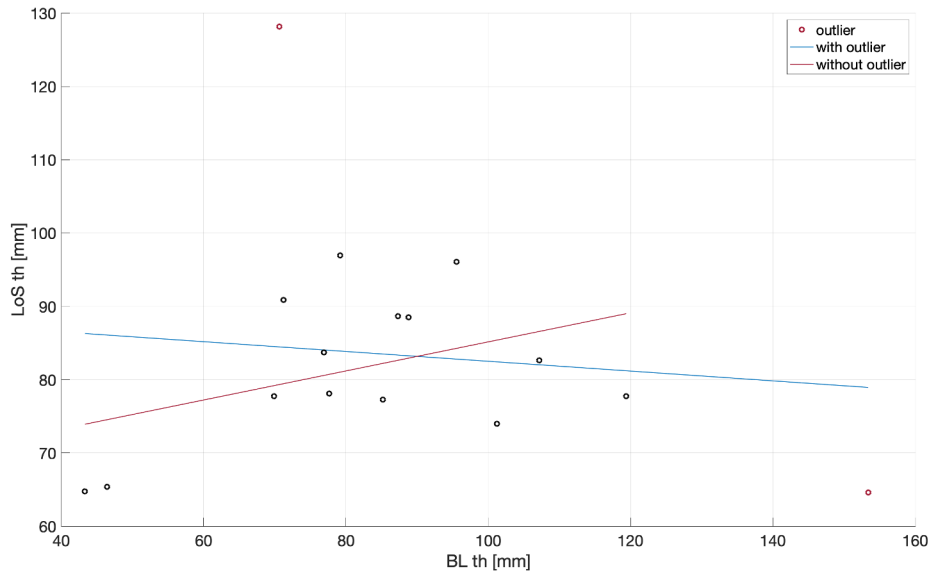
Figure 3.14: Correlation between the anterior component of BL-threshold and LoS-threshold ; red circle indicate outlier, straights are the regression lines
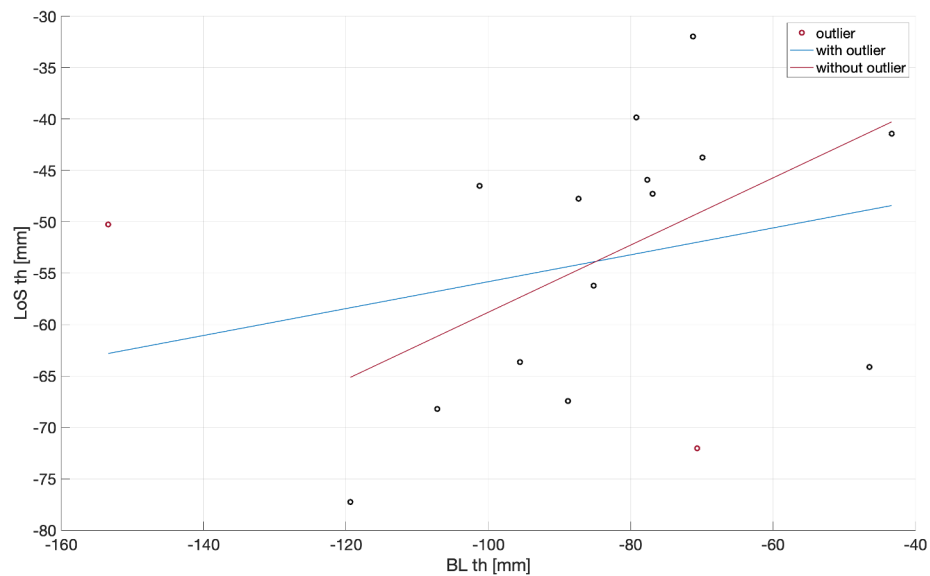

Figure 3.15: Correlation between the posterior component of BL-threshold and LoS-threshold ; red circle indicate outlier, straights are the regression lines

	R	p-value	n
Anterior with outlier	-0.1138	0.6749	16
Anterior without outlier	**0.4169**	0.1380	14
Left with outlier	-0.0747	0.7833	16
Left without outlier	0.0191	0.9434	14
Right with outlier	-0.0232	0.9320	16
Right without outlier	-0.1567	0.5927	14
Posterior with outlier	0.2646	0.3219	16
Posterior without outlier	**0.5204**	0.0564	14

Table 3.6: Correlations between BL- and LoS-threshold separated by direction component

3.6 sPT-scenario

After we determined the BL- and LoS-threshold for each system, the next step was to evaluate their performance during the postural transitions. In the sPT-scenario the participant bent forward, shifting his CoP and CoM. The postural transition was stable and the subject did not loose balance at any point.

Figure 3.16 depicts the CoP/ CoM trajectories of subject 5's transitions 1-3 of trial 3 together with the calculated BL- and LoS-threshold for each system. We notice that the BL-threshold was exceeded in all three systems. The LoS-threshold was also exceeded in the IS-system and IMU-system in transition 3, though not in the FP-system. In contrast, subject 8 never exceeded the thresholds during the stable postural transition (cf. Figure 3.17).

Table 3.7 outlines the maximal distance between the CoP/ CoM trajectory recorded by each system and its respective BL- and LoS-threshold. Positive values indicate that the CoP/ CoM reached a point beyond the threshold and thus crossed it.
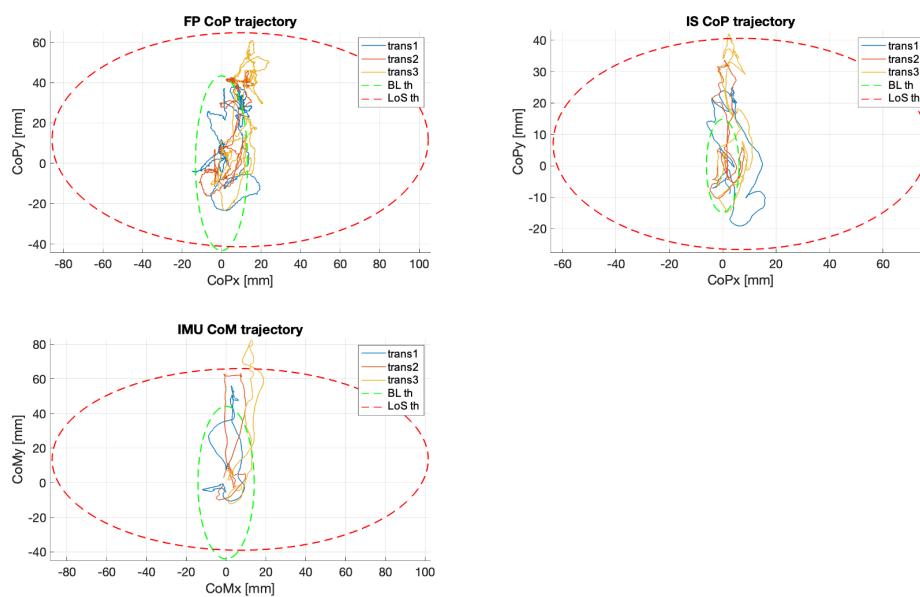
Figure 3.16: CoP/ CoM trajectories of the three transitions (trans1-3) of trial 3 during the sPT-scenario and the calculated BL- and LoS-threshold for each system (Subject 5)
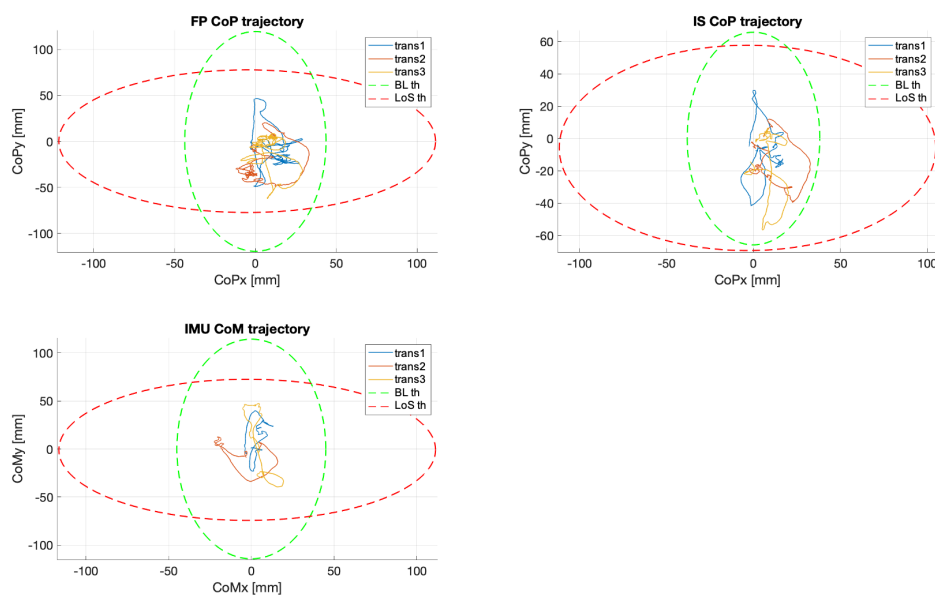
Figure 3.17: CoP/ CoM trajectories of the three transitions (trans1-3) of trial 3 during the sPT-scenario and the calculated BL- and LoS-threshold for each system (Subject 8)

| | Subject 5 | | | | Subject 8 | | | |
	Trans1	Trans2	Trans3	Mean	Trans1	Trans2	Trans3	Mean
FP BLth	-4.5064	2.5118	17.8062	5.2705	-40.7817	-55.9706	-40.3128	-45.6884
FP LoSth	-17.6722	-19.0300	-3.4835	-13.3952	-28.0936	-27.9852	-14.6834	-23.5874
IS BLth	10.1755	18.9665	27.1998	18.7806	-23.8707	-26.2553	-9.1420	-19.7560
IS LoSth	-7.4535	-6.8882	1.5921	-4.2499	-27.6994	-29.8518	-12.6794	-23.4102
IMU BLth	11.8502	19.1021	38.0867	23.0130	-41.3868	-42.0752	-41.0728	-41.5116
IMU LoSth	-9.8511	-2.5811	16.4146	1.3275	-32.8572	-40.6774	-25.1646	-32.8997

Table 3.7: Maximal distance between the CoP/ CoM trajectory and respective threshold during the three transitions of trial 3; unit: [mm], positive values indicate that the threshold is crossed

If we look at the maximum displacement in anterior direction during the sPT-scenario (cf. Figure 3.18), we observe large variations across the subjects ranging from less than 30mm to more than 110mm as measured by the FP-system. Differences between the systems' means are significant ($F(2, 30) = 43.26, p = 0.0000, \eta_p^2 = 0.74, f = 1.7$); especially the IMU-system measured a greater displacement. Detailed results are listed in Table A.2 in the Appendix.

The FP-system's measurements and performance were regarded as the reference. Thus, we compared the differences in maximal distances between the IS-system and IMU-system by calculating the distance discrepancy Δd between the FP-system's distance values and the IS-system's or IMU-system's values, respectively.

The Δd-values across all subjects grouped by system and threshold-type are shown in Figure 3.19. We clearly see a larger variance in Δd of the IMU-system compared to the IS-system. A value of zero means that there is no discrepancy between the maximal distance values of the FP-system and the IS-system or IMU-system. Negative values indicate that distance values lie above those identified by the FP-system, so the CoP/ CoM reached either closer to the corresponding threshold or exceeded it by a larger scale than did the CoP recorded by the FP-system. Most values lie below zero and are therefore greater than the reference. The IS-system's LoS-threshold comes closest to the reference and shows a small variance among the subjects. It also demonstrates a significant better performance than the BL-threshold. On first sight, results of the IMU-system's BL- and LoS-threshold seem to be similar.

Differences in mean values between the factor combinations were statistically evaluated in a two-way repeated measure ANOVA. We found no significant main effect for the factor 'System' ($F(1, 15) = 2.6, p = 0.1277, \eta_p^2 = 0.1477$) but a medium effect size of $f = 0.42$ according to Cohen. There is a trend towards a difference between the IS-system and IMU-system regarding the accuracy with which they can track the CoP's or CoM's position to a defined threshold. There is a significant main effect for the factor 'Threshold' ($F(1, 15) = 7.1, p = 0.0176, \eta_p^2 = 0.3214$) with a large effect size of $f = 0.69$. So the BL-threshold seems to significantly differ from the LoS-threshold. Besides the two main effects there is also a significant interaction between 'System' and 'Threshold' ($F(1, 15) = 25.1, p = 0.0002, \eta_p^2 = 0.6263$) with a very large effect size of $f = 1.29$. This seems plausible when we look at Figure 3.19 once more: The difference between BL-threshold and LoS-threshold is greater within the IS-system than within the IMU-system.

In order to evaluate the differences between each factor combination separately, we carried out a post-hoc test. The results are presented in Table 3.8. The difference in the BL-threshold between the two systems is less than 1mm but more than 13mm considering the LoS-threshold. The distance discrepancy of the IS-system's LoS-threshold is 11.37mm lower than the discrepancy of the BL-threshold.
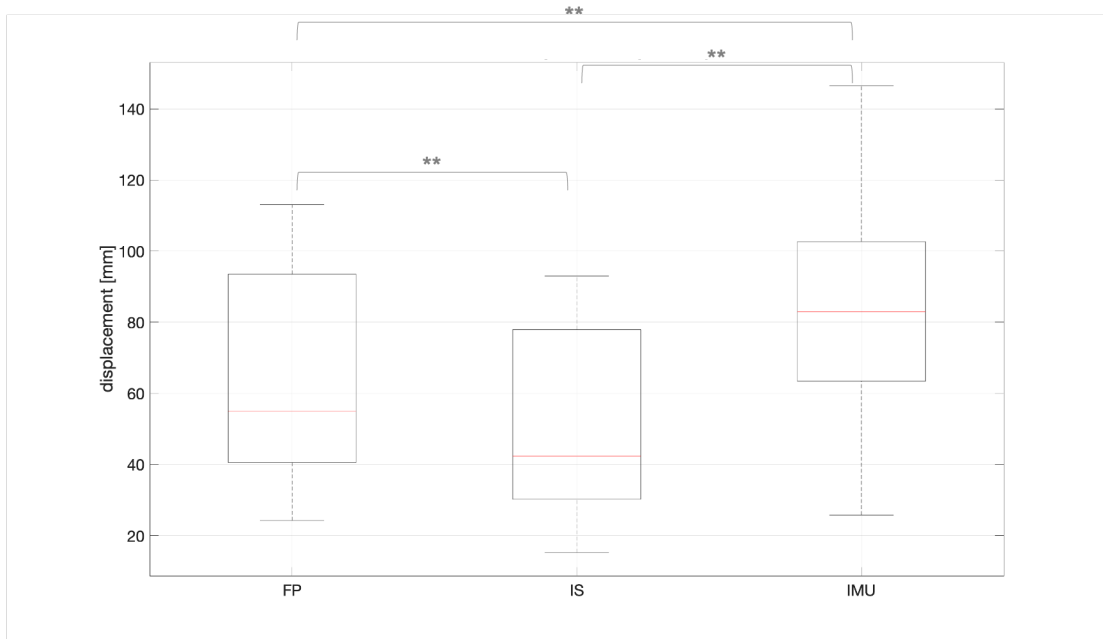
Figure 3.18: Maximum displacement in anterior direction during the sPT-scenario across all subjects measured by the different systems; red line = median, whiskers = min/max, * = p<0.05, ** = p<0.01
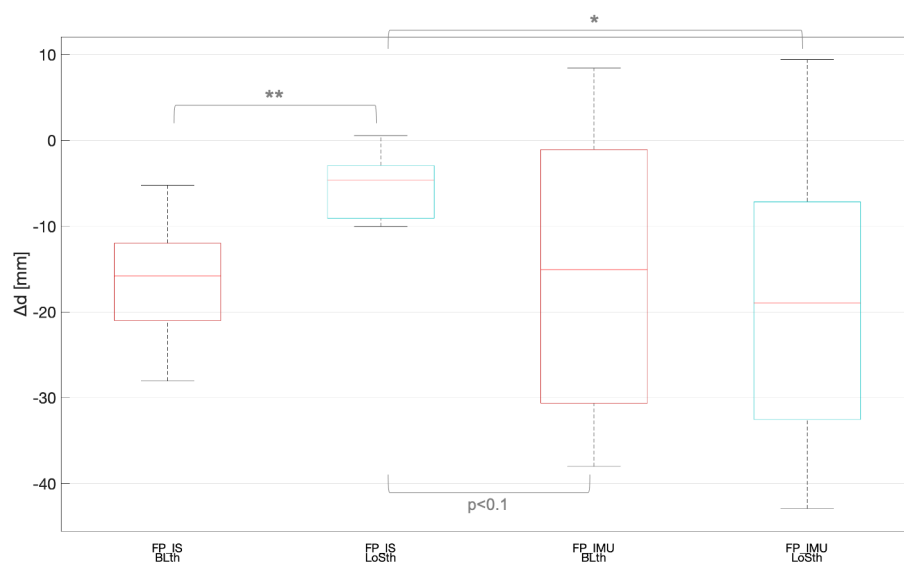

Figure 3.19: Distance discrepancy Δd between the CoP's (recorded by the FP-system) maximal distance from the respective threshold and the CoP's (IS-system) and CoM's (IMU-system) corresponding values; red line = median, whiskers = min/max, * = p<0.05, ** = p<0.01

	Difference	StdError	p-value
FP-IS BLth vs FP-IS LoSth	-11.373	2.0940	0.0004**
FP-IS BLth vs FP-IMU BLth	-0.7436	3.9328	0.9975
FP-IS BLth vs FP-IMU LoSth	1.9874	4.4197	0.9687
FP-IS LoSth vs FP-IMU BLth	10.6300	4.0415	0.0769
FP-IS LoSth vs FP-IMU LoSth	13.3610	4.3704	0.0359*
FP-IMU BLth vs FP-IMU LoSth	2.7311	2.1977	0.6108

Table 3.8: Results of the Tukey-Kramer post-hoc test regarding differences in means of Δd between factor combinations of 'System' and 'Threshold' in the sPT-scenario's evaluation; unit 'Difference': [mm]; * = p<0.05, ** = p<0.01

3.7   uPT-scenario

Investigating the systems' performances in the uPT-scenario, we evaluated each direction separately. Data recordings of the postural transitions were split into the different directions and then tested for statistical significance between the groups' means. This time, we also considered the combined threshold (COMB) in the analysis.

uPT - Anterior

Figure 3.20 and Figure 3.21 show the CoP/ CoM trajectories during the uPT-scenario in anterior direction of subject 5 and subject 8. Trajectories are plotted from the beginning of the postural transition until the tipping point was reached. Hence, the path's end-point corresponds to the tipping point. We observe a certain sway around the initial position, resulting from the forward bending, followed by a continuous motion in anterior direction. Because the IS-system's coordinate system is not fixed to the environment but to the participant, we can observe sudden changes in the CoP trajectory at the point when the subject tipped over and made impulsive movements. BL- and LoS-threshold of the systems were exceeded in all trials, except in the FP-system in trial 3 of subject 8, where the subject did not exceed the BL-threshold before she or he reached the tipping point.
Table 3.9 gives the exact time discrepancies for each trial and threshold of subject 5 and 8. Positive values indicate that the threshold was exceeded after the tipping point was reached. In trial 3 of subject 8 we have a time discrepancy Δt of 30ms which corresponds to the case mentioned.
In the statistical analysis we considered the mean over the three trials of each subject. Figure 3.22 presents the results for each threshold across all subjects. Because all values lie below zero, all threshold were on average crossed before the tipping point was reached. The IS-system's BL-threshold shows a great variance in Δt; values range from -500ms to around -7500ms before the tipping point.
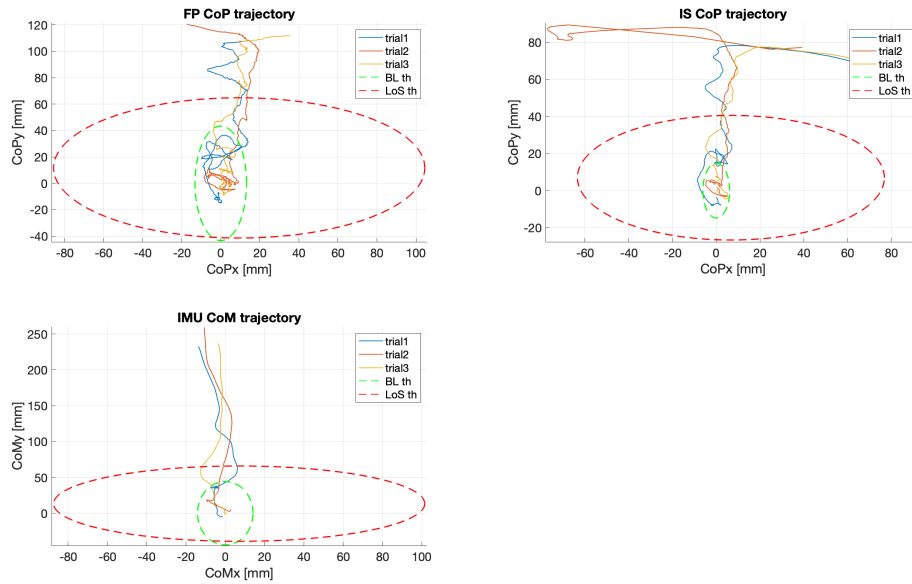
Figure 3.20: CoP/ CoM trajectories of trial 1-3 during the sPT-scenario in anterior direction and the calculated BL- and LoS-threshold for each system (Subject 5)
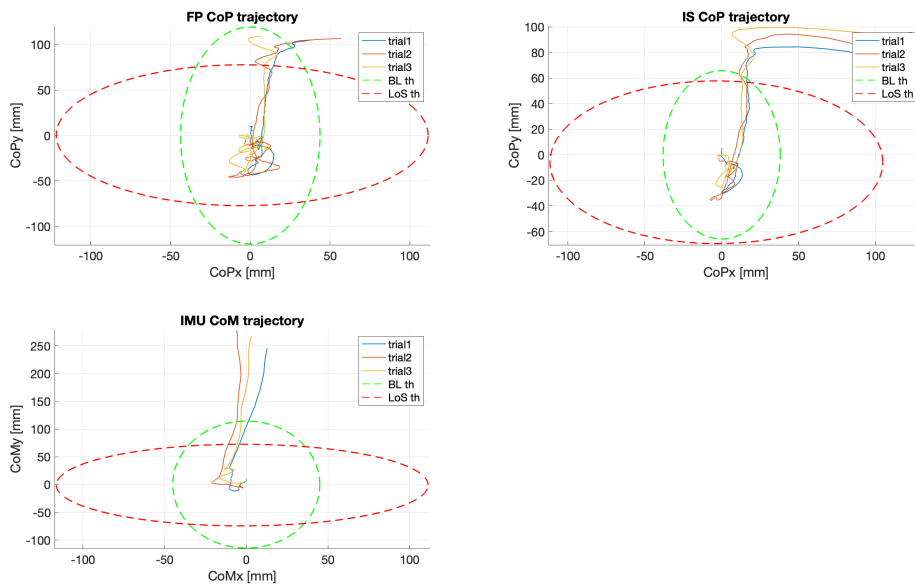
Figure 3.21: CoP/ CoM trajectories of trial 1-3 during the sPT-scenario in anterior direction and the calculated BL- and LoS-threshold for each system (Subject 8)

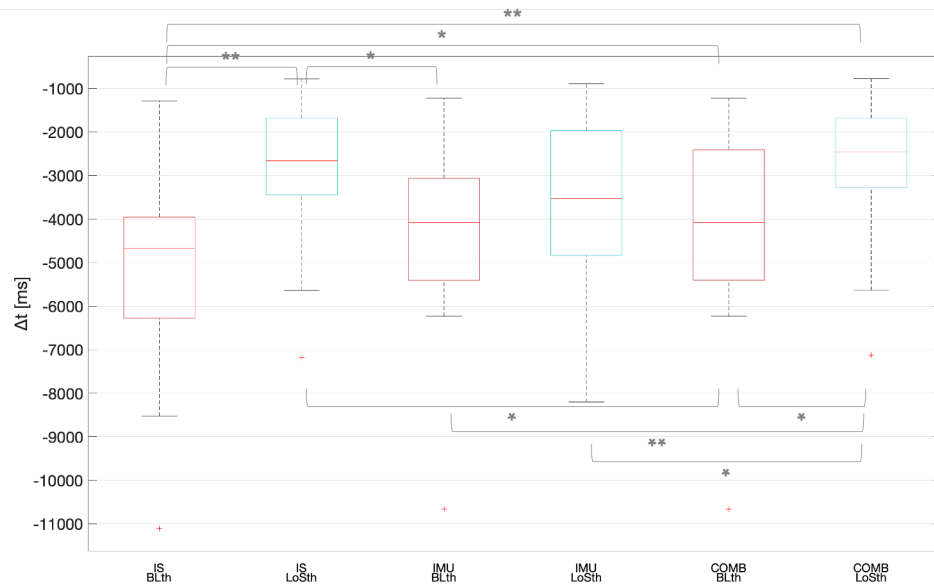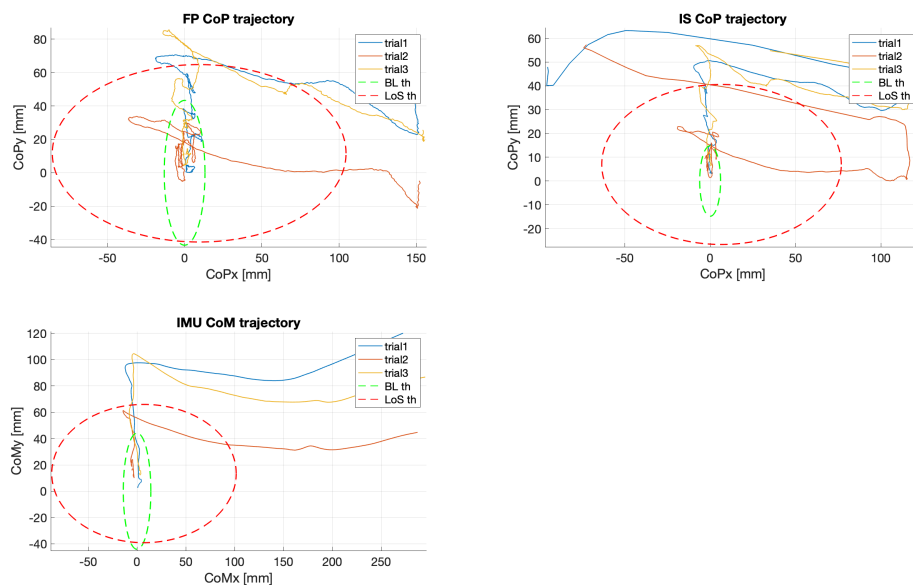| | Subject 5 | | | | Subject 8 | | | |
	Trial1	Trial2	Trial3	Mean	Trial1	Trial2	Trial3	Mean
FP BLth	-4460	-1790	-2550	-2933.33	-110	-70	30	-50.00
FP LoSth	-1600	-1280	-1890	-1590.00	-390	-600	-460	-483.33
IS BLth	-5480	-2270	-3440	-3730.00	-540	-730	-730	-666.67
IS LoSth	-1900	-1580	-2040	-1840.00	-570	-870	-780	-740.00
IMU BLth	-2640	-2100	-3240	-2660.00	-550	-730	-570	-616.67
IMU LoSth	-2080	-1720	-2380	-2060.00	-950	-1100	-850	-966.67

Table 3.9: Time discrepancy Δt between the timepoint the subject exceeded the respective threshold and the tipping point during the uPT-scenario anterior; unit: [ms], positive values indicate that the threshold was crossed after the tipping point was reached
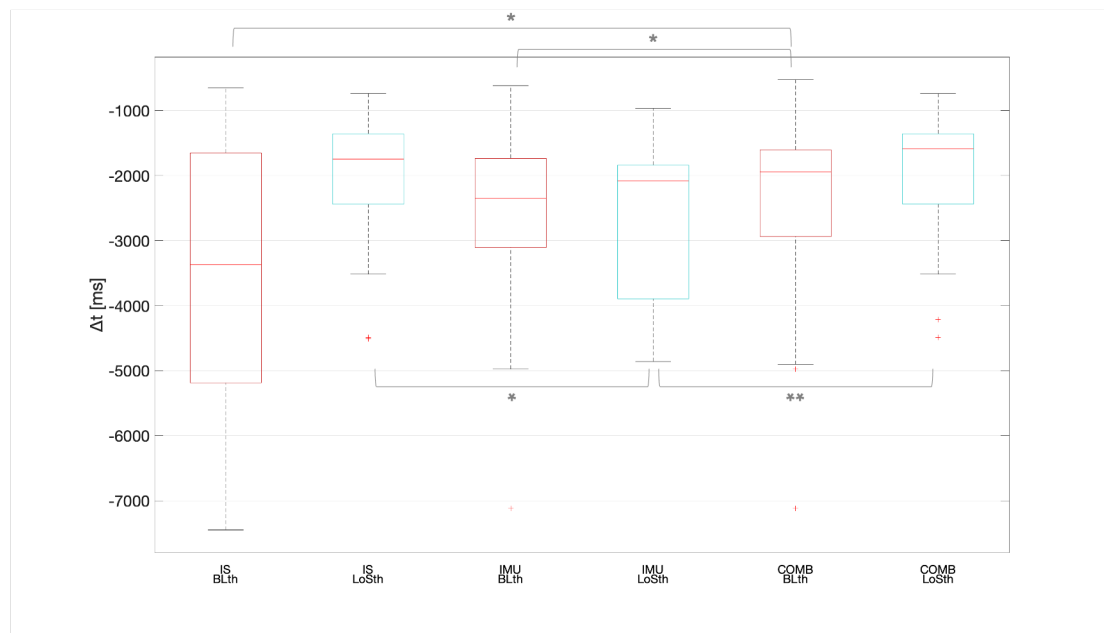
Figure 3.22: Time discrepancy Δt between the timepoint the subject exceeded the respective threshold and the tipping point during the uPT-scenario anterior; red line = median, whiskers = min/max, * = $p < 0.05$, ** = $p < 0.01$

We transformed the data taking their natural logarithms in order to meet the assumption of normal distribution. We got a significant effect for the factor 'System' ($F(2,30) = 9.4, p = 0.0025, \eta_p^2 = 0.3853$) with a large effect size of $f = 0.79$ and the interaction of the factors 'System' and 'Threshold' ($F(2,30) = 18.66, p = 0.0000, \eta_p^2 = 0.5544$) with a very large effect size of $f = 1.12$. The post-hoc test found a significant difference in Δt between the IMU-system's LoS-threshold and the IS-system's and combined LoS-threshold, respectively. All results are listed in Table A.3 in the Appendix.

uPT - Left

Figure 3.23 depicts the results of the uPT-scenario in left direction. The statistical analysis revealed a significant main effect for both the factor 'System' ($F(2,30) = 5.32, p = 0.0235, \eta_p^2 = 0.262$) with an effect size of $f = 0.6$ and the factor 'Threshold' ($F(1.15) = 17.00, p = 0.0009, \eta_p^2 = 0.53$) with an effect size of $f = 1.06$. There is also an significant effect for the interaction between the factors ($F(2.30) = 11.35, p = 0.0019, \eta_p^2 = 0.43$) with a large effect size of $f = 0.87$. The results indicate that time discrepancy Δt is shorter for the LoS-threshold than for the BL-threshold and shorter in the IS-system than the IMU-system. Differences between means of the BL-threshold and LoS-threshold reach from 2287ms within the IS-system to 759ms within the IMU-system. The difference between IS LoS-threshold and IMU LoS-threshold lies at 757ms. We observed a similar trend in the combined threshold. All results are listed in Table A.5 in the Appendix together with exemplary results of subject 5 and 8.

uPT - Right

Figure 3.24 and Figure 3.25 show the CoP/ CoM trajectories of subject 5 and subject 8 during the uPT-scenario in right direction. We see that the CoP and CoM first shifted to anterior once the subjects bent forward and then right when moving to the right. In the IS-system's CoP trajectory the sudden quick movements, once the tipping point is reached, are clearly discernible. In trial 1 and 3, subject 5 already passed the BL- and LoS-threshold by the time he bent forward. Subject 8's CoP and CoM stayed closer to the initial position and only passed the threshold when he moved to the right.

Table 3.10 contains the detailed time discrepancies and we notice that these are higher in trail 1 and 3 of subject 5, the trails where he already passed the thresholds during the forward bending. In trail 2 differences between subject 5 and 8 are less than 1000ms.

Looking at the results across all subjects (cf. Figure 3.26), we observe a high variance in the IS BL-threshold's results with values ranging from -1500ms to one case of -10500ms. This one subject exceeded the threshold early on in the beginning of the postural transition.

Figure 3.23: Time discrepancy Δt between the timepoint the subject exceeded the respective threshold and the tipping point during the uPT-scenario left; red line = median, whiskers = min/max, * = p<0.05, ** = p<0.01

Figure 3.24: CoP/ CoM trajectories of trial 1-3 during the sPT-scenario in right direction and the calculated BL- and LoS-threshold for each system (Subject 5)
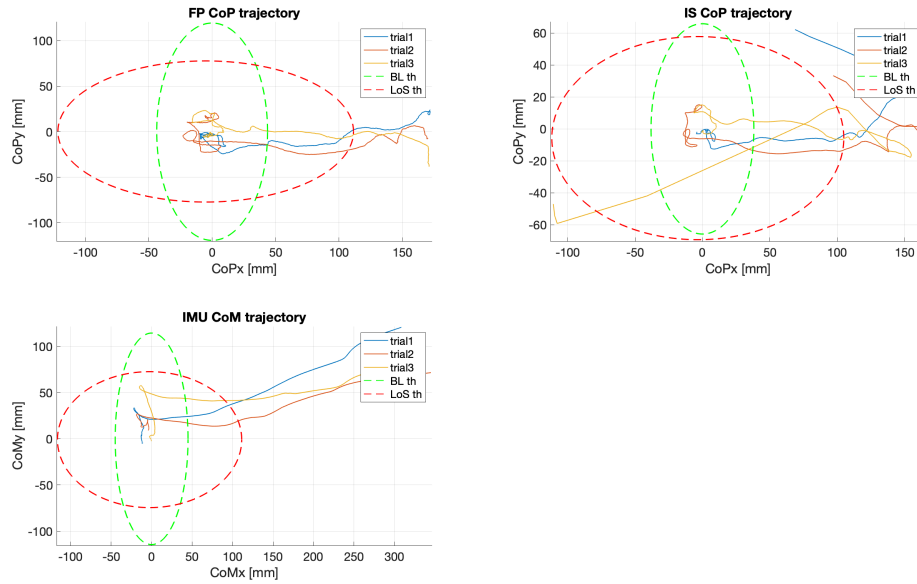
Figure 3.25: CoP/ CoM trajectories of trial 1-3 during the sPT-scenario in right direction and the calculated BL- and LoS-threshold for each system (Subject 8)

	Subject 5				Subject 8			
	Trial1	Trial2	Trial3	Mean	Trial1	Trial2	Trial3	Mean
FP BLth	-3510	-1890	-3900	-3100.00	-1710	-1460	-1080	-1416.67
FP LoSth	-2260	-810	-2940	-2003.33	-820	-1060	-550	-810.00
IS BLth	-5520	-4680	-5360	-5186.67	-1790	-1500	-1380	-1556.67
IS LoSth	-2620	-1040	-3250	-2303.33	-1020	-1160	-800	-993.33
IMU BLth	-4330	-2630	-4100	-3686.67	-1340	-1360	-1070	-1256.67
IMU LoSth	-3440	-750	-3380	-2523.33	-820	-920	-710	-816.67

Table 3.10: Time discrepancy Δt between the timepoint the subject exceeded the respective threshold and the tipping point during the uPT-scenario right; unit: [ms]
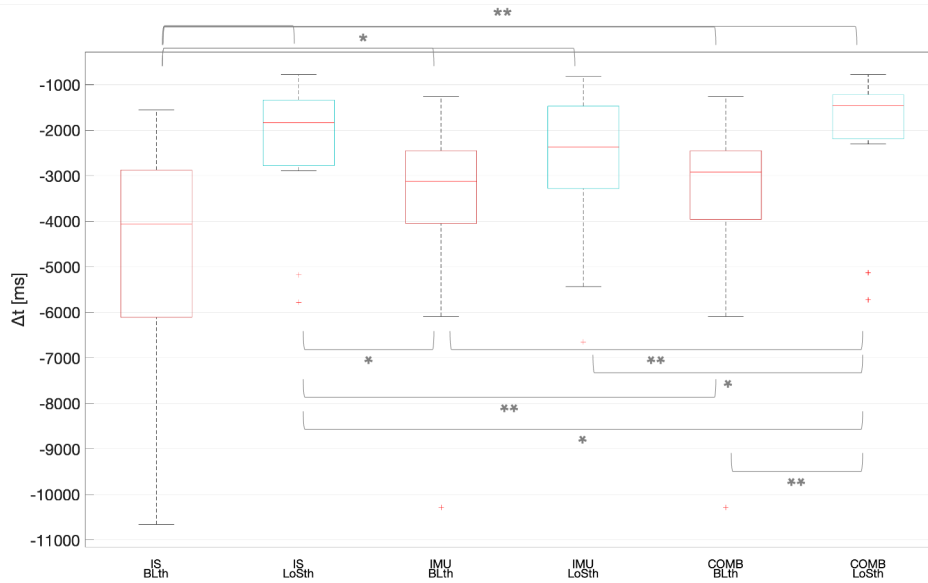
Figure 3.26: Time discrepancy Δt between the timepoint the subject exceeded the respective threshold and the tipping point during the uPT-scenario right; red line = median, whiskers = min/max, * = p<0.05, ** = p<0.01

The statistical test gave a significant effect of the factor 'System' ($F(2, 30) = 6.56, p = 0.0159, \eta_p^2 = 0.3, f = 0.66$) and the factor 'Threshold' ($F(1, 15) = 39.25, p = 0.0000, \eta_p^2 = 0.72$) with a very large effect size of $f = 1.62$ as well as a significant effect of the interaction ($F(2, 30) = 10.14, p = 0.0016, \eta_p^2 = 0.4$) with an effect size of $f = 0.82$. But we need to interpret these main effects with caution because of the high variation in the group 'IS Blth'. The post-hoc test revealed several significant differences, of particular interest are the differences between the group 'IS Blth' and each other group's mean and the difference between the combined BL- and LoS-threshold. All results are listed in Table A.6 in the Appendix.

Trends and differences are similar to the left direction, except the single low value in the group 'IS BLth'. In both directions, the LoS-threshold's Δt is shorter than the BL-threshold's one within all systems.

uPT - Posterior

Finally, Figure 3.27 depicts the results of the unstable postural transition in posterior direction. Again, the group 'IS BLth' shows a high variability and the post-hoc test revealed significant differences compared to all other groups except the IS-system's LoS-threshold and IMU-system's BL-threshold. The statistical test calculated a significant effect of the factor 'System' ($F(2, 30) = 11.49, p = 0.0025, \eta_p^2 = 0.43$) with an effect size of $f = 0.88$ but not the factor 'Threshold' or the interaction
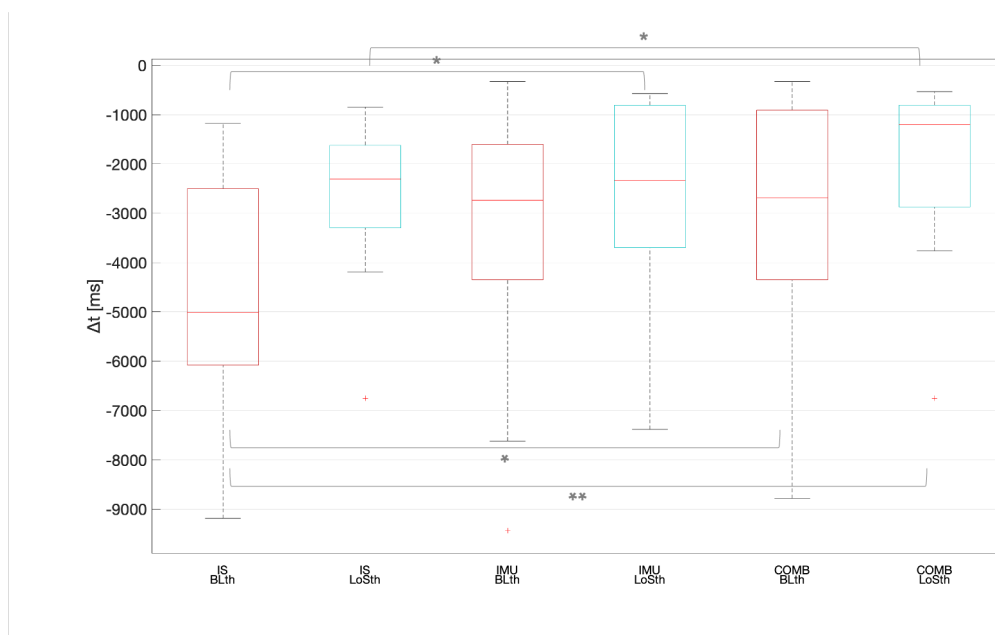
Figure 3.27: Time discrepancy Δt between the timepoint the subject exceeded the respective threshold and the tipping point during the uPT-scenario posterior; red line = median, whiskers = min/max, * = p<0.05, ** = p<0.01

between the factors. Again we need to treat the main effect with caution because of the large variability in the group 'IS Blth'. The post-hoc test only revealed one significant difference between the other groups, namely the IS-system's and combined LoS-threshold. All results are listed in Table A.8 in the Appendix.

Like in anterior direction (cf. Figure 3.22), we observe only a significant main effect for the factor 'System', though in both directions the LoS-threshold's Δt is shorter compared to the BL-threshold within all systems. Worth to mention is the small difference between the IS-system's and IMU-system's LoS-threshold of less than 18ms in posterior direction.

Exemplary results of subject 5 and 8 are presented in the Appendix.

3.8 Reduced segmentation

In the last part of the data analysis we looked into the differences between the two approaches how to segment the human body in the IMU-system's CoM-calculation. In the first approach, we defined 16 segments according to Hedegaard et al. [HAMJ+20], in the second approach we defined only three segments (upper body, left leg and right leg) by combining the original 23 segments during the segment CoM's calculation. Go to Figure A.7 in the Appendix for detailed information. We refer to the CoM calculated according to the first approach as the 'CoM' and to the alternative one as the 'CoMred'. Standard deviations (SD) during the baseline measurements
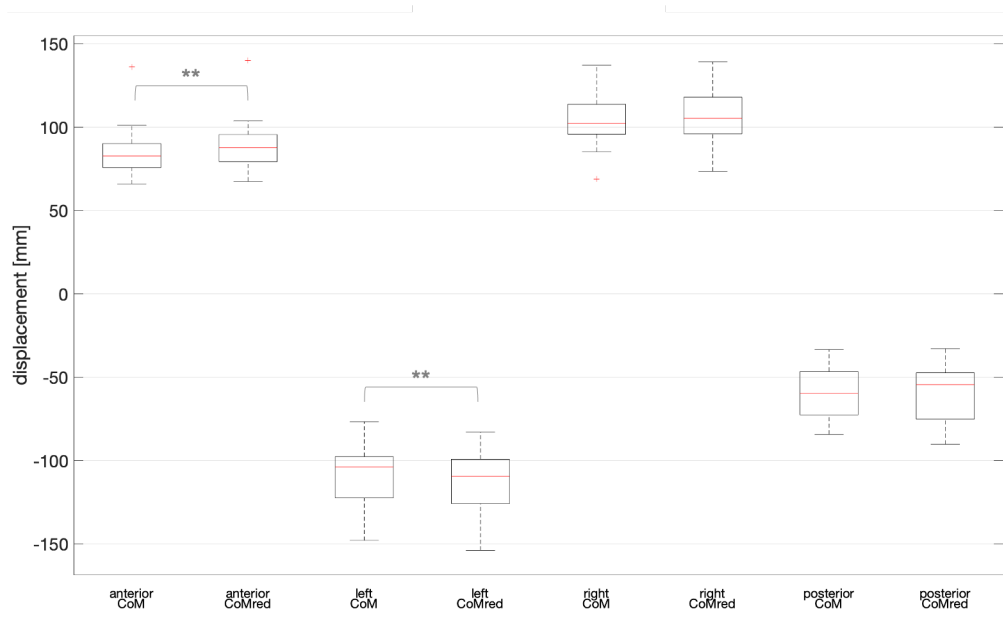
Figure 3.28: Differences in in each direction's LoS between the CoM and CoMred; red line = median, whiskers = min/max, * = p<0.05, ** = p<0.01

and the LoS of the IMU-system were calculated for both approaches and compared to see whether there are any significant differences.

A t-Test revealed that the SDs in both directions do not significantly differ between the CoM and CoMred. In medio-lateral direction the average SDs differ by only 0.02mm ($t = -1.78, p = 0.0938, n = 16$), in anterior-posterior direction by 0.06mm ($t = -1.24, p = 0.233, n = 16$). Detailed figures can be found in the Appendix.

Figure 3.28 shows the differences in the LoS in each direction between the CoM and CoMred. We notice that the CoMred's LoS are broader compared to the CoM's ones. The CoMred's LoS anterior is significantly larger by 4.03mm ($t = -5.85, p = 0.0000, n = 16$), the LoS left is significantly larger by even 5.14mm ($t = 4.17, p = 0.0008, n = 16$). LoS right and LoS posterior differ by 1.86mm and 0.07mm.

3.9   Summary

To sum the results up, we obtained differences between the IS-system thresholds and IMU-system thresholds. Differences between both systems are more distinctly for the LoS-threshold than they are for the BL-threshold, mainly because there is a great variability in the BL-threshold's results across the subjects. Regarding the LoS-thresholds, the IS-system demonstrates the best performance. The IS-system's LoS-threshold has a significant lower distance discrepancy Δd by 13mm compared to the IMU-system's one and a shorter time discrepancy Δt, except during the uPT in posterior direction, where results are similar. Values of the combined thresholds

are similar to these of the IS-system.

Within the systems, the LoS-threshold shows a better performance than the BL-threshold. The LoS-threshold has a lower Δd in the IS-system and shorter Δt, and thus achieves more similar results to the reference. Only during the uPT in anterior direction the IMU-system's LoS-thresholds achieved a similar Δt with a difference of only 8ms in favor of the BL-threshold. In the other cases, differences lie between 650ms and 2325ms in favor of the LoS-threshold.

Speaking of the two threshold-types, we found a large positive, though not significant, correlation between the BL- and LoS-threshold of 0.42 and 0.52 in anterior and posterior direction.

Comparing the two CoM-calculation approaches, we found no large or significant differences in the postural sway. The LoS differed significantly in anterior and left direction, though only by a small scale of 4mm and 5mm.

Chapter 4

Discussion

4.1 A Novel Approach

To the best of our knowledge there is no previous study which utilized the CoM-displacement measured by an IMU-system to control biofeedback in the context of postural control. As presented in the introduction, most studies considered the trunk's inclination (angle) or angular velocity as the parameter which defines the threshold and thus controls the biofeedback. There are studies though, which estimated the CoM's position based on IMU sensors to classify body postures and postural transitions; for example to predict activity and energy expenditure [FSS+17, HAMJ+20, PSCB20]. Other researchers have used IMU measures to assess balance performance, mostly in dynamic balance during gait and physical activities [LDP04, FWSV+12, DBRM19]. So it is not arbitrary to implement such a control scheme. A biofeedback system based on the CoM-displacement tackles the problems reported when using the trunk's inclination or angular velocity because it does not focus on the orientation of one body segment but the whole body's position [NMAP+12]. On the downside, we require more than one IMU sensor to estimate the CoM's position and a comparably high processing power for the calculation. But our results show that the CoM based on the segmentation of the body into three segments only marginally differs from the CoM based on 16 segments. There are no significant differences in the baseline postural sway and differences in the LoS, though significant, range around 5%. We have to keep in mind though that the calculations are in both cases based on the output of all sensors. We highly encourage future studies to further investigate this aspect.

4.2 Threshold Parameters

We looked at two parameters which defined our thresholds and could potentially control biofeedback. Postural sway was defined as the variance in CoP and CoM trajectories during baseline measurements. We observed high variations in the base-

line postural sway across the subjects, indicating that this metric is highly individual. This coincides with findings by Yamamoto et al. who classified the variation as an individual-specific factor as well [YSS$^+$15]. They suggest that spectral parameters in the CoP trajectory's frequency and amplitude are less individual-specific. We further observed this trend in the sPT- and uPT-scenario's results where the BL-threshold shows a higher variation across the subjects than the LoS-threshold does. So spectral parameters might be better suited to define a threshold based on baseline measurements. Even more so, because the BL-threshold does not show any correlation to the LoS-threshold in the medio-lateral direction and is comparably narrow. The BL-threshold is proportional to the baseline postural sway (cf. Equation 2.5), so the higher the postural sway the broader the threshold. Therefore, it is reasonable why the BL-threshold is smaller in the medio-lateral than the anterior-posterior direction because in the latter direction the body is more stable in a bipedal stand.

The LoS-threshold, on the other hand, is based on the displacement a person can voluntarily reach. It is also an individual-specific factor but better considers the person's voluntary ability to control his balance. Our findings support this argument as the LoS-threshold has a lower distance and time discrepancy and shows a better performance than the BL-threshold.

4.3   Implications

Considering the BL-threshold, our findings implicate that a person with a higher postural sway needs a broader threshold because he reaches the tipping point later than a person with a small postural sway does. This is contradicting findings in previous studies that postural sway increases with age and that older adults have a smaller range of motion and narrower LoS [TSL$^+$17, JJW$^+$19]. So in fact, they would need tighter thresholds.

Our results suggest that a LoS-based threshold is better qualified to control biofeedback because it shows a more reliable performance and smaller difference to the reference system than the BL-threshold does. Differences between the two threshold parameters are not statistically significant in all systems but only in particular cases, so that we cannot accept the hypothesis H_3. We cannot statistically proof that the LoS-threshold is in general more reliable but our results indicate so.

One might argument that it is difficult to assess LoS in the elderly. We claim that it is not important to determine the extremest limits but the range a person is comfortable to move in. It is more important that we assess voluntarily reachable limits and based on these we could adjust the threshold. So instead of defining 90% of the LoS, as we did in this study, one could take 110% of the 'comfortable LoS' to account for the fact that the person did not reach the extremest limits during the assessment. The exact percentage would need further investigation including a larger sample. Alternatively, one could also implement an algorithm which learns

the optimal ratio based on previous situations where a feedback was triggered. Our results show a considerable variability in the CoP/ CoM trajectories of some subject across the trials. Looking at Figure 3.16, it seems that subject 5 increased his or her range of motion with each transition in the trial and crossed the LoS-threshold in the last one. So it might be more effective to define a flexible threshold, which adjusts itself based on the user's previous movements.

Furthermore, the results indicate that a PPS-system, like the IS-system, is more reliable than the IMU-system because it shows less variance in the output across all subjects and a smaller distance and time discrepancy compared to the IS-system. This is in particular the case for the IS-system's LoS-threshold. Once again, we cannot statistically proof that the PPS-system thresholds is in general more reliable than the IMU-system ones and therefore cannot accept hypothesis H_1. From a practical perspective, a PPS-system is easier to implement and integrate into daily activities than an IMU-system.

We cannot confirm that a combined threshold is more reliable than the threshold of one single system but that the combined threshold shows a similar performance to the IS-system's thresholds. So we cannot accept the hypothesis H_2 and our results suggest an opposite trend.

4.4 Practical Context

So far, we have mostly compared the systems in relation to each other, now we want to bring the absolute values into context. During the baseline measurement we recorded standard deviations (SD) in medio-lateral direction of 0.25 - 3.6mm in the PPS-system and 0.6 - 3.3mm in the IMU-system (cf. Figure 3.4). These are below mean values of 4mm reported by Kirchner et al. where older adults stood quietly on a force plate in a bipedal hip-width position. [KSGH13]. In anterior-posterior direction they report an average SD of 5.4mm which is above the 0.9 - 6.5mm measured in this study (cf. Figure 3.5). Differences might result from the various stance width and age of participants. The shape and absolute displacement of the CoP and CoM trajectories are similar with results found in the literature [LDP04, TFWA15]. The LoS, we measured in this study, correspond to values reported by Thomsen et al. who collected data from a sample of similar age and body dimensions [TSL$^+$17].

The IS-system's LoS-threshold showed a 11mm lower distance discrepancy Δd compared to the BL-threshold and 13mm lower Δd compared to the IMU-system's LoS-threshold. If we compare the Δd-values to the maximum displacement in anterior during the sPT-scenario (cf. Figure 3.18), the Δd of 11mm corresponds to 18% of the average maximum displacement measured by the reference system. A Δd of 13mm corresponds to 21%. Further compared to the ranges during baseline measurements, the discrepancies are considerable.

Our findings suggest that the IS-system's LoS-threshold is most reliable in triggering

a biofeedback compared to the other systems. We measured average time discrepancies Δt of around -1600ms, -2600ms, -1800ms and -2300ms (anterior, left, right and posterior) for this threshold during the uPT-scenario. This means that the subjects on average crossed the IS-system's LoS-threshold 2075ms before the tipping point. Do we compare this time discrepancy to average reaction times on vibrotactile stimuli, differences are large. Bao et al. compared reaction times between younger and older adults and between different body locations to which they applied the vibrotactile stimulus [BSK+19]. They report reaction times of 200 - 250ms in the younger and 250 - 300ms in the older adults. The reaction time was shorter the closer to the brain the stimulus was sensed. These are values for scenarios where the subjects were fully focused on the stimulus. In a dual-task scenario, reaction times increased to 500 - 600ms. Still, the average Δt values measured in this study are three to four times higher than these reaction times, so one could argue that the biofeedback signal would be triggered too early. On the other hand, we measured extreme Δt values of less than 600ms in all thresholds, so in some cases feedback would be triggered too late. This shows once more the variability between subjects. And an early feedback would give elderly people enough time to react properly.

4.5   Limitations

This study compared different concepts how to control a biofeedback system. Even though our results revealed differences between the concepts and parameters, we want to discuss potential limitations.

We simplified the human body and its biomechanics and assume in our calculations that the human body is composed of a chain of rigid body segments. Furthermore, our proportions are based on results of previous studies, namely these of Zatsiorsky and Seluyanov in 1990. But we adjusted the proportions to the subject's body dimensions. This procedure is widely applied among researchers and accepted as a good approximation of the human's kinematics [FSS+17, DBRM19, HAMJ+20].

We calculated the insole's CoP according to the weighted-mean-approach, where the force/ pressure of each sensor is weighted by its corresponding location in the insole. In a 2018 study, Hu et al. point out that the accuracy of the CoP's position in this approach depends on the locations and amount of sensors [HZP+18]. Certain locations and the areas covered by each sensor are potential sources for errors. They mention, however, that this error becomes smaller the denser the sensors are installed. Because the *medilogic* insoles employ up to 240 sensors, we neglected the potential error and used the weighted-mean-approach.

The tipping point's detection is another limitation in the technical setup. We could notice a distinctive peak in the vertical force measured by the force plate once the subject tipped over but the scale and time frame varied, making it difficult to automatically analyze. A trigger below the shoe's sole might help to determine more exactly the tipping point, as the point when the sole leaves the ground.

Other potential limitations result from the study design. Our sample of subjects contains only young adults, of who all do sports regularly. Nearly half of the participants reported that they frequently need to handle balance instabilities during their exercises. A future biofeedback system, however, will be designed for older adults or patients with neurological impairments. So it is important to verify the results in a cohort closer to the target one. Previous studies suggest that sensation and balance control differs between young and older adults [MWW$^+$15, JVD13].

All measurements of one subject were done consecutively on a single day with a rather short period where the participant could accustom to the systems and exercises. We tried to handle potential deviating behavior by repeating each exercise over three trials and considering the mean value. Yet, some subjects improved or changed their behavior over the trials. Thomsen et al. already pointed out that a valid determination of the LoS would need at least eight trials [TSL$^+$17]. So we recommend more detailed and standardized measures on the exact threshold parameters. One variable, which might have an influence on the subject's balance, are the shoes. We asked the participants to wear tight sport shoes, but we observed that subjects controlled their balance differently depending on the soles shape. Flat thin soles provided a better sense of the ground while thick round soles led to more tiny movements.

4.6 Future work

As already mentioned in the beginning of this discussion, we are not able to finally answer the question which IMU locations are necessary to reliably estimate the CoM's position. Measurements of postural sway and LoS should be repeated with an IMU-system, which allows the user to access each sensor's output separately. This way, one could compare the estimated CoM of different sensor sets or evaluate each sensor location in a Principal Component Analysis.

Our results suggest that a PPS-system is more reliable in triggering biofeedback. Insoles are also easy to integrate in shoes, so future research should focus on the exact tracking of the CoP by means of mobile PPS-based systems. We come to the conclusion that a LoS-threshold is more reliable than one based on the baseline postural sway. But as mentioned before, alternative less individual-specific parameters might provide even better results. Control parameters for a threshold should be investigated in more detail.

The reliability and validity of a potential biofeedback device should further be evaluated in a cohort closer to the target user group and also in different environmental settings. Our study was limited to one particular feet position, other positions, such as semi-tandem stance, should be explored as well. We tried to put our measured time discrepancies into context with reported reaction times but the optimal timing a elderly person needs to react on feedback and prevent a fall should be studied further.

Chapter 5

Conclusion

This study compared a PPS-system, using pressure insoles, and an IMU-system regarding their performance to reliably trigger a feasible biofeedback. We compared the time discrepancy between the point the potential feedback would be triggered and the actual tipping point when the person lost balance. The shorter this discrepancy the more accurate and reliable the system. Furthermore, we contrasted a threshold based on the postural sway during baseline measurements with a threshold based on the subject's LoS. We evaluated what influence the factors 'System' and 'Threshold' have on the time discrepancy. Though not significantly in all factor combinations, our results indicate that the LoS-based threshold has a shorter time discrepancy, and the PPS-system triggers a signal closer to the tipping point than the IMU-system. We come to the conclusion that the LoS-based threshold of the PPS-system is most reliable because time discrepancy and variance among the subjects are lowest in this case. A combined threshold of both systems gave similar results to the PPS-system. The average time discrepancies are still high though compared to reaction times on vibrotactile stimuli. We should further investigate the threshold's exact definition and consider alternative parameters, other than the postural sway or LoS. They might be better suited and less individual-specific. A potential biofeedback device should finally be tested under various circumstances and in a cohort closer to the target user group.

Appendix A

Additional Figures & Tables

A.1   Correlation BL- & LoS-threshold
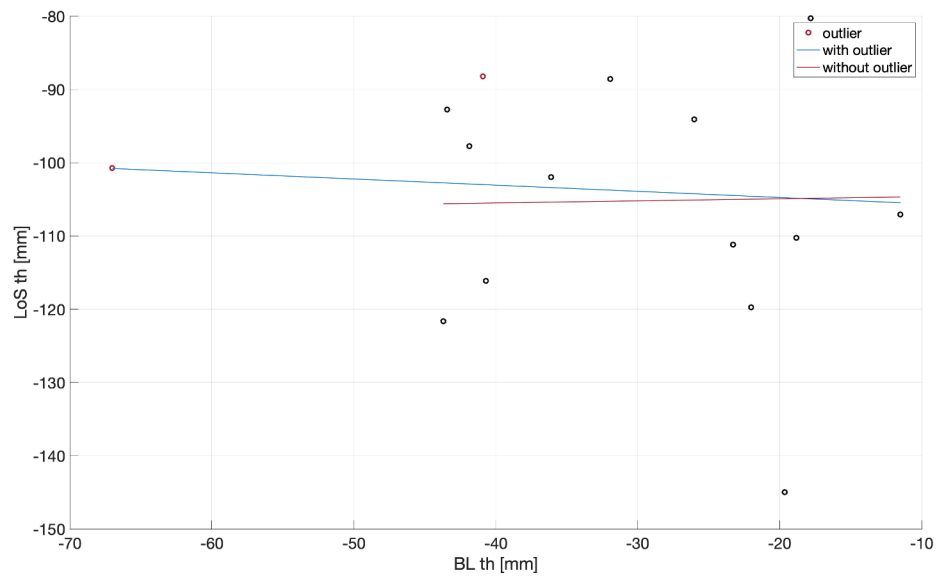
Figure A.1: Correlation between the left component of BL-threshold and LoS-threshold ; red circle indicate outlier, straights are the regression lines
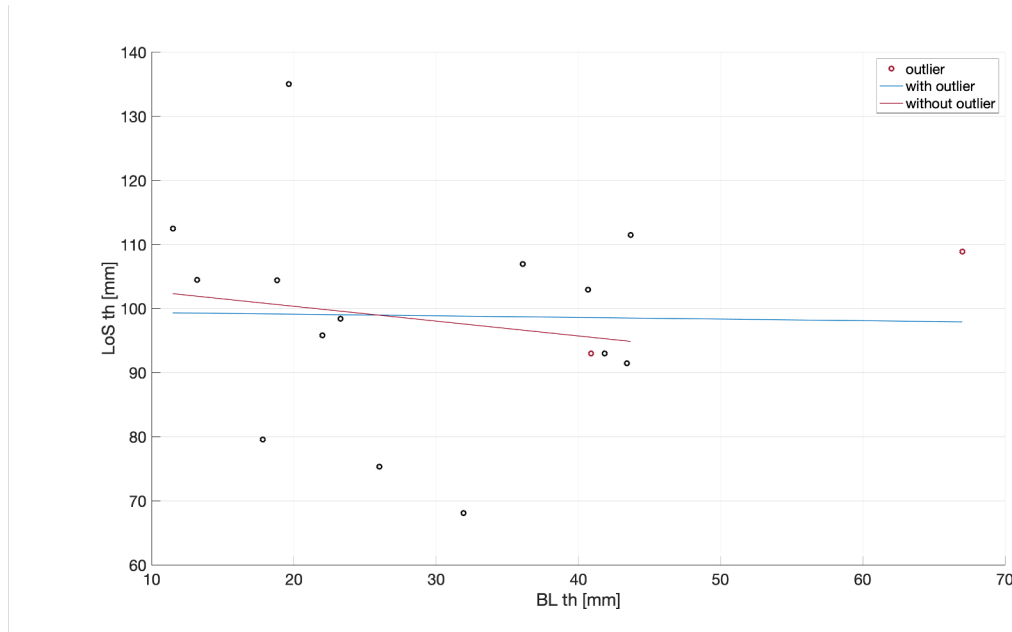
Figure A.2: Correlation between the right component of BL-threshold and LoS-threshold ; red circle indicate outlier, straights are the regression lines

	R	p-value	n
Anterior with outlier	-0.1138	0.6749	16
Anterior without outlier	**0.4169**	0.1380	14
Left with outlier	-0.0747	0.7833	16
Left without outlier	0.0191	0.9434	14
Right with outlier	-0.0232	0.9320	16
Right without outlier	-0.1567	0.5927	14
Posterior with outlier	0.2646	0.3219	16
Posterior without outlier	**0.5204**	0.0564	14

Table A.1: Correlations between BL- and LoS-threshold separated by direction component

A.2 sPT-scenario

	Difference	StdError	p-value
FP vs IS	12.0210	1.4988	0.0000**
FP vs IMU	-19.4990	4.0150	0.0006**
IS vs IMU	-31.5200	4.0900	0.0000**

Table A.2: Results of the Tukey-Kramer post-hoc test regarding differences in means between the systems' maximal displacement in anterior direction during the sPT-scenario; unit 'Difference': [mm]; * = p<0.05, ** = p<0.01

A.3 uPT-scenario

	Difference	Difference (transformed)	StdError (transformed)	p-value (transformed)
IS BLth vs IS LoSth	-1381.90	0.4169	0.1533	0.1287
IS BLth vs IMU BLth	-779.17	0.2221	0.0817	0.1293
IS BLth vs IMU LoSth	-771.25	0.1392	0.1785	0.9668
IS BLth vs COMB BLth	-925.83	0.3073	0.0827	0.0209*
IS BLth vs COMB LoSth	-1426.90	0.4365	0.1524	0.1002
IS LoSth vs IMU BLth	602.71	-0.1948	0.1013	0.4261
IS LoSth vs IMU LoSth	610.62	-0.2777	0.0716	0.0152*
IS LoSth vs COMB BLth	456.04	-0.1096	0.1126	0.9197
IS LoSth vs COMB LoSth	-45.00	0.0196	0.0140	0.7261
IMU BLth vs IMU LoSth	7.92	-0.0829	0.1260	0.9841
IMU BLth vs COMB BLth	-146.67	0.0852	0.0251	0.0382*
IMU BLth vs COMB LoSth	-647.71	0.2144	0.0982	0.3002
IMU LoSth vs COMB BLth	-154.58	0.1681	0.1382	0.8223
IMU LoSth vs COMB BLth	-655.63	0.2973	0.0653	0.0042**
COMB BLth vs COMB LoSth	-501.04	0.1292	0.1106	0.8449

Table A.3: Results of the Tukey-Kramer post-hoc test regarding differences in means between the factors 'System' and 'Threshold' in the uPT-scenario's (anterior) evaluation; unit 'Difference': [mm], unit 'Difference (transformed)': [log(mm)]; * = p<0.05, ** = p<0.01
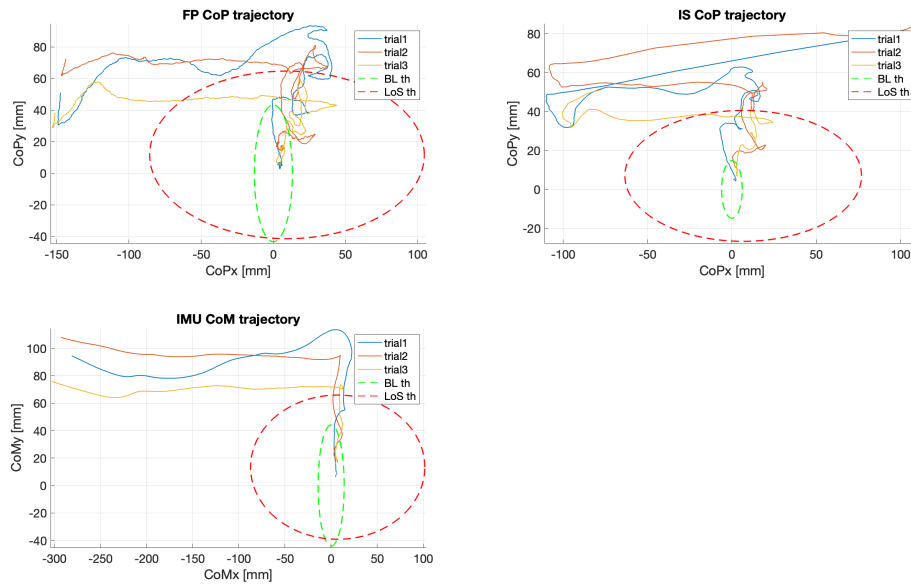
Figure A.3: CoP/ CoM trajectories of trial 1-3 during the sPT-scenario in left direction and the calculated BL- and LoS-threshold for each system (Subject 5)
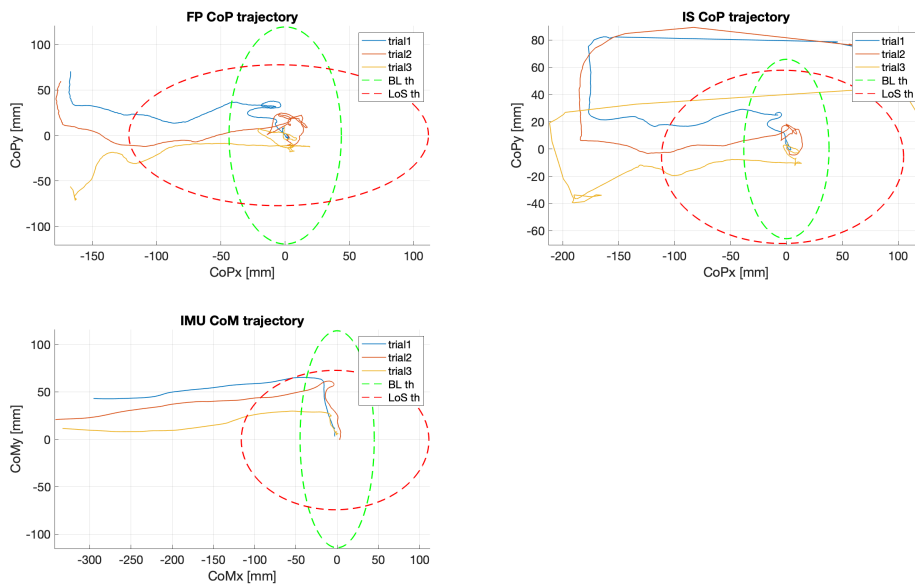
Figure A.4: CoP/ CoM trajectories of trial 1-3 during the sPT-scenario in left direction and the calculated BL- and LoS-threshold for each system (Subject 8)

	Subject 5				Subject 8			
	Trial1	Trial2	Trial3	Mean	Trial1	Trial2	Trial3	Mean
FP BLth	-5150	-4610	-5160	-4973.33	-1130	-1170	-1040	-1113.33
FP LoSth	-3600	-3360	-1310	-2756.67	-530	-660	-590	-593.33
IS BLth	-5690	-5220	-5470	-5460.00	-1340	-1300	-1220	-1286.67
IS LoSth	-3940	-3730	-3220	-3630.00	-810	-830	-710	-783.33
IMU BLth	-5110	-4390	-4910	-4803.33	-1290	-1280	-1110	-1226.67
IMU LoSth	-3860	-3350	-3290	-3500.00	-1080	-890	-700	-890.00

Table A.4: Time discrepancy Δt between the timepoint the subject exceeded the respective threshold and the tipping point during the uPT-scenario left; unit: [ms], positive values indicate that the threshold was crossed after the tipping point was reached

	Difference	Difference (transformed)	StdError (transformed)	p-value (transformed)
IS BLth vs IS LoSth	-2286.90	0.6289	0.1248	0.0017**
IS BLth vs IMU BLth	-771.04	0.1596	0.0687	0.2441
IS BLth vs IMU LoSth	-1530.00	0.3760	0.1257	0.0800
IS BLth vs COMB BLth	-878.96	0.1975	0.0564	0.0312*
IS BLth vs COMB LoSth	-2394.20	0.6724	0.1239	0.0008**
IS LoSth vs IMU BLth	1515.80	-0.4693	0.1237	0.0179*
IS LoSth vs IMU LoSth	756.88	-0.2529	0.1031	0.1995
IS LoSth vs COMB BLth	1407.90	-0.4314	0.1288	0.0415*
IS LoSth vs COMB LoSth	-107.29	0.0434	0.0301	0.7016
IMU BLth vs IMU LoSth	-758.96	0.2164	0.1094	0.3974
IMU BLth vs COMB BLth	-107.92	0.0379	0.0244	0.6400
IMU BLth vs COMB LoSth	-1623.10	0.5127	0.1131	0.0043**
IMU LoSth vs COMB BLth	651.04	-0.1785	0.1143	0.6331
IMU LoSth vs COMB BLth	-864.17	0.2963	0.0906	0.0482*
COMB BLth vs COMB LoSth	-1515.20	0.4749	0.1195	0.0127*

Table A.5: Results of the Tukey-Kramer post-hoc test regarding differences in means between the factors 'System' and 'Threshold' in the uPT-scenario's (left) evaluation; unit 'Difference': [mm], unit 'Difference (transformed)': [log(mm)]; * = p<0.05, ** = p<0.01

	Difference	Difference (transformed)	StdError (transformed)	p-value (transformed)
IS BLth vs IS LoSth	-2325.60	0.7424	0.1187	0.0002**
IS BLth vs IMU BLth	-925.83	0.2398	0.0672	0.0275*
IS BLth vs IMU LoSth	-1827.30	0.5610	0.1578	0.0282*
IS BLth vs COMB BLth	-1003.80	0.2637	0.0632	0.0087**
IS BLth vs COMB LoSth	-2617.10	0.9011	0.1147	0.0000**
IS LoSth vs IMU BLth	-1399.80	-0.5026	0.0978	0.0014**
IS LoSth vs IMU LoSth	498.33	-0.1814	0.1306	0.7328
IS LoSth vs COMB BLth	1321.90	-0.4786	0.0965	0.0019**
IS LoSth vs COMB LoSth	-291.46	0.1587	0.0460	0.0345*
IMU BLth vs IMU LoSth	-901.46	0.3212	0.1140	0.1086
IMU BLth vs COMB BLth	-77.92	0.0240	0.0131	0.4786
IMU BLth vs COMB LoSth	-1691.20	0.6613	0.0831	0.0000**
IMU LoSth vs COMB BLth	823.54	-0.2972	0.1183	0.1818
IMU LoSth vs COMB BLth	-789.79	0.3401	0.1016	0.0416*
COMB BLth vs COMB LoSth	-1613.30	0.6374	0.0834	0.0000**

Table A.6: Results of the Tukey-Kramer post-hoc test regarding differences in means between the factors 'System' and 'Threshold' in the uPT-scenario's (right) evaluation; unit 'Difference': [mm], unit 'Difference (transformed)': [log(mm)]; * = p<0.05, ** = p<0.01
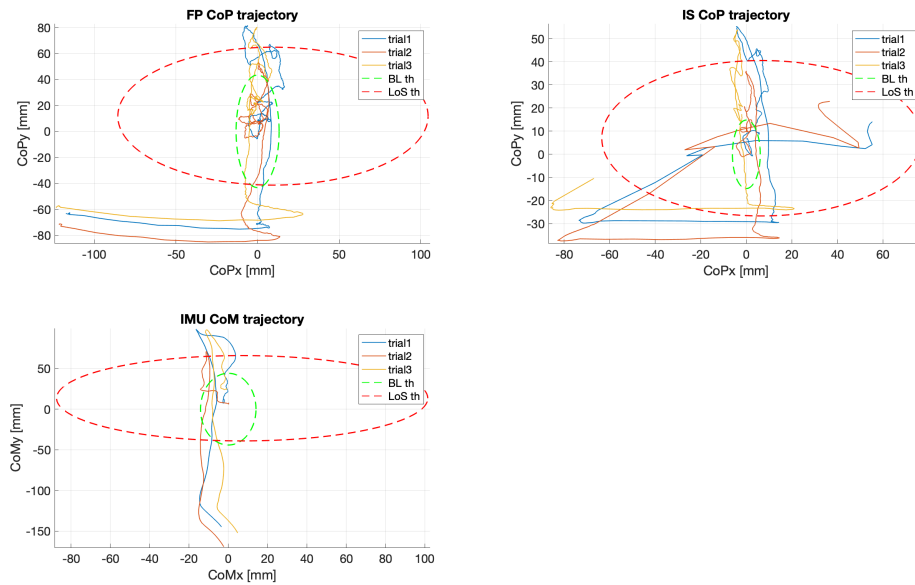
Figure A.5: CoP/ CoM trajectories of trial 1-3 during the sPT-scenario in posterior direction and the calculated BL- and LoS-threshold for each system (Subject 5)
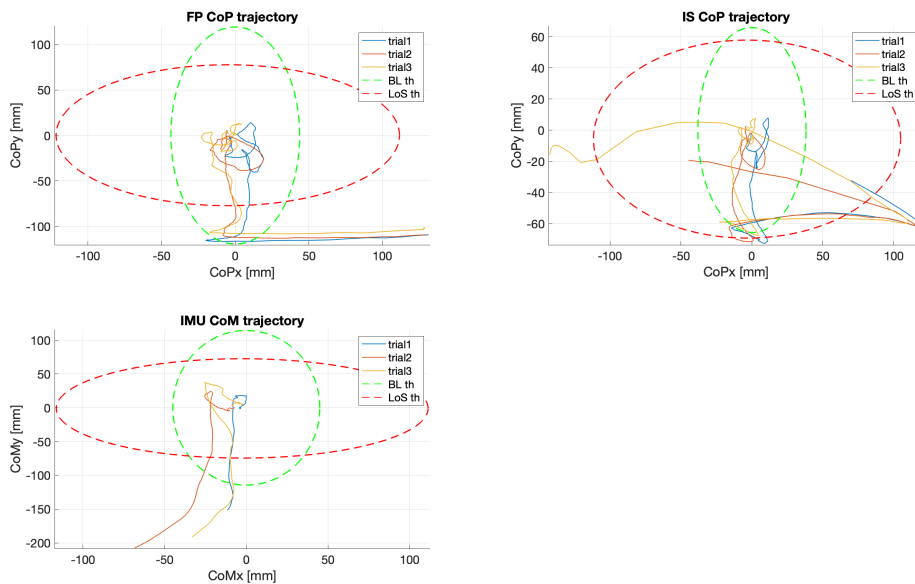
Figure A.6: CoP/ CoM trajectories of trial 1-3 during the sPT-scenario in posterior direction and the calculated BL- and LoS-threshold for each system (Subject 8)

| | Subject 5 | | | | Subject 8 | | | |
	Trial1	Trial2	Trial3	Mean	Trial1	Trial2	Trial3	Mean
FP BLth	-3800	-2510	-3890	-3400.00	-290	-240	-220	-250.00
FP LoSth	-2860	-1000	-2800	-2220.00	-1050	-940	-860	-950.00
IS BLth	-5600	-4800	-7130	-5843.33	-1250	-1140	-1140	-1176.67
IS LoSth	-3220	-1240	-3100	-2520.00	-1180	-1100	-400	-893.33
IMU BLth	-3990	-3970	-4010	-3990.00	-220	-490	-280	-330.00
IMU LoSth	-3290	-2270	-3260	-2940.00	-540	-660	-520	-573.33

Table A.7: Time discrepancy Δt between the timepoint the subject exceeded the respective threshold and the tipping point during the uPT-scenario posterior; unit: [ms], positive values indicate that the threshold was crossed after the tipping point was reached

	Difference	Difference (transformed)	StdError (transformed)	p-value (transformed)
IS BLth vs IS LoSth	-2030.20	0.5494	0.1711	0.0537
IS BLth vs IMU BLth	-1388.80	0.5616	0.1789	0.0611
IS BLth vs IMU LoSth	-2048.10	0.7021	0.1869	0.0193*
IS BLth vs COMB BLth	-1529.60	0.6424	0.1689	0.0176*
IS BLth vs COMB LoSth	-2684.20	0.9812	0.1776	0.0007**
IS LoSth vs IMU BLth	641.46	0.0122	0.2276	1.0000
IS LoSth vs IMU LoSth	-17.92	0.1526	0.1745	0.9470
IS LoSth vs COMB BLth	500.62	0.0930	0.2374	0.9985
IS LoSth vs COMB LoSth	-653.96	0.4318	0.1118	0.0157*
IMU BLth vs IMU LoSth	-659.38	0.1404	0.1810	0.9676
IMU BLth vs COMB BLth	-140.83	0.0808	0.0503	0.6074
IMU BLth vs COMB LoSth	-1295.40	0.4196	0.1983	0.3303
IMU LoSth vs COMB BLth	518.54	-0.0597	0.1887	0.9995
IMU LoSth vs COMB BLth	-636.04	0.2791	0.0932	0.0796
COMB BLth vs COMB LoSth	-1154.60	0.3388	0.2050	0.5794

Table A.8: Results of the Tukey-Kramer post-hoc test regarding differences in means between the factors 'System' and 'Threshold' in the uPT-scenario's (posterior) evaluation; unit 'Difference': [mm], unit 'Difference (transformed)': [log(mm)]; * = p<0.05, ** = p<0.01

A.4   Reduced Segmentation
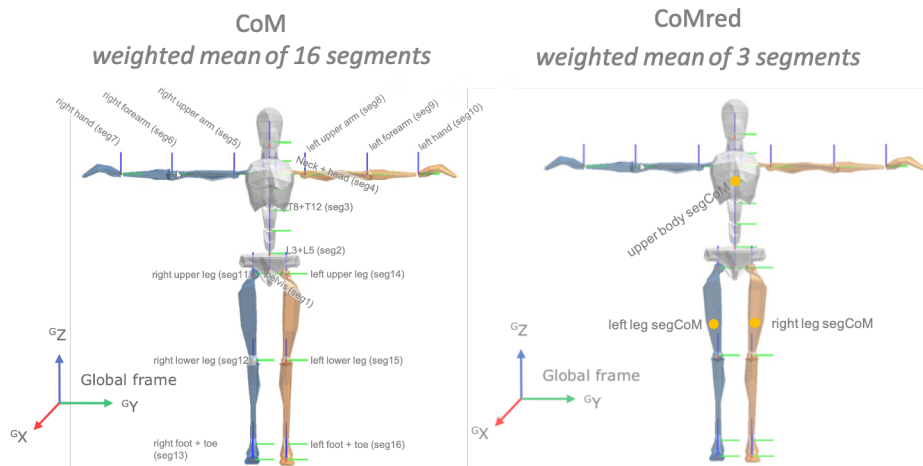
Figure A.7: Visualization of the two segmentation approaches of the CoM and CoMred (graphic from *Xsens* user manual and modified by author)
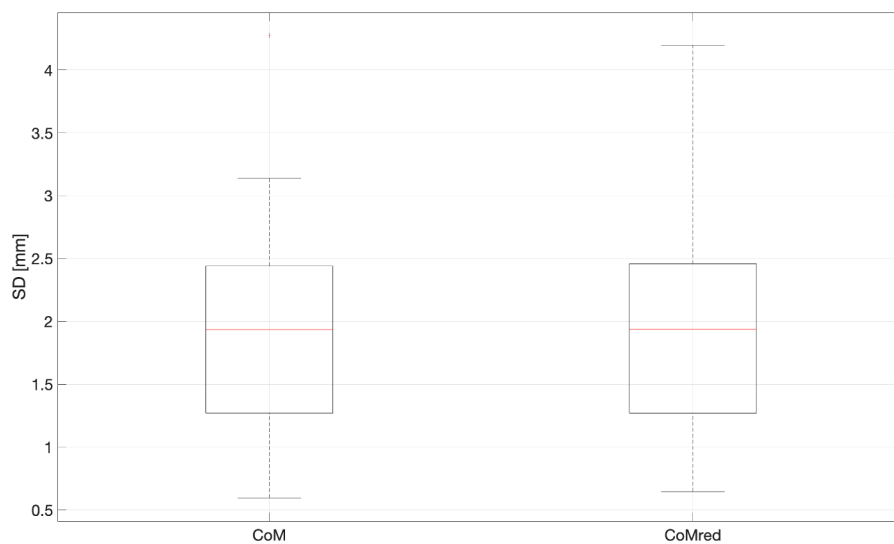
Figure A.8: Differences in the baseline SD medio-lateral between the CoM and CoMred; red line = median, whiskers = min/max, * = p<0.05, ** = p<0.01

Figure A.9: Differences in the baseline SD anterior-posterior between the CoM and CoMred; red line = median, whiskers = min/max, * = p<0.05, ** = p<0.01

List of Figures

Acronyms and Notations

ap anterior-posterior

BL baseline

BoS Base of Support

BW Body Weight

CoM Center of Mass

CoP Center of Pressure

DoF degrees of freedom

DV Dependent Variable

FP Force Plate

FSO Full Scale Output

GRF Ground Reaction Force

IMU Inertial Measurement Unit

IS Insoles

LoS Limits of Stability

MEMS Microelectromechanical System

ml medio-lateral

OMC Optical Motion Capturing

PPS Plantar Pressure Sensor

sPT stable postural transition

SSR Solid-state Relay

TUG Timed Up and Go test

uPT unstable postural transition

Bibliography

[AAB⁺17]   Atefeh Aboutorabi, Mokhtar Arazpour, Mahmood Bahramizadeh, Farzam Farahmand, and Reza Fadayevatan. Effect of vibration on postural control and gait of elderly subjects: a systematic review. *Aging Clinical and Experimental Research*, 30(7):713–726, 2017. `doi: 10.1007/s40520-017-0831-7`.

[ADH⁺20]   Arash Atrsaei, Farzin Dadashi, Clint Hansen, Elke Warmerdam, Benoit Mariani, Walter Maetzler, and Kamiar Aminian. Postural transitions detection and characterization in healthy and patient populations using a single waist sensor. *Journal of NeuroEngineering and Rehabilitation*, 17(1), Mar 2020. `doi:10.1186/s12984-020-00692-4`.

[ALHPI⁺18] Christopher Moufawad El Achkar, Constanze Lenbole-Hoskovec, Anisoara Paraschiv-Ionescu, Kristof Major, Christophe Buela, and Kamiar Aminian. Classification and characterization of postural transitions using instrumented shoes. *Medical Biological Engineering Computing*, 56(8):1403–1412, Dec 2018. `doi:10.1007/s11517-017-1778-8`.

[AOL⁺15]   Muhammad Raheel Afzal, Min-Kyun Oh, Chang-Hee Lee, Young Sook Park, and Jungwon Yoon. A portable gait asymmetry rehabilitation system for individuals with stroke using a vibrotactile feedback. *BioMed Research International*, 2015:1–16, 2015. `doi:10.1155/2015/375638`.

[AS10]   A.u. Alahakone and S.m.n.a. Senanayake. A real-time system with assistive feedback for postural control in rehabilitation. *IEEE/ASME Transactions on Mechatronics*, 15(2):226–233, 2010. `doi:10.1109/tmech.2010.2041030`.

[BFC⁺20]   Giulia Ballardini, Valeria Florio, Andrea Canessa, Giorgio Carlini, Pietro Morasso, and Maura Casadio. Vibrotactile feedback for improving standing balance. *Frontiers in Bioengineering and Biotechnology*, 8, 2020. `doi:10.3389/fbioe.2020.00094`.

[BRK94]   B.j. Benda, P.o. Riley, and D.e. Krebs. Biomechanical relationship
           between center of gravity and center of pressure during standing. *IEEE
           Transactions on Rehabilitation Engineering*, 2(1):3–10, 1994. `doi:10.`
           `1109/86.296348`.

[BSK+19]   Tian Bao, Lydia Su, Catherine Kinnaird, Mohammed Kabeto, Peter B.
           Shull, and Kathleen H. Sienko. Vibrotactile display design: Quantify-
           ing the importance of age and various factors on reaction times. *Plos
           One*, 14(8), 2019. `doi:10.1371/journal.pone.0219737`.

[CBG+19]   Kavin Chandrasekaran, Luke Buquicchio, Walter Gerych, Emmanuel
           Agu, and Elke Rundensteiner. Get up!: Assessing postural activ-
           ity transitions using bi-directional gated recurrent units (Bi-GRUs)
           on smartphone motion data. *2019 IEEE Healthcare Innovations
           and Point of Care Technologies, (HI-POCT)*, 2019. `doi:10.1109/`
           `hi-poct45284.2019.8962729`.

[CCD+15]   Simona Crea, Christian Cipriani, Marco Donati, Maria Chiara Car-
           rozza, and Nicola Vitiello. Providing time-discrete gait information by
           wearable feedback apparatus for lower-limb amputees: Usability and
           functional validation. *IEEE Transactions on Neural Systems and Re-
           habilitation Engineering*, 23(2):250–257, 2015. `doi:10.1109/tnsre.`
           `2014.2365548`.

[cdc17]   Important facts about falls, Feb 2017. URL: `https://www.cdc.gov/`
           `homeandrecreationalsafety/falls/adultfalls.html`.

[CDR+14]   Simona Crea, Marco Donati, Stefano De Rossi, Calogero Oddo, and
           Nicola Vitiello. A wireless flexible sensorized insole for gait analysis.
           Sensors, 14(1):1073–1093, 2014. `doi:10.3390/s140101073`.

[CGD+18]   Francesco Caputo, Alessandro Greco, Egidio D'Amato, Immacolata
           Notaro, and Stefania Spada. IMU-based motion capture wearable sys-
           tem for ergonomic assessment in industrial environment. *Advances
           in Human Factors in Wearable Technologies and Game Design Ad-
           vances in Intelligent Systems and Computing*, pages 215–225, 2018.
           `doi:10.1007/978-3-319-94619-1_21`.

[CT17]   Ramon Cuevas-Trisan. Balance problems and fall risks in the el-
           derly. *Physical Medicine and Rehabilitation Clinics of North America*,
           28(4):727–737, 2017. `doi:10.1016/j.pmr.2017.06.006`.

[DBRM19]   Gisele Francini Devetak, Roberta Castilhos Detanico Bohrer, Andre
           Luiz Felix Rodacki, and Elisangela Ferretti Manffra. Center of mass in
           analysis of dynamic stability during gait following stroke: A systematic

review. *Gait Posture*, 72:154–166, 2019. `doi:10.1016/j.gaitpost.`
`2019.06.006.`

[DSL19]   Steven Diaz, Jeannie B. Stephenson, and Miguel A. Labrador. Use of
            wearable sensor technology in gait, balance, and range of motion anal-
            ysis. *Applied Sciences*, 10(1):234, 2019. `doi:10.3390/app10010234.`

[FSS⁺17]   Benedikt Fasel, Joerg Spoerri, Pascal Schuetz, Silvio Lorenzetti, and
            Kamiar Aminian. An inertial sensor-based method for estimating the
            athletes relative joint center positions and center of mass kinematics in
            alpine ski racing. *Frontiers in Physiology*, 8, Jan 2017. `doi:10.3389/`
            `fphys.2017.00850.`

[FWSV⁺12]   M. J. Floor-Westerdijk, H. H. Schepers, P. H. Veltink, E. H. F. Van
            Asseldonk, and J. H. Buurke. Use of inertial sensors for ambula-
            tory assessment of center-of-mass displacements during walking. *IEEE
            Transactions on Biomedical Engineering*, 59(7):2080–2084, 2012. `doi:`
            `10.1109/tbme.2012.2197211.`

[HAMJ⁺20]   Mathias Hedegaard, Amjad Anvari-Moghaddam, Bjorn K. Jensen, Ce-
            cilie B. Jensen, Mads K. Pedersen, and Afshin Samani. Prediction
            of energy expenditure during activities of daily living by a wearable
            set of inertial sensors. *Medical Engineering Physics*, 75:13–22, 2020.
            `doi:10.1016/j.medengphy.2019.10.006.`

[HGM⁺16]   Aodhan Hickey, Brook Galna, John C. Mathers, Lynn Rochester, and
            Alan Godfrey. A multi-resolution investigation for postural transition
            detection and quantification using a single wearable. *Gait Posture*,
            49:411–417, 2016. `doi:10.1016/j.gaitpost.2016.07.328.`

[HLBB19]   Klaas A. Hartholt, Robin Lee, Elizabeth R. Burns, and Ed F. Van
            Beeck. Mortality from falls among US adults aged 75 years or older,
            2000-2016. *Jama*, 321(21):2131, Apr 2019. `doi:10.1001/jama.2019.`
            `4185.`

[HZP⁺18]   Xinyao Hu, Jun Zhao, Dongsheng Peng, Zhenglong Sun, and Xingda
            Qu. Estimation of foot plantar center of pressure trajectories with low-
            cost instrumented insoles using an individual-specific nonlinear model.
            Sensors, 18(2):421, 2018. `doi:10.3390/s18020421.`

[JJW⁺19]   Jonas Johansson, Ewa Jarocka, Goeran Westling, Anna Nordstroem,
            and Peter Nordstroem. Predicting incident falls: Relationship between
            postural sway and limits of stability in older adults. *Human Movement
            Science*, 66:117–123, 2019. `doi:10.1016/j.humov.2019.04.004.`

[JVD13]   Jitka Jancova Vseteckova and Nicholas Drey. What is the role body sway deviation and body sway velocity play in postural stability in older adults? *Acta medica (Hradec Kralove)*, 56(3):117–123, 2013.

[KBS+16]   Angelos Karatsidis, Giovanni Bellusci, H. Schepers, Mark De Zee, Michael Andersen, and Peter Veltink. Estimation of ground reaction forces and moments during gait using only inertial motion capture. *Sensors*, 17(12):75, 2016. `doi:10.3390/s17010075`.

[KFG+18]   Herman Kingma, Lilian Felipe, Marie-Cecile Gerards, Peter Gerits, Nils Guinand, Angelica Perez-Fornos, Vladimir Demkin, and Raymond Van De Berg. Vibrotactile feedback improves balance and mobility in patients with severe bilateral vestibular loss. *Journal of Neurology*, 266(S1):19–26, May 2018. `doi:10.1007/s00415-018-9133-z`.

[KJBC18]   Kavisha Khanuja, Jaclyn Joki, Gloria Bachmann, and Sara Cuccurullo. Gait and balance in the aging population: Fall prevention using innovation and technology. *Maturitas*, 110:51–56, 2018. `doi:10.1016/j.maturitas.2018.01.021`.

[KSGH13]   M. Kirchner, P. Schubert, T. Getrost, and C.t. Haas. Effect of altered surfaces on postural sway characteristics in elderly subjects. *Human Movement Science*, 32(6):1467–1479, 2013. `doi:10.1016/j.humov.2013.05.005`.

[LDP04]   D Lafond, M Duarte, and F Prince. Comparison of three methods to estimate the center of mass during balance assessment. *Journal of Biomechanics*, 37(9):1421–1426, 2004. `doi:10.1016/s0021-9290(03)00251-3`.

[Lev96]   Paolo De Leva. Adjustments to zatsiorsky-seluyanovs segment inertia parameters. *Journal of Biomechanics*, 29(9):1223–1230, 1996. `doi:10.1016/0021-9290(95)00178-6`.

[LFT18]   Beom-Chan Lee, Alberto Fung, and Timothy A. Thrasher. The effects of coding schemes on vibrotactile biofeedback for dynamic balance training in parkinsonâs disease and healthy elderly individuals. *IEEE Transactions on Neural Systems and Rehabilitation Engineering*, 26(1):153–160, 2018. `doi:10.1109/tnsre.2017.2762239`.

[LPJ+18]   Cunguang Lou, Chenyao Pang, Congrui Jing, Shuo Wang, Xufeng He, Xiaoguang Liu, Lei Huang, Feng Lin, Xiuling Liu, Hongrui Wang, and et al. Dynamic balance measurement and quantitative assessment using wearable plantar-pressure insoles in a pose-sensed virtual environment. *Sensors*, 18(12):4193, 2018. `doi:10.3390/s18124193`.

[mat]   Model IMU, GPS, and INS/GPS. URL: `https://www.mathworks.com/help/fusion/gs/model-imu-gps-and-insgps.html`.

[MMD17]   Sumit Majumder, Tapas Mondal, and M. Deen. Wearable sensors for remote health monitoring. *Sensors*, 17(12):130, 2017. `doi:10.3390/s17010130`.

[MP20]   John McLester and Peter St. Pierre. *Applied biomechanics: concepts and connections*. Jones Bartlett Learning, 2020.

[MWL+16]   Christina Ma, Duo Wong, Wing Lam, Anson Wan, and Winson Lee. Balance improvement effects of biofeedback systems with state-of-the-art wearable sensors: A systematic review. *Sensors*, 16(4):434, 2016. `doi:10.3390/s16040434`.

[MWW+15]   Christina Ma, Anson Wan, Duo Wong, Yong-Ping Zheng, and Winson Lee. A vibrotactile and plantar force measurement-based biofeedback system: Paving the way towards wearable balance-improving devices. *Sensors*, 15(12):31709–31722, 2015. `doi:10.3390/s151229883`.

[NMAP+12]   W. Nanhoe-Mahabier, J.h. Allum, E.p. Pasman, S. Overeem, and B.r. Bloem. The effects of vibrotactile biofeedback training on trunk sway in parkinsons disease patients. *Parkinsonism Related Disorders*, 18(9):1017–1021, 2012. `doi:10.1016/j.parkreldis.2012.05.018`.

[PDRP00]   Alexandra S Pollock, Brian R Durward, Philip J Rowe, and John P Paul. What is balance? *Clinical Rehabilitation*, 14(4):402–406, 2000. `doi:10.1191/0269215500cr342oa`.

[PJA90]   Ilmari Pyykko, Pirkko Jantti, and Heikki Aalto. Postural control in elderly subjects. *Age and Ageing*, 19(3):215–221, 1990. `doi:10.1093/ageing/19.3.215`.

[PSCB20]   Gaspare Pavei, Francesca Salis, Andrea Cereatti, and Elena Bergamini. Body center of mass trajectory and mechanical energy using inertial sensors: a feasible stride? *Gait Posture*, 2020. `doi:10.1016/j.gaitpost.2020.04.012`.

[Rag96]   Maria Ragnarsdottir. The concept of balance. *Physiotherapy*, 82(6):368–375, 1996. `doi:10.1016/s0031-9406(05)66484-x`.

[RKSL17]   A. Rommel, J. Kottner, R. Suhr, and N. Lahmann. Haeufigkeit von stuerzen unter klienten ambulanter pflegedienste. *Zeitschrift fuer Gerontologie und Geriatrie*, 52(1):3–9, 2017. `doi:10.1007/s00391-017-1215-5`.

[Sal10]   Brooke Salzman. Gait and balance disorders in older adults. *American Family Physican*, 82(1):61–68, Jul 2010. URL: `www.aafp.org/afp`.

[SK08]   Bruno Siciliano and Oussama Khatib. *Springer handbook of robotics*. Springer, 2008.

[Ste20]   Nicholas Stergiou. *Biomechanics and gait analysis*. Academic Press, 2020.

[TFWA15]   Adin Ming Tan, Franz Konstantin Fuss, Yehuda Weizman, and Michael F. Azari. Centre of pressure detection and analysis with a high-resolution and low-cost smart insole. *Procedia Engineering*, 112:146–151, 2015. `doi:10.1016/j.proeng.2015.07.190`.

[TSL+17]   Mikkel Hojgaard Thomsen, Nicolai Stottrup, Frederik Greve Larsen, Ann-Marie Sydow Krogh Pedersen, Anne Grove Poulsen, and Rogerio Pessoto Hirata. Four-way-leaning test shows larger limits of stability than a circular-leaning test. *Gait Posture*, 51:10–13, 2017. `doi:10.1016/j.gaitpost.2016.09.018`.

[VCDP06]   Nicolas Vuillerme, Olivier Chenu, Jacques Demongeot, and Yohan Payan. Controlling posture using a plantar pressure-based, tongue-placed tactile biofeedback system. *Experimental Brain Research*, 179(3):409–414, 2006. `doi:10.1007/s00221-006-0800-4`.

[Vie06]   Lucas Vieira. A gyroscope, Oct 2006. accessed on 21.12.2020. URL: `https://en.wikipedia.org/wiki/Gyroscope#/media/File:3D_Gyroscope.png`.

[WHCR14]   Saunders N. Whittlesey, Joseph Hamill, Graham E. Caldwell, and D. Gordon E. Robertson. *Research methods in biomechanics*. Human Kinetics, 2014.

[who07]   WHO global report on falls prevention in older age, Mar 2007. URL: `https://www.who.int/ageing/publications/Falls_prevention7March.pdf`.

[WWD+93]   Robert Whipple, Leslie Wolfson, Carol Derby, Devender Singh, and Jonathan Tobin. 10 altered sensory function and balance in older persons. *Journal of Gerontology*, 48(Special Issue):71–76, 1993. `doi:10.1093/geronj/48.special_issue.71`.

[WWSK01]   C. Wall, M.s. Weinberg, P.b. Schmidt, and D.e. Krebs. Balance prosthesis based on micromechanical sensors using vibrotactile feedback of tilt. *IEEE Transactions on Biomedical Engineering*, 48(10):1153–1161, 2001. `doi:10.1109/10.951518`.

[YSS$^+$15]   Tomohisa Yamamoto, Charles E. Smith, Yasuyuki Suzuki, Ken Kiyono, Takao Tanahashi, Saburo Sakoda, Pietro Morasso, and Taishin Nomura. Universal and individual characteristics of postural sway during quiet standing in healthy young adults. *Physiological Reports*, 3(3), 2015. `doi:10.14814/phy2.12329`.